UNIVERSITY OF CALIFORNIA SAN DIEGO

Noisy Binary Search: Practical Algorithms and Applications

A dissertation submitted in partial satisfaction of the
requirements for the degree
Doctor of Philosophy

in

Electrical Engineering
(Communication Theory and Systems)

by

Sung-En Chiu

Committee in charge:

Professor Tara Javidi, Chair
Professor Todd Kemp
Professor Piya Pal
Professor Bhaskar D. Rao
Professor Ruth J. Williams

2019

The dissertation of Sung-En Chiu is approved, and it is acceptable in quality and form for publication on microfilm and electronically:

_____

_____

_____

_____

_____

Chair

University of California San Diego

2019

DEDICATION

To my family.

TABLE OF CONTENTS

LIST OF FIGURES

LIST OF TABLES

ACKNOWLEDGEMENTS

First, I am greatly indebted to my advisor, Tara Javidi, who support financially and work patiently with me.

I would like to give thanks to my thesis committees, Bhaskar Rao, Piya Pal, Todd Kemp, and Ruth Williams. In particular, I thank Prof Bhaskar Rao, whom I worked with in my first three years of Ph.D. He guided and shaped the original path of my Ph.D. study.

I would like to express my thanks to my collaborators Anusha Lalitha, and Nancy Ronquillo. They helped a lot in the works of this dissertation.

I would also like to give appreciations to my lab-mates Chang-Heng Wang, Yongxi Lu, Shekar Shubhanshu, Yacong Ding, David Ho, Jing Liu, PhuongBang Nguyen, Anh Nguyen, Furkan Kovasoglu, Ritwik Giri, Elina Nayebi, Maher AlShoukairi, Igor Fedorov, Alican Nalci. The conversations with them are a significant component of my work toward this dissertation.

I thank my friends from Taiwan, including Hsin-Ming Lin, Yeng-Tsun Peng, Jeng-Hau Lin, Pei-Chain Chih, Chia-Hung Liu.

I thank my church, Lord's Grace CBCSD, where I receive a lot of help in life, prayer supports, and wonderful fellowship. I thank my small group Crossroads, Bowen Ouyang, Ray Chu, Ivy Tsai, Andrew Ling, Stephanie Toh, Erica Yeh, David and Shirley Liu, Joyce Tan, Jeff Syang, Hao Zheng, Tavis Lam, Raymond Lam, Ezra Fu. I thank Erica Yeh, who provides spiritual support in my last few months of preparing this dissertation. I thank Derek and Leah Wong, Enoch and Luice Kang, Allen and Caroline Wei, Andrew and Anges See, Victor and Monica Ho, Raymond and Nina Luck , Michael and Eva Liew, Samuel and Eulalia Chen, William and Winnie Soo Hoo, Tom and Connie Tye, for their hosting and caring for me. I thank the worship team: Jiawei and Esther Chen, Victor Ho, Jeff and Vicky Uy, John Mokili; I thank choir: Ming Chu, Eric and Ellen, Katie Kong, and Rochelle Wu, for we worship and praise God together. I thank Pastor Justin Sim for his prayer and leading the whole church, praying for my thesis and final defense.

I thank my Uncle CT Chang, who offers me a lot of support in life.

I thank my parents, sister, family, and friends in Taiwan for their support of my Ph.D. journey. This dissertation is dedicated to them.

I thank God who has brought me here in the U.S this far and more to go.

Chapter 2, in part, is a reprint of the material as it appears in the paper: Sung-En Chiu and Tara Javidi. ”Sequential Measurement-Dependent Noisy Search.” 2016 IEEE Information Theory Workshop (ITW). IEEE, 2016. The dissertation author was the primary investigator and author of this paper.

Chapter 2, in full, is currently being prepared for submission for publication as Sung-En Chiu and Tara Javidi, ”Query Dependent Noisy Search.” The dissertation author was the primary investigator and author of this material.

Chapter 3, in full, is a reprint of the material as it appears in the paper: Sung-En Chiu, Anusha Lalitha and Tara Javidi, ”Bit-wise Sequential Coding with Feedback.” 2018 IEEE International Symposium on Information Theory (ISIT). IEEE, 2018. The dissertation author was the primary investigator and author of this paper.

Chapter 4, in full, has been submitted for publication as Sung-En Chiu, Nancy Ronquillo and Tara Javidi, ”Active Learning and CSI Acquisition for mmWaveInitial Alignment,” available on arXiv:1812.07722. The dissertation author was the primary investigator and author of this paper.

VITA

2008	Bachelor of Engineering, National Chiao Tung University, Taiwan
2010	Master of Science, National Chiao Tung University, Taiwan
2019	Doctor of Philosophy, University of California San Diego

PUBLICATIONS

S.-E. Chiu, N. Ronquillo, and T. Javidi, "Active Learning and CSI acquisition for mmWave Initial Alignment", *arXiv preprint arXiv:1812.07722, submitted to IEEE J. Sel. Areas in Communications*

Y. Ding, S.-E. Chiu, and B. D. Rao, "Bayesian channel estimation algorithms for massive MIMO systems with hybrid analog-digital processing and low resolution ADCs," *IEEE J. Sel. Topics in Signal Processing*, vol. 12, no. 3, pp. 499-513, Jun. 2018.

S. H. Fouladi, S.-E. Chiu, B. D. Rao, and I. Balasingham, "Recovery of Independent Sparse Sources From Linear Mixtures Using Sparse Bayesian Learning," *IEEE Transactions on Signal Processing.*, vol. 66, no. 24, pp. 6332-6346, Dec. 2018.

S.-E. Chiu, F. T. Chien, and R. Y. Chang, "On the Diversity of Noncoherent Distributed Space-Frequency Coded Relay Systems With Relay Censoring," *IEEE Transactions on Communications*, vol. 62 no. 10, pp. 3491-3503, Oct. 2014

S.-E. Chiu, A. Lalitha, and T. Javidi, "Bit-wise Sequential Coding with Feedback," IEEE International Symposium on Information Theory (ISIT) ,pp. 321-325, June 2018.

Y. Ding, S.-E. Chiu, and B. D. Rao, "Sparse recovery with quantized multiple measurement vectors," In *Proc. 51st Asilomar Conf. Signals Syst. Comput.*, pp. 845-849, Oct. 2017.

S.-E. Chiu and T. Javidi, (2016, September). "Sequential measurement-dependent noisy search," *Information Theory Workshop (ITW)*, pp. 221-225, Sept. 2016.

S.-E. Chiu, and B. D. Rao, "Correlation learning on joint support recovery for more sources than measurements," *Sensor Array and Multichannel Signal Processing Workshop (SAM)*, July 2016.

ABSTRACT OF THE DISSERTATION

Noisy Binary Search: Practical Algorithms and Applications

by

Sung-En Chiu

Doctor of Philosophy in Electrical Engineering
(Communication Theory and Systems)

University of California San Diego, 2019

Professor Tara Javidi, Chair

This dissertation addresses the problem of searching a target within a region by sequential queries with noisy responses. A Bayesian decision maker is responsible for collecting observation samples to enhance his knowledge about the actual location speedily. When the response is noiseless, the classical binary search solves such a problem optimally. Noisy binary search, on the other hand, has also been formulated and studied extensively in theory over the past 60 years since Horstein (1963). However, the algorithms developed in noisy binary search problem find limited practical applications in real-world engineer problem. Motivated by bridging theory and practice, we formulate the noisy binary search problem by identifying realistic scenarios and

constraints that naturally rises with practical applications such as spectrum sensing in cognitive communication, AoA estimation by adaptive beamforming in large antenna array system, visual image inspection, bit-wise data transmission, heavy hitter detection in network system, etc.

The first part of the dissertation (Chapter 2) focuses on theoretical understanding and developing noisy binary search algorithms under those practical constraints. Three algorithms $sortPM$, $dyaPM$, $hiePM$ are proposed. Using the extrinsic Jensen Divergence from information theory, we provide upper bound for the expected search time of each of the algorithms. By comparing with an information theoretic lower bound, we demonstrate the asymptotic optimality and suboptimality of the proposed algorithms (asymptotic in the resolution of the target location).

The second part of the dissertation applies the proposed $hiePM$ to practical problems. In particular, Chapter 3 demonstrates the application of $hiePM$ on the data transmission problem with noiseless feedback. The dyadic hierarchical query area of $hiePM$ relates directly to the bit representation of the data stream. This method simplifies the corresponding adaptive encoding scheme significantly and allows a bit-wise encoding. Chapter 4 considers the initial beam alignment problem in 5G mmWave communication using beamforming. With a single-path channel model, the problem is reduced to actively searching the Angle-of-Arrival (AoA) of the signal sent from the user to the Base Station (BS). $hiePM$ is applied to adaptively and sequentially choose the beamforming from the hierarchical beamforming codebook. The proposed algorithm is compared to prior works of initial beam alignment that employs linear beam search, repeat binary search, or random beam search, respectively, and gives the state-of-art performance in terms of both AoA estimation error at the end of the initial alignment, and the spectral efficiency during the communication phase.

Chapter 1

Introduction

This dissertation addresses the problem of searching a target within a region by sequential queries. A Bayesian decision maker is responsible for collecting observation samples to enhance his knowledge about the true location speedily. When the response is noiseless, the classical binary search solves such a problem optimally. The problem of binary noisy search for a target with query-independent noise [1–7] have been studied extensively in the literature. Relying on connections with feedback coding, [2, 3] proposed a noisy variant of the binary search algorithm. For a general channel with feedback, [8] proposed a scheme, referred to as Posterior Matching, generalizing the noisy binary search algorithm. In particular, [8] established the rate-optimality where we define the targeting rate as the ratio of the logarithm of the search resolution over the number of queries. By allowing for random search time, [7] proposed two-phase schemes that achieve the optimal rate-reliability trade-off where reliability is defined to be the ratio of the logarithm of error probability over the (expected) number of queries.

In many applications of interest, such as spectrum sensing [9] in cognitive radio, AoA estimation in initial beam alignment (Chapter 4), and heavy hitter detection [10] in Networking, the noise statistics of the observation is usually *query-dependent*. In particular, querying a larger size region is often prone to return a noisier measurement than querying a smaller region. With

binary measurements and Bernoulli noise, for instance, this noise behavior means that the false alarm and miss detection of each query can be thought of a non-decreasing function of the size of the query set.

Motivated by practical applications, in this dissertation, we study the problem of query-dependent noisy search. Chapter 2 is dedicated to formulating in detail the target localization problem where at any given time, an agent can choose a region to query for the presence of the target in that region. Each query is assumed to be subjected to an additive noise whose variance is an increasing function of the size of the query region. Motivated by practical applications such as initial beam alignment in array processing, heavy hitter detection in Networking, and visual search in robotics, we proposed adaptive algorithms with the following essential metrics: *query time complexity*, *computational and memory complexity*, *query geometry (the shape of the query set)* and *query cardinality (cardinality of the collection of query sets that are allowed to be chosen from)*. Three novel search strategies: sorted Posterior Matching ($sortPM$), dyadic Posterior Matching ($dyaPM$) and hierarchical Posterior Matching ($hiePM$), are proposed. Each of them has its advantages in different applications. In particular, $sortPM$, by a sorting operation, greedily reduces the noise variance of each query, with the compromise of query geometry and query cardinality (by sorting, the chosen query set can be any measurable set). With minor sacrifice in the query noise, we design $dyaPM$ under the constraint that the agent can only query connected sets, which aims at applications where connected query sets are favorable. Lastly, we design $hiePM$ by further limiting the query set to be the sets in noiseless bisection. Hence $hiePM$ not only enjoys a hierarchical query structure, but the query cardinality of $hiePM$ is small. These benefits make $hiePM$ suitable for applications such as beamforming in array processing that requires pre-construction and storage of the query sets. We demonstrate a low (computational and memory) complexity implementation of the three strategies, which shows a logarithmic improvement over search strategies in the literature of query-dependent noisy search. Furthermore, with the Extrinsic Jensen Shannon (EJS) Divergence, we provide a unified

asymptotic analysis (asymptotic in resolution and error probability) on the time complexity. In particular, we derive upper bounds on the expected search time with respect to the resolution and error probability of the final estimate of the target location. To our surprise, even though $dyaPM$ is designed under a connected query constraint, both $sortPM$ and $dyaPM$ achieves asymptotic optimality in time complexity whereas $hiePM$ is near-optimal in the asymptotic performance. Numerically, we show that all the proposed search strategies have superior non-asymptotic performance.

In Chapter 3, we demonstrate the application of the proposed $hiePM$ in the feedback coding problem (corresponding to query-independent noise). In particular, we consider the problem of bit-wise channel coding over a Binary Symmetric Channel (BSC) with feedback. While it is known that feedback does not increase the capacity of a memoryless channel, it is believed to simplify the coding schemes for some channels. The most significant one is the Binary Erasure Channel (BEC) where capacity is achieved by a simple sequential bit-wise repetition code under which each bit is (re-)transmitted until it is received. This sequential bit-wise feedback code has the added advantage that it can be used for streaming applications over BECs. In contrast, there is no known sequential bit-wise code with feedback that can achieve a non-zero transmission rate for a BSC. For example, under Posterior Matching for a binary input channel with feedback, also known as Horstein scheme, each message is considered in its entirety in a block coding manner. We apply $hiePM$ to this problem and proposes a sequential feedback coding scheme, $bitPM$, with a hierarchical bit-wise structure that generalizes repetition codes. This scheme is shown to achieve a strictly positive rate for a large class of binary input channels including a BSC with arbitrary cross-over probability $p \in (0, \frac{1}{2})$.

In Chapter 2, we demonstrate another application of $hiePM$ in Millimeter-wave (mmWave) communication. MmWave communication with large antenna arrays is a promising technique to enable extremely high data rates due to the large available bandwidth in mmWave frequency bands. Besides, given the knowledge of an optimal directional beamforming vector, large antenna

arrays have been shown to overcome both the severe signal attenuation in mmWave as well as the interference problem. However, fundamental limits on the achievable learning rate of an optimal beamforming vector remain. This chapter considers the problem of adaptive and sequential optimization of the beamforming vectors during the initial access phase of communication. With a single-path channel model, the problem is reduced to actively learning the Angle-of-Arrival (AoA) of the signal sent from the user to the Base Station (BS). We, therefore, propose to use $hiePM$ for designing sequential beamforming for estimating the AoA. For any given resolution and error probability of the estimated AoA, an upper bound on the expected search time of the proposed algorithm is derived via Extrinsic Jensen-Shannon Divergence. The upper bound demonstrates that the search time of the proposed algorithm asymptotically matches the performance of the noiseless bisection search up to a constant factor, in effect, characterizing the AoA acquisition rate. Furthermore, the upper bound shows that the acquired AoA error probability decays exponentially fast with the search time with an exponent that is a decreasing function of the acquisition rate. Numerically, the proposed algorithm is compared with prior work, where a significant improvement of the system communication rate is observed. Most notably, in the relevant regime of low (-10dB to $+5$dB) raw SNR, this establishes the first practically viable solution for initial access and, hence, the first demonstration of stand-alone mmWave communication.

Notations used in this dissertation are as follows. We use boldface letters to represent vectors. We write boldface $\mathbf{b}_{\mathcal{I}}$ to denote a vector of length $|\mathcal{I}|$ with elements from $\{b_i\}_{i\in\mathcal{I}}$. Similarly, we also write $\mathbf{b}_{1:l}$ to be a length l vector with elements being the first l elements in $\mathbf{b}$. We write $\mathbf{b}^{\downarrow}$ to denote sorted element of a vector $\mathbf{b}$ in descending order, $i.e.$, $b_i^{\downarrow}$ represents the ith largest element of $\mathbf{b}$. For a set of indices S, we write non-bold $b_S \equiv \sum_{i\in S} b_i$ to be the summation of all elements in $\mathbf{b}_S$. Similarly for a set collection $\mathcal{I} = \{I_1, I_2, ..., I_n\}$, we write $\mathbf{b}_{\mathcal{I}} = (b_{I_1}, b_{I_2}, ..., b_{I_n})$. We use $[x]$ to denote the integer closet to a real number x. We denote the space of probability mass functions on set $\mathcal{X}$ as $P(x)$. We denote the Kullback-Leibler

(KL) divergence between distribution P and Q by $D(P\|Q) = \sum_x P(x) \log \frac{P(x)}{Q(x)}$. The mutual information between random variable X and Y is defined as $I(X;Y) = \sum_{x,y} p(x,y) \log \frac{p(x,y)}{p(x)p(y)}$, where $p(x,y)$ is the joint distribution, and $p(x)$ and $p(y)$ are the marginals of X and Y. Let Bern(p) denote the Bernoulli distribution with parameter p, and $I(q,p)$ denote the mutual information of the input $X \sim$ Bern(q) and the output Y of a BSC channel with crossover probability p. Let $C_1(p) := D(\text{Bern}(p)\|\text{Bern}(1-p))$. Let $\mathbb{E}[\cdot]$ denote the expectation. We use $|S_t|$ to represent the counting measure of a discrete set S_t (cardinality of S_t). $\mathcal{CN}(\boldsymbol{\mu}, \boldsymbol{\Sigma})$ denotes multivariate complex Gaussian distribution and $\mathcal{CN}(\mathbf{x}; \boldsymbol{\mu}, \boldsymbol{\Sigma})$ with mean μ and covariance matrix $\boldsymbol{\Sigma}$. Rice(μ, σ^2) denotes and Rician distribution and Rice$(x; \mu, \sigma^2) := \frac{x}{\sigma^2} \exp\left(\frac{-(x^2+\mu^2)}{2\sigma^2}\right) J_0(\frac{x\mu}{\sigma^2})$ denotes its probability density function, where $J_0(\cdot)$ is the modified Bessel function of the first kind with order zero.

Chapter 2

Sequential Query-Dependent Noisy Search

In this chapter, we formulate the target localization problem. We proposed and analyzed three novel search strategies, sorted Posterior Matching ($sortPM$), dyadic Posterior Matching ($dyaPM$) and hierarchical Posterior Matching ($hiePM$).

2.1 Introduction

We consider a target search problem where at any given time, an agent can choose a query set to query for the presence of the target in that set. By the query, the agent receives a noisy measurement regarding the presence of the target in the set that the agent chooses. The agent conducts multiple queries where each query set is chosen adaptively and strategically based on previous (noisy) measurements. The main focus of this chapter is to design, analyze, and compare various search strategies under the setting of realistic noise models.

The problem of binary noisy search for a target with query-independent noise [1–7] have been studied extensively in the literature. Relying on connections with feedback coding, [2, 3] proposed a noisy variant of the binary search algorithm. For a general channel with feedback, [8] proposed a scheme, referred to as Posterior Matching, generalizing the noisy binary search

algorithm. In particular, [8] established the rate-optimality where the targeting rate is defined as the ratio of the logarithm of the search resolution over the number of queries. By allowing for random search time, [7] proposed two-phase schemes that achieve the optimal rate-reliability trade-off where reliability is defined to be the ratio of the logarithm of error probability over the (expected) number of queries.

In many applications of interest, such as spectrum sensing [9] in cognitive radio, AoA estimation in initial beam alignment (Chapter 4), and heavy hitter detection [10] in networking, the noise statistics of the observation is usually *query-dependent*. In particular, querying a larger size region is often prone to return a noisier measurement than querying a smaller region. With binary measurements and Bernoulli noise, for instance, this noise behavior means that the false alarm and miss detection of each query can be thought of a non-decreasing function of the size of the query set.

The problem of noisy search with query-dependent noise was first introduced in [6], where the author proposed a search strategy, maxEJS, that designs the query set by maximizing the Extrinsic Jensen Shannon (EJS) divergence (a function of the posterior) exhaustively over all possible query sets. However, the prohibitive complexity of the exhaustive maximization of EJS divergence renders maxEJS impractical in many applications. Furthermore, even though the functional EJS relates well to the sequential analysis, [6] fails to give tight asymptotic bounds for the expected search time.

By using the technique of random coding, [11] constructed a three-phase random search scheme (here we refer to as 3rand) and proved that the scheme achieves a tight upper and lower asymptotic bounds for the expected search time, which sets the fundamental limits and behavior of the query-dependent noise search problem. In particular, while it is known [12] that feedback (corresponds to adaptivity) does not increase capacity (corresponds to targeting rate) in channel coding problem (corresponds to query independent noise), adaptivity is shown to

[0]thus we will refer to the noisy variant of binary search algorithm as median Posterior Matching, medianPM

be essential [11] and can increase not only reliability but also the targeting rate compared with non-adaptive strategies. The strategy 3rand is, however, constructed primarily for asymptotic analytical/proof purposes. Indeed, non-asymptotically 3rand performs poorly and highly depends on the parameters that determine the transition between the three phases. Furthermore, the optimal estimator for 3rand is of high complexity (the same as the optimal decoder of random coding).

Motivated by practical applications such as initial beam alignment in array processing, heavy hitter detection in networking, and visual search in robotics, in this dissertation we study the problem of query-dependent noisy search with the following important metrics: *query time complexity*, *computational and memory complexity*, *query geometry (the shape of the query set)* and *query cardinality (cardinality of the collection of query sets that are allowed to be chosen from)*. We proposed three novel search strategies, sorted Posterior Matching ($sortPM$), dyadic Posterior Matching ($dyaPM$) and hierarchical Posterior Matching ($hiePM$), where each of which has its advantages in different applications. In particular, $sortPM$, by a sorting operation, greedily reduces the noise variance of each query, with the compromise of query geometry and query cardinality (by sorting, the chosen query set can be any measurable set). With minor sacrifice in the query noise, we design $dyaPM$ under the constraint that the agent can only query connected sets, which aims at applications where connected query sets are favorable. Lastly, we design $hiePM$ by further limiting the query set to be the sets in noiseless bisection. Hence $hiePM$ not only enjoys a hierarchical query structure, but the query cardinality of $hiePM$ is small. These benefits make $hiePM$ suitable for applications such as beamforming in array processing that requires pre-construction and storage of the possible query sets.

We demonstrate a low (computational and memory) complexity implementation of the three strategies, which shows an exponential improvement (logarithmic complexity) over search strategies in the literature of query-dependent noisy search (maxEJS and 3rand). Furthermore, with the Extrinsic Jensen Shannon (EJS) Divergence [13] , we provide a unified asymptotic analysis (asymptotic in resolution and error probability) on the time complexity. In particular, we

derive upper bounds on the expected search time with respect to the resolution and error probability of the final estimate of the target location. To our surprise: even though $dyaPM$ is designed under a connected query constraint, both $sortPM$ and $dyaPM$ achieves asymptotic optimality in query time complexity; whereas $hiePM$ is near-optimal in the asymptotic performance. Numerically, we show that all the proposed search strategies have superior non-asymptotic performance compared with that of 3rand. Notably, although $hiePM$ is asymptotically sub-optimal, its non-asymptotic performance in some regime is even better than that of $sortPM$ and $dyaPM$.

2.2 Problem Setup

We consider the problem of searching for a point target in the unit interval, where the target is uniformly placed on the unit interval. We wish to estimate the target position on the unit interval to a particular resolution $\frac{1}{\delta}$. In other words, the distance between the estimate and the actual target is smaller than or equal to δ. Given a target the resolution $\frac{1}{\delta}$ that is determined and fixed in advance, without loss of generality, we can discretize the problem by quantizing the area into δ sub-intervals before the search process begins.

We now formulate the problem with finite resolution $\frac{1}{\delta}$.More precisely, let us divide the unit interval $[0, 1]$ into $\frac{1}{\delta}$ sub-intervals (referred to as bins), where $\frac{1}{\delta}$, without loss of generality, is assumed to be an integer. Let θ be the index of the bin that contains the target. We wish to estimate θ by sequentially choosing (possible random) any query sets $S_t \subseteq \{1, 2, ..., \frac{1}{\delta}\}$. Let $X_t = \mathbb{1}(\theta \in S_t)$ denote the clean binary signal indicating whether the target is in the query set S_t. The agent obtains a corrupted version Y_t of X_t, with noise level that corresponds to the size of the query set $|S_t|$. Specifically, the agent obtains

$$Y_t = X_t \oplus Z_t(S_t) \tag{2.1}$$

where $\oplus$ denotes exclusive OR operation, and $Z_t(S_t)$ is the variable of Bernoulli noise where

its statistics depends on the query set S_t. In particular, we assume that $Z_t(S_t) \sim \text{Bern}(p(|S_t|))$ where $p : (0, 1) \to (0, \frac{1}{2})$ is a continuous and non-decreasing function.

After τ queries, the agent declares the target index $\hat{\theta}$. The search is said to have *resolution* $\frac{1}{\delta}$ and *reliability* ϵ if

$$\mathbb{P}(\mid \hat{\theta}_\tau \neq \theta \mid \leq \delta) \geq 1 - \epsilon. \tag{2.2}$$

A sequential query strategy consists of a *query function* γ that determines a sequence of the query sets S_t, $t = 1, 2, 3...$, a stopping time τ, and an estimator $\hat{\theta}_\tau$ of the index of the target position. The strategy γ is said to be *adaptive* if the choice of the query S_t is a random set measurable with respect to the sigma-filed generated by Y_1^{t-1}; otherwise, the strategy is said to be *non-adaptive*. The search is said to be fixed-length if τ is determined in advance and independently of observations Y_1^τ; otherwise, the search is said to be variable-length, $i.e.$ if τ is a random stopping time with respect to the sequence of observations $Y_1, Y_2, ...$ Finally, we consider the uniform Bayesian prior $\pi_i(0) = \mathbb{P}(\theta = i) = \delta$. It is sufficient for us to consider strategies that select the next query set $S_t \subseteq \{1, 2, ..., \frac{1}{\delta}\}$ based on the vector of posterior probability $\boldsymbol{\pi}(t)$ whose ith element is denoted by

$$\pi_i(t) = \mathbb{P}(\theta = i \mid Y_1^{t-1}), \quad i = 1, 2, ..., \frac{1}{\delta}. \tag{2.3}$$

In other word, the deterministic and adaptive strategy γ can be represented by the function:

$$\gamma : \Delta_\delta \to 2^{\{1,2,...,\frac{1}{\delta}\}} \tag{2.4}$$

where Δ_δ is the probability simplex of dimension $\frac{1}{\delta}$.

We characterize the performance of search strategies by the following:

i) *The Query Time Complexity*:

We are interested in search strategies that can find the target location accurately (with

resolution $\frac{1}{\delta}$) and reliability (with confidence $1-\epsilon$) as quickly as possible. We measure the asymptotic time complexity by how the expected number of queries $\tau_{\epsilon,\delta}$ scales with the resolution $\frac{1}{\delta}$ and the reliability ϵ.

ii) *The Computational and Memory Complexity*:

There are memory and computational requirements for computing the query set S_t at every query time t, as well as computing the final estimate $\hat{\theta}$. Specifically, adaptive selection of S_t requires updating the posterior vector. There is also the computation complexity associated with the mapping γ from $\boldsymbol{\pi}(t)$ to the next query set S_{t+1}.

iii) *The Query Geometry and the Query Cardinality*:

In many practical settings, the choice of the query set S_t cannot be arbitrary. Let $\mathcal{A} \subseteq \mathcal{S} \equiv 2^{\{1,2,...,\frac{1}{\delta}\}}$ be the set of allowable query sets, i.e. $S_t \in \mathcal{A}$. We evaluate the algorithms in terms of the geometric complexity of sets in $\mathcal{A}$. One possible interesting choice of $\mathcal{A}$, motivated by the visual search [6] and initial beam alignment (Chapter 4) applications, is when $\mathcal{A} = \mathcal{I} := \{\{i : a \leq i \leq b\} : 1 \leq a < b \leq \frac{1}{\delta}\}$, i.e. when the query sets are constrained to be contiguous intervals. In such case, we say that the search strategy is with a connected/contiguous query geometry. On the other hand, we define the query cardinality as the cardinality of $\mathcal{A}$. A smaller query cardinality is favorable for applications where the construction of the query set itself is non-trivial and a pre-construction with a codebook-based approach is preferable (e.g. the beam alignment problem in Chapter 4).

Note that by tracking the posterior vector $\boldsymbol{\pi}(t)$ of length $\frac{1}{\delta}$ with Bayes' rule, the computational and memory complexity are both at least of order $O(\frac{1}{\delta})$. Now, the connected query geometry of $\mathcal{I}$ offers an immediate reduction of computational and memory complexity in tracking the posterior. In particular, we have

Lemma 2.1. *For connected query geometry $S_n \in \mathcal{I} := \{\{i : a \leq i \leq b\} : 1 \leq a < b \leq \frac{1}{\delta}\}$, $n = 1, 2, ..., t$ with uniform prior $\pi_i(0) = \delta$ for all i, the posterior at time t can be written as a*

simple function with at most $2t+1$ *intervals. Specifically, there exist some* $\mathcal{I}^{(t)} = \{I_u^{(t)} : u = 1, 2, ..., 2t\} \subseteq \mathcal{I}$ *where* $I_u^{(t)}$ *are disjoint partitions* $\{1, 2, ..., \frac{1}{\delta}\} = \cup_{u=0}^{2t} I_u^{(t)}$ *such that*

$$\pi_i(t) = \sum_{u=0}^{2t} \frac{\pi_{I_u^{(t)}}}{|I_u^{(t)}|} \mathbb{1}_{I_u^{(t)}}(i). \tag{2.5}$$

Proof. (2.5) is true for $t = 0$ with uniform prior and $I_0 = \{1, 2, ..., \frac{1}{\delta}\}$. By Procedure 2.1 and Math Induction, we conclude the assertion. □

Procedure 2.1: Sequential Quantization and Bayes' Rule

Input: $(\boldsymbol{\pi}_{\mathcal{I}^{(t)}}(t), \mathcal{I}^{(t)}, S_{t+1}, Y_{t+1})$ where $S_{t+1} = \{i : s_1 \le i \le s_2\}$;

Output: $(\boldsymbol{\pi}_{\mathcal{I}^{(t+1)}}(t+1), \mathcal{I}^{(t+1)})$;

Find $I_{t_1}^{(t)}, I_{t_2}^{(t)}$ such that $s_1 \in I_{t_1}^{(t)}$ and $s_2 \in I_{t_2}^{(t)}$;

for $0 \le u < t_1$ **do**

  $I_u^{(t+1)} = I_u^{(t)}$, $\pi_{I_u^{(t+1)}}(t) = \pi_{I_u^{(t)}}(t)$;

$I_{t_1}^{(t+1)} = [\min I_{t_1}, s_1 - 1]$, $\pi_{I_{t_1}^{(t+1)}}(t) = \frac{|I_{t_1}^{(t+1)}|}{|I_{t_1}^{(t)}|} \pi_{I_{t_1}^{(t)}}(t)$;

$I_{t_1+1}^{(t+1)} = [s_1, \max I_{t_1}]$, $\pi_{I_{t_1+1}^{(t+1)}}(t) = \frac{|I_{t_1+1}^{(t+1)}|}{|I_{t_1}^{(t)}|} \pi_{I_{t_1}^{(t)}}(t)$;

for $t_1 + 2 \le u < t_2 + 1$ **do**

  $I_u^{(t+1)} = I_{u-1}^{(t)}$, $\pi_{I_u^{(t+1)}}(t) = \pi_{I_{u-1}^{(t)}}(t)$;

$I_{t_2+1}^{(t+1)} = [\min I_{t_2}, s_2 - 1]$, $\pi_{I_{t_2+1}^{(t+1)}}(t) = \frac{|I_{t_2+1}^{(t+1)}|}{|I_{t_2}^{(t)}|} \pi_{I_{t_2}^{(t)}}(t)$;

$I_{t_2+2}^{(t+1)} = [s_2, \max I_{t_2}]$, $\pi_{I_{t_2+2}^{(t+1)}}(t) = \frac{|I_{t_2+2}^{(t+1)}|}{|I_{t_2}^{(t)}|} \pi_{I_{t_2}^{(t)}}(t)$;

for $t_2 + 3 \le u <\le 2t + 2$ **do**

  $I_u^{(t+1)} = I_{u-2}^{(t)}$, $\pi_{I_u^{(t+1)}}(t) = \pi_{I_{u-2}^{(t)}}(t)$;

Bayes' rule:

$$\pi_{I_u^{(t+1)}}(t+1) = \frac{\pi_{I_u^{(t+1)}}(t)\, \mathbb{P}(Y_{t+1} \mid X_{t+1} = \mathbb{1}(t_1 + 1 \le u \le t_2 + 1))}{\sum_{u'=0}^{2t+2} \pi_{I_{u'}^{(t+1)}}(t)\, \mathbb{P}(Y_{t+1} \mid X_{t+1} = \mathbb{1}(\theta \in I_{u'}^{(t+1)}))} \tag{2.6}$$

By lemma 2.1 and procedure 2.1, we see that the complexity of tracking the posterior is of order $O(\tau)$ under the connected query geometry. Therefore, this benefit offers a logarithmic

Table 2.1: Comparisons between different search strategies and Main results

	Asym. # Query Rate: $\lim_\delta \frac{\log(1/\delta)}{\mathbb{E}[\tau_{\epsilon,\delta}]}$	Computation (each query)	Memory Complexity	Query Geom.	Query Card.
medianPM [2]	$I(\frac{1}{2}, p_{\max})$	$O(\log \frac{1}{\delta})$	$O(\log \frac{1}{\delta})$	conn.	$O(\frac{1}{\delta})$
maxEJS [6]	$I(\frac{1}{2}, p_{\min})$	$O(2^{\frac{1}{\delta}})$	$O(\frac{1}{\delta})$	disj.	$O(2^{\frac{1}{\delta}})$
3rand [11]	$I(\frac{1}{2}, p_{\min})$	$O(\frac{1}{\delta})$[1]	$O(\frac{1}{\delta})$	disj.	$O(2^{\frac{1}{\delta}})$
$sortPM$	$I(\frac{1}{2}, p_{\min})$ [Thm2.1]	$O(\frac{1}{\delta}\log\frac{1}{\delta})$ [2]	$O(\frac{1}{\delta})$	disj.	$O(2^{\frac{1}{\delta}})$
$dyaPM$	$I(\frac{1}{2}, p_{\min})$ [Thm2.3]	$O(\log \frac{1}{\delta})$	$O(\log \frac{1}{\delta})$	conn.	$O((\frac{1}{\delta})^2)$
$hiePM$	$I(\frac{1}{3}, p_{\min})$ [Thm2.2]	$O(\log \frac{1}{\delta})$	$O(\log \frac{1}{\delta})$	conn.	$O(\frac{1}{\delta})$

Optimal error exponent $\lim_\epsilon \frac{\log(1/\epsilon)}{\mathbb{E}[\tau_{\delta,\epsilon}]} = C_1(p[\delta])$ is achieved by most of these algorithm except medianPM where the error exponent is only of $I(\frac{1}{2}, p_{\max})$.

order of reduction for the computational and memory complexity from $O(\frac{1}{\delta})$ to $O(\log \frac{1}{\delta})$ (we will show that $\tau = O(\log(\frac{1}{\delta}))$ for all the proposed algorithms)

Lastly, we use the rate-reliability pair to capture the asymptotic query time complexity:

Definition 2.1. *A family of search strategies $\gamma_{\epsilon,\delta}$ with resolution $\frac{1}{\delta}$, reliability ϵ, and stopping time $\tau_{\epsilon,\delta}$ are said to achieve a maximum rate R and a maximum reliability E respectively if and only if*

$$R = \lim_{\delta\to 0} \frac{\log(\frac{1}{\delta})}{\mathbb{E}[\tau_{\epsilon,\delta}]}, \quad E = \lim_{\epsilon\to 0} \frac{\log(\frac{1}{\epsilon})}{\mathbb{E}[\tau_{\epsilon,\delta}]}. \tag{2.7}$$

2.3 Proposed Search Strategies and Main Results

In this section, we introduce three proposed search strategies: sorted Posterior Matching ($sortPM$), dyadic Posterior Matching ($dyaPM$), and hierarchical Posterior Matching ($hiePM$). We give a summary of our main results and complexity comparisons in Table 2.1

[1] we count the complexity of random search by the optimal decoder which requires a tracking of the posterior vector. It's possible to reach $O(poly(\log \frac{1}{\delta}))$ for both memory and computation by trading memory with computation via other codes rather than random coding

[2] By a more sophisticated implementation using sequential quantization, it is possible to implement $sortPM$ with both memory and computational complexity of order $O((\log \frac{1}{\delta})(\log\log \frac{1}{\delta}))$

2.3.1 Sorted Posterior Matching

First, we present sorted Posterior Matching ($sortPM$) [14] by the idea of sorting the posterior vector $\boldsymbol{\pi}(t)$ together with Posterior Matching [8]. In particular, we apply the $sortPM$ on the sorted posterior $\boldsymbol{\pi}^{\downarrow}(t)$. Let $k^* = \arg\min_k |\pi^{\downarrow}_{[1,k]}(t) - 1/2|$, under $sortPM$

$$S_{t+1} = \gamma_s(\boldsymbol{\pi}(t)) = \{i : \sigma_t(i) \in [1, k^*]\}, \tag{2.8}$$

is queried, where and σ_t is the corresponding sorting operation such that $\pi_i(t) \equiv \pi^{\downarrow}_{\sigma_t(i)}(t)$.

Algorithm 2.1: Sorted Posterior Matching

Input: resolution $\frac{1}{\delta}$, error probability ϵ, fixed stopping time n, *stopping-criterion*
Output: estimate of the target location $\hat{\theta}$ after τ queries
Initialization: $\pi_i(0) = \delta$ for all $i = 1, 2, ..., 1/\delta$,
for $t = 0, 1, ...$ **do**
    # Design the search region by sorted posterior

$$\begin{aligned} k^* &= \arg\min_k \ |\pi^{\downarrow}_{[1,k]}(t) - 1/2| \\ S_{t+1} &= \gamma_s(\boldsymbol{\pi}(t)) = \{i : \sigma_t(i) \in [1, k^*]\}, \end{aligned} \tag{2.9}$$

    # Take next measurement
    $Y_{t+1} = \mathbb{1}(\theta \in S_{t+1}) \oplus Z_{t+1}$
    # Posterior update by Bayes' Rule
    $\boldsymbol{\pi}(t+1) \leftarrow Y_{t+1}, \boldsymbol{\pi}(t)$
    # Stopping criteria
    case: stopping-criterion = fixed length (FL)
    if $t + 1 = n$ **then**
        break;
    case: stopping-criterion = variable length (VL)
    if $\max_i \pi_i(t+1) > 1 - \epsilon$ **then**
        break;
$\tau = t + 1$ (length of the search)
$\hat{\theta} = \arg\max_i \pi_i(\tau)$

Theorem 2.1. *The expected search time of $sortPM$ of achieving resolution $\delta > 0$ and reliability*

$0 < \epsilon < 1$ *can be upper bounded by*

$$E[\tau_{\epsilon,\delta}] \leq \frac{\log(1/\delta)}{I(1/2, p[\alpha])} + \frac{\log(1/\epsilon)}{C_1(p[\delta])} + o(\frac{1}{\delta\epsilon}), \tag{2.10}$$

for any fixed $\alpha > (e \log \frac{1}{\delta\epsilon})^{-K_s}$*, where* $K_s > 0$ *a constant defined in Lemma A.1.*

Remark 2.1. *By first taking* $\delta \to 0$ *and then* $\alpha \to 0$*, Theorem 2.1 together with the corresponding converse theorem [Theorem 1 in [6]] implies that* $sortPM$ *achieves the best possible acquisition rate* $I(1/2, p_{\min})$ *and the best reliability exponent* $C_1(p[\delta])$ *(by taking* $\epsilon \to 0$*).*

Remark 2.2. *Even though* $sortPM$*, as well as prior works such as* $maxEJS$ *[6] and 3-phase random search [11], are asymptotically optimum in time complexity under query-dependent noise, there's no constraint on the query set they choose. This unstructured query geometry prevents them from many applications where connected query set or other specific geometry is preferred (such as visual search [6]). Furthermore, the query cardinality of these algorithms are of a prohibitive order* $O(2^{\frac{1}{\delta}})$

2.3.2 Hierarchical Posterior Matching

Motivated by the need of the connected query geometry, here we proposed a novel low-complexity search strategy which we call Hierarchical Posterior Matching, $hiePM$. $HiePM$ utilizes the hierarchical query geometry that is used in the noiseless binary search. For the brevity of presentation, we assume that $\frac{1}{\delta} = 2^L$ for some $L > 0$. The hierarchical query geometry is therefore written as $\mathcal{H} = \{H_l^m : l = 0, 1, 2, ..., m = 0, 1, 2, ..., 2^l - 1\}$ where $H_l^m = \{m2^{L-l} + 1, m2^{L-l} + 2, ..., (m + 1)2^{L-l}\}$. This query geometry, as shown in Fig. 2.1, can be represented by a binary tree recursively by

$$H_l^m = H_{l+1}^{2m} \cup H_{l+1}^{2m+1}, \;\; l = 0, 1, 2, 3, ..., L. \tag{2.11}$$

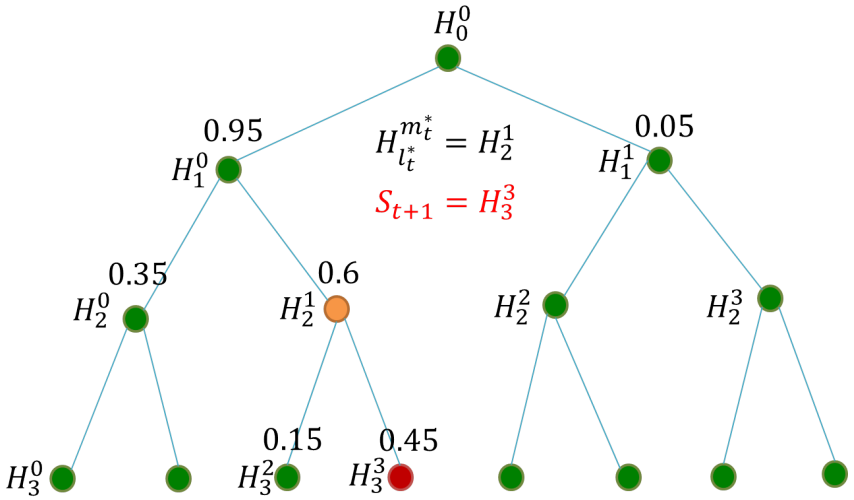

Figure 2.1: Binary search tree and the posterior for a given time t

Since $\mathcal{H} \subseteq \mathcal{I}$, $hiePM$ has a connected query geometry.

Now, $hiePM$ applies the Posterior Matching hierarchically along the binary tree as follows: let

$$\begin{aligned} l_t^* &= \arg\max_{l} \left\{ \max_{m} \pi_{H_l^m}(t) \geq \frac{1}{2} \right\}, \\ m_t^* &= \arg\max_{m} \ \pi_{H_{l_t^*}^m}(t), \end{aligned} \tag{2.12}$$

and the hierarchical half posterior matching with

$$(l_{t+1}, m_{t+1}) = \arg\min_{(l',m') \in \{(l_t^*, m_t^*), (l_t^*+1, 2m_t^*), (l_t^*+1, 2m_t^*+1)\}} \left| \pi_{H_{l'}^{m'}}(t) - \frac{1}{2} \right|, \tag{2.13}$$

$hiePM$ queries $S_{t+1} = H_{l_{t+1}}^{m_{t+1}}$ (The whole procedure of $hiePM$ is summarized in Algorithm 2.2).

Theorem 2.2. *The expected search time of $hiePM$ for achieving resolution $\delta > 0$ and reliability $0 < \epsilon < 1$ can be upper bounded by*

$$E[\tau_{\epsilon,\delta}] \leq \frac{\log(1/\delta)}{I(1/3, p[2^{-l}])} + \frac{\log(1/\epsilon)}{C_1(p[\delta])} + o(\frac{1}{\delta\epsilon}), \tag{2.15}$$

Algorithm 2.2: Hierarchical Posterior Matching

Input: resolution $\frac{1}{\delta} = 2^L$, error probability ϵ, fixed stopping time n, *stopping-criterion*

Output: estimate of the target location $\hat{\theta}$ after τ queries

Initialization: $\boldsymbol{\pi}_{\mathcal{I}^{(0)}}(0) = 1, \mathcal{I}^{(0)} = \{(1, 2, ..., 2^L)\}$

for $t = 1, 2, ...$ **do**

$l_t^* = \arg\max_l \left\{\max_m \pi_{H_l^m}(t) \geq \frac{1}{2}\right\}$;

$m_t^* = \arg\max_m \pi_{H_{l_t^*}^m}(t)$;

Match half posterior along the hierarchy l

$$(l_{t+1}, m_{t+1}) = \underset{(l',m')\in\{(l_t^*,m_t^*),(l_t^*+1,2m_t^*),(l_t^*+1,2m_t^*+1)\}}{\arg\min} \left|\pi_{H_{l'}^{m'}}(t) - \frac{1}{2}\right|; \quad (2.14)$$

$S_{t+1} = H_{l_{t+1}}^{m_{t+1}}$;

Take next measurement

$Y_{t+1} = \mathbb{1}(\theta \in S_{t+1}) \oplus Z_{t+1}$

Posterior update by Bayes' Rule (Procedure 2.1)

$(\boldsymbol{\pi}_{\mathcal{I}^{(t+1)}}(t+1), \mathcal{I}^{(t+1)}) \leftarrow (\boldsymbol{\pi}_{\mathcal{I}^{(t)}}(t), \mathcal{I}^{(t)}, S_{t+1}, Y_{t+1})$;

Stopping criteria

case: stopping-criterion = fixed length (FL)

if $t + 1 = n$ **then**

break;

case: stopping-criterion = variable length (VL)

if $\max_i \pi_i(t+1) > 1 - \epsilon$ **then**

break;

$\tau = t + 1$ (length of the search)

$\hat{\theta} = \arg\max_i \pi_i(\tau)$

for any fixed $l > 0$ such that $2^{-l} > (e \log \frac{1}{\delta\epsilon})^{-K_h}$, where $K_h > 0$ is a constant defined in Lemma A.3.

Remark 2.3. *As shown in Algorithm 2.2, both the computational and memory complexity are dominated by tracking the posterior representation $\boldsymbol{\pi}_{\mathcal{I}^{(t)}}, \mathcal{I}^{(t)}$ in Procedure 2.1. By Theorem 2.2 we know that the computational and memory complexity is of order $O(\log \frac{1}{\delta})$.*

Remark 2.4. *The hierarchical query geometry $\mathcal{H}$ not only is connected but also is of a hierarchical structure, which is suitable for the applications such as heavy hitter detection in*

networking [10] (monitoring pre-fix IP addresses) and bit-wise coding (Chapter 3). Furthermore, the query cardinality is only $|\mathcal{H}| = O(\frac{1}{\delta})$, rendering $hiePM$ a great candidate for beamforming applications as we will see in Chapter 4.

Remark 2.5. *Taking $\epsilon \to 0$, we see that $hiePM$ achieves the best possible error exponent $C_1(p\min)$. However, the achievable acquisition rate of $hiePM$ by Theorem 2.2, is only $I(1/3, p_{\min}) < I(1/2, p_{\min})$. It remains an open problem of the best achievable acquisition rate when we restrict the query area S_{t+1} to be hierarchical intervals. In the case of measurement independent noise ($p[x] \equiv p$), the simulation study in Chapter 3 suggests that $hiePM$ achieves an acquisition rate that is very close but is strictly less than the optimal rate $I(1/2, p)$.*

2.3.3 Dyadic Posterior Matching

By using the hierarchical query $\mathcal{H}$, $hiePM$ gives a solution that allows for constraints on the connectedness of query geometry. However, we do see that $hiePM$ loses the asymptotic optimality in time complexity. In this subsection, we proposed another low-complexity search strategy which we call dyadic Posterior Matching, $dyaPM$.

By the same procedure as in $hiePM$, $dyaPM$ first finds the smallest binary interval that contains more than half posterior, i.e. $H_{l_t^*}^{m_t^*} = \{m_t^* 2^{L-l_t^*} + 1, m_t^* 2^{L-l_t^*} + 2, ..., (m_t^* + 1)2^{L-l_t^*}\}$ as in equation (2.12). The $dyaPM$ algorithm then applies the Posterior Matching within $H_{l_t^*}^{m_t^*}$ by

$$S_{t+1} = [m_t^* 2^{L-l_t^*} + 1, k^*] \tag{2.16}$$

where $k^* = \arg\min_k |\pi_{[m_t^* 2^{L-l_t^*}+1,k]}(t) - 1/2|$ (The whole procedure of $dyaPM$ is summarized in Algorithm 2.3).

Theorem 2.3. *The expected search time of $dyaPM$ of achieving resolution $1/\delta$ and reliability*

Algorithm 2.3: Dyadic Posterior Matching

Input: resolution $\frac{1}{\delta}$, error probability ϵ, fixed stopping time n, *stopping-criterion*
Output: estimate of the target location $\hat{\theta}$ after τ queries
Initialization: $\boldsymbol{\pi}_{\mathcal{I}^{(0)}}(0) = 1, \mathcal{I}^{(0)} = \{(1, 2, ..., 2^L)\}$
for $t = 1, 2, ...$ **do**
    $l_t^* = \arg\max_l \left\{\max_m \pi_{H_l^m}(t) \geq \frac{1}{2}\right\}$;
    $m_t^* = \arg\max_m \pi_{H_{l_t^*}^m}(t)$;
    $k^* = \arg\min_k |\pi_{[m_t^* 2^{L-l_t^*}+1,k]}(t) - 1/2|$;
    $S_{t+1} = [m_t^* 2^{L-l_t^*} + 1, k^*]$;
    # Take next measurement
    $Y_{t+1} = \mathbb{1}(\theta \in S_{t+1}) \oplus Z_{t+1}$
    # Posterior update by Bayes' Rule (Procedure 2.1)
    $(\boldsymbol{\pi}_{\mathcal{I}^{(t+1)}}(t+1), \mathcal{I}^{(t+1)}) \leftarrow (\boldsymbol{\pi}_{\mathcal{I}^{(t)}}(t), \mathcal{I}^{(t)}, S_{t+1}, Y_{t+1})$;
    # Stopping criteria
    case: stopping-criterion = fixed length (FL)
    if $t + 1 = n$ **then**
        break;
    case: stopping-criterion = variable length (VL)
    if $\max_i \pi_i(t+1) > 1 - \epsilon$ **then**
        break;
$\tau = t + 1$ (length of the search)
$\hat{\theta} = \arg\max_i \pi_i(\tau)$

$0 < \epsilon < 1$, *can be upper bounded by*

$$E[\tau_{\epsilon,\delta}] \leq \frac{\log(1/\delta)}{I(1/2, p[2^{-l}])} + \frac{\log(1/\epsilon)}{C_1(p[\delta])} + o(\frac{1}{\delta\epsilon}), \tag{2.17}$$

for any fixed $l > 0$ *such that* $2^{-l} > (e \log \frac{1}{\delta\epsilon})^{-K_d}$, *where* $K_d > 0$ *a constant defined in Lemma A.2.*

Remark 2.6. *By taking* $\delta \to 0$ *and then* $l \to \infty$, *we conclude that* $dyaPM$ *achieves the best possible acquisition rate* $I(1/2, p_{\min})$. *And by taking* $\epsilon \to 0$, $dyaPM$ *achieves the best reliability exponent* $C_1(\delta)$. *To the best of our knowledge,* $dyaPM$ *is the first and the only known algorithm with connected query geometry that achieves asymptotic optimality under query-dependent noise*

Remark 2.7. *As shown in Algorithm 2.3, both the computational and memory complexity are again dominated by tracking the posterior representation* $\boldsymbol{\pi}_{\mathcal{I}^{(t)}}, \mathcal{I}^{(t)}$ *in Procedure 2.1. By Theorem 2.3 we know that the computational and memory complexity of* $dyaPM$ *is of order* $O(\log \frac{1}{\delta})$.

2.3.4 Asymptotic Results

To illustrate the asymptotic results from Theorem 2.1-2.3, here we present the achievable rate-reliability (R, E) pair from Definition 2.1. As an example, we use the noise profile $p[x] = 0.1 + 0.5x$ and obtain the rate-reliability region In Fig. 2.2, where we have $p_{\min} = 0.1$, $p_{\max} = p[\frac{1}{2}] = 0.35$. By Theorem 2.1-2.3, any (R, E) pairs below the corresponding curves are achievable by the corresponding algorithm. In fact, further by the converse theorem from [Theorem 1 in [6]], we have the converse: any (R, E) pair above the blue line is not achievable by any algorithm.

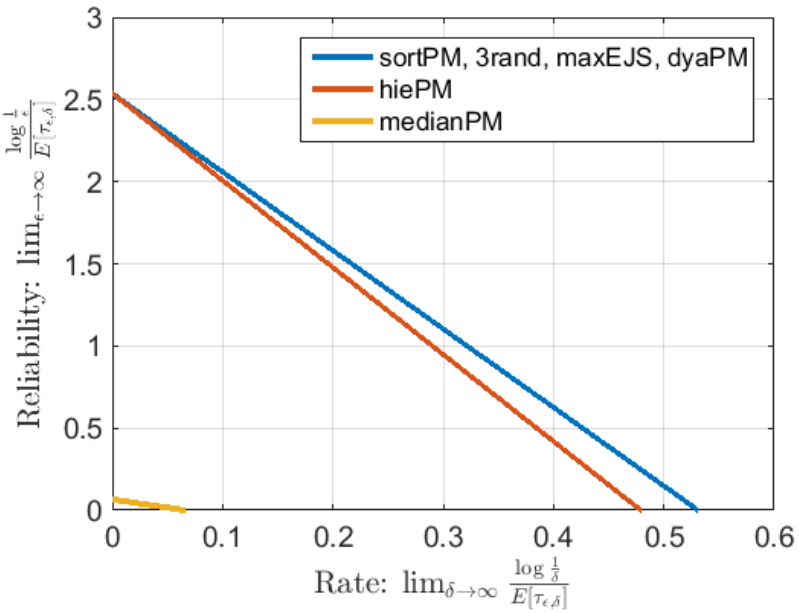

Figure 2.2: Achievable rate-reliability region
The noise profile is set to be $p[x] = 0.1 + 0.5x$, which means $p_{\min} = 0.1$, $p_{\max} = p[\frac{1}{2}] = 0.35$.

2.4 Numerical Examples

In this section, we give numerical comparisons amongst various algorithms. We study the error probability versus the number of queries at a fixed resolution. We compare all the algorithms under query-dependent Bernoulli noise where $p[\delta|S|]$ is linearly increasing in $|S|$. For applications of our algorithm under different noise profiles as well as non-Bernoulli noise, we refer readers to Chapter 4. The proposed algorithms sortPM, dyaPM, and hiePM are as described in Sec. 2.3. The median binary search from [2, 8] is denoted as medianPM. The 3 phase random search from [11] is denoted as 3rand. We use algorithm-VL to represent the variable length termination of the algorithm where the number of queries is reported in its expectation value. Likewise, we use algorithm-FL to represent the fixed length termination of the algorithm.

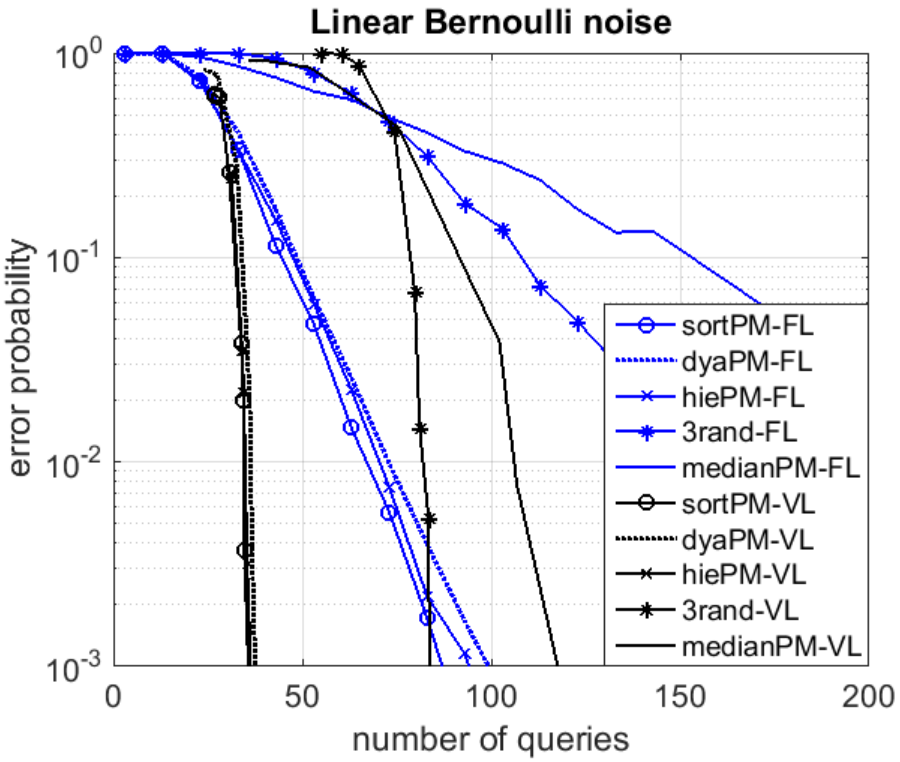

Figure 2.3: Error probability vs. number of queries: linear noise case
We set resolution $\frac{1}{\delta} = 2^{15}$ and Bernoulli noise with linear flipping probability $p[\delta|S|] = 0.1 + \delta|S|/2$

As we see in Fig. 2.3, the proposed algorithms $sortPM$, $dyaPM$, and $hiePM$ enjoys

the optimal error exponent $C_1(p[\delta])$ with variable length (VL) operation for both measurement independent and query-dependent noise, as predicted by Theorem 2.1, 2.3, and 2.2. Notably, even with the restriction of contiguous query area, $dyaPM$ and $hiePM$ perform almost the same as $sortPM$ both asymptotically and non-asymptotically in reliability. As we expect, the medianPMfails in generalization to query-dependent noise (Fig. 2.3). On the other hand, while 3rand is also asymptotically optimal in reliability with VL operation, we see that there is an obvious non-asymptotic performance gap compared with our proposed algorithms. We also summarized the performance of each of the algorithms with fixed length (FL) operation. While the full characterizations of FL error exponent with respect to the noise profile $p[\cdot]$ is still an open problem, here by the superior numerical performance of the proposed algorithms, we can conclude the applicability of the proposed algorithms under different settings.

(Note that for 3rand, we modified and enhanced the algorithm from [11] by tracking and using the posterior to determine the phase transition. In particular, in phase-1 coarse search, we chop the area into 8 coarse bins and randomly choose 4 out of 8 as a query area for each query. If one of the coarse bin accumulates more than $1-\epsilon_1 = 0.99$, then the process switches to phase-2 where half of the fine resolution bins $(1/\delta)$ within the $1-\epsilon_1$ coarse bin is randomly selected as query area. If the posterior of the coarse bin from phase-1 decreases under $1-\epsilon_1$ during phase-2, then the process switches back to phase-1. If otherwise during the phase-2 random search, one of the fine resolution $(1/\delta)$ accumulates more than $1-\epsilon_2 = 0.5$, then the process switches to phase-3 confirmation phase where only the $1-\epsilon_2$ fine bin is selected as query area. If the fine bin posterior drops under $1-\epsilon_2$ during phase-3 confirmation, then the process switches back to phase-2 random search (as opposed to [11] where the whole process is started over if the confirmation phase gives a NACK decision). This modification of a sequential 3rand allows us to run the 3rand algorithm with both fixed length and variable length.)

2.5 Discussion: Finite Resolution vs. Variable Resolution

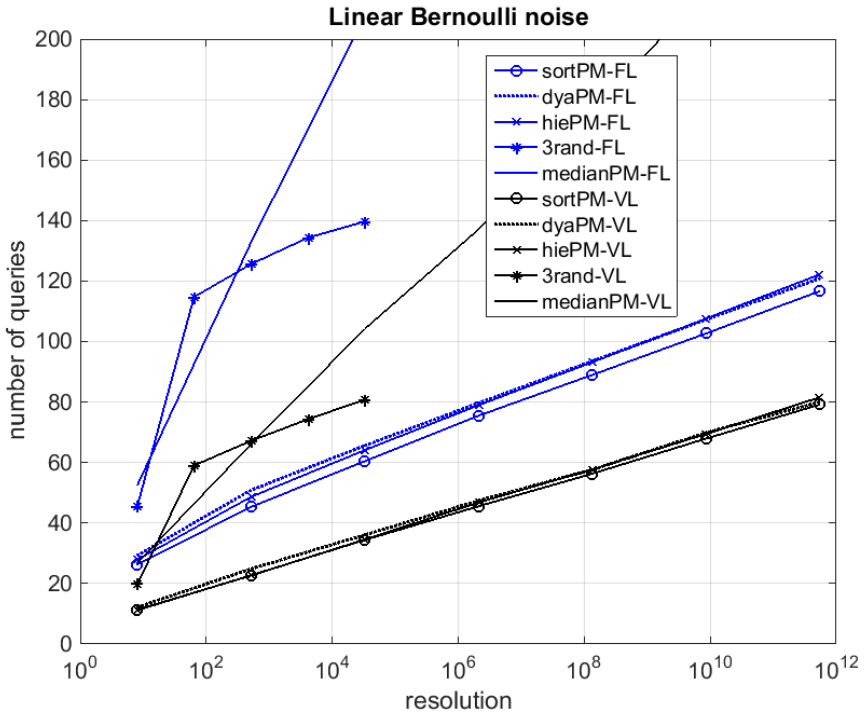

Figure 2.4: Resolution vs. Number of Queries: linear noise case
We set error probability $\epsilon = 0.02$ and Bernoulli noise with linear flipping probability $p[\delta|S|] = 0.1 + \delta|S|/2$

For pre-determined and fixed finite resolution $\frac{1}{\delta}$, the logarithmic scaling between resolution and (expected) number of queries is predicted by Theorem 2.1-2.3 and verified by simulation in Fig. 2.4. However, We note that although we formulate the search problem with finite and pre-determined resolution $\frac{1}{\delta}$, the original search problem operates on a continuous area (interval $[0, 1]$). Indeed, our proposed algorithms $dyaPM$ and $hiePM$ are free of pre-quantization and can operate on the continuous area with a natural sequential quantization-refinement which allows a variable resolution. For better comparison, in this chapter, we discuss under pre-quantization and focus on the fixed resolution case. We refer readers to Chapter 4 for an application of the proposed algorithm operating with a variable resolution that is sequentially determined. Furthermore, we also note that while we focus on binary noise in this chapter for the brevity of presentation, our

framework can be modified to deal with various forms of noise corruption by adapting the Bayes' rule accordingly (see Chapter 4 Sec. 4.3.4 for examples).

2.6 Appendix: query-independent noise

Here for reference, we append the performance of the algorithms under query-independent noise, which can be seen as a special case of query-dependent noise with $p[x] \equiv p_0$ for all x. In Fig. 2.5, we observe minor variations in the error probability between the proposed algorithms and medianPM, and a non-asymptotic gap of 3rand. See Chapter 3 for an application of the proposed algorithm $hiePM$ to the case of query-independent noise in the feedback coding problem.

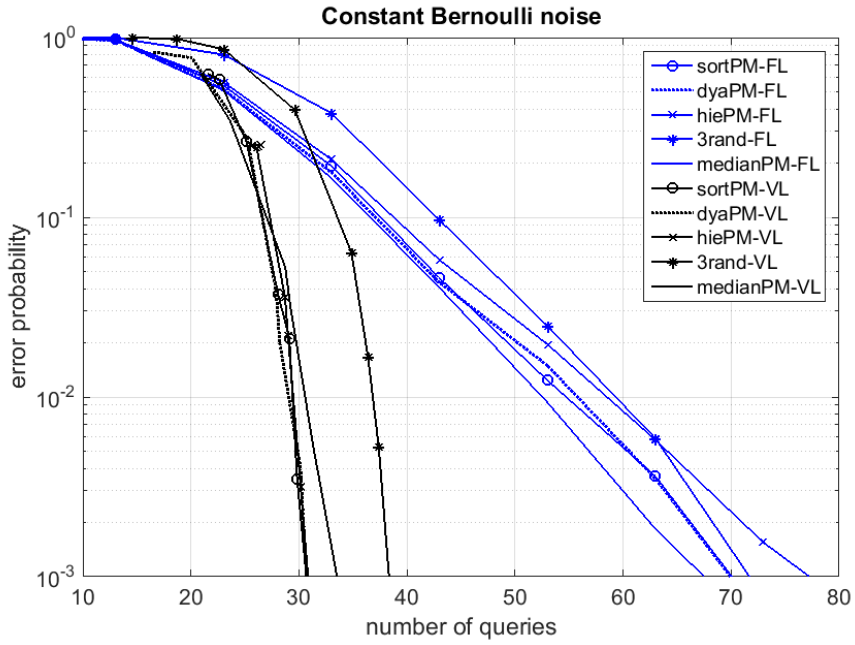

Figure 2.5: Error probability vs. number of queries: constant noise case
We set resolution $\frac{1}{\delta} = 2^{15}$ and Bernoulli noise with constant flipping probability $p[\delta|S|] = 0.1$

Chapter 2, in part, is a reprint of the material as it appears in the paper: Sung-En Chiu and Tara Javidi. "Sequential Measurement-Dependent Noisy Search." 2016 IEEE Information Theory Workshop (ITW). IEEE, 2016. The dissertation author was the primary investigator and author of

this paper.

Chapter 2, in full, is currently being prepared for submission for publication as Sung-En Chiu and Tara Javidi, ”Query-Dependent Noisy Search.” The dissertation author was the primary investigator and author of this material.

Chapter 3

Bit-wise Sequential Coding with Feedback

Even though $hiePM$ is developed for query-dependent noise in Chapter 2, we demonstrate the application of $hiePM$ in the feedback coding problem (corresponding to query-independent noise). We apply $hiePM$ to the feedback coding problem and proposes a sequential feedback coding scheme, $bitPM$, with a hierarchical bit-wise structure that generalizes repetition codes. This scheme is shown to achieve a strictly positive rate for a large class of binary input channels including a BSC with arbitrary cross-over probability $p \in (0, \frac{1}{2})$.

3.1 Introduction

Consider the problem of transmitting information over a noisy channel in the presence of perfect output feedback, i.e., the transmitter has a perfect observation of the received signal. While it is known that the presence of the feedback does not increase the capacity of a memoryless channel [12], one hopes to utilize the feedback to simplify the encoding scheme significantly. This folk belief that feedback can simplify the encoding is based on the construction of the optimal code for the Binary Erasure Channel (BEC) with perfect output feedback. More specifically, the simple sequential scheme that sends the message bit-by-bit via persistent retransmission of bits achieves the optimal transmission rate–reliability trade-off for a BEC.

Unfortunately and counter-intuitively, similar simple bit-wise sequential codes that achieve a positive rate of transmission over other noisy channels remain. For instance, the transmission rate of the noisy variant of the bit-by-bit repetition code over a Binary Symmetric Channel (BSC) is strictly zero for all values of crossover probability $p \in (0, \frac{1}{2})$. Conversely, no known capacity-achieving feedback code has a bit-wise sequential structure. For example, under Posterior Matching, each message is considered in its entirety in a block coding manner. To the best of our knowledge, the only sequential bit-wise feedback code over BSCs has been considered by Simsek et. al. in [15]. However, the analysis in [15] only applies to BSCs where the crossover probability is extremely small.

In this chapter, we provide the first sequential feedback code with a bit-wise nested structure that generalizes the simple repetition codes. By using the Extrinsic Jensen Shannon (EJS) divergence, this scheme is shown to achieve a strictly positive rate for a BSC with arbitrary crossover probability $p \in (0, \frac{1}{2})$. We also show that this result can be generalized to a large class of binary input channels.

3.2 Problem Setup

A Binary Symmetric Channel (BSC) with cross-over probability $p \in (0, \frac{1}{2})$ has the following channel transition probabilities when an input symbol $x \in \{0, 1\}$ is transmitted:

$$p(y|x) = \begin{cases} 1-p, & y = x, \\ p, & y \neq x. \end{cases} \tag{3.1}$$

A transmitter wishes to send a source message with bit representation $\mathbf{b}_{1:n}$ of length n where each bit is independently and identically distributed ($i.i.d.$) with distribution $B(\frac{1}{2})$. At time t, we assume that the causal noiseless feedback of past channel outputs $\mathbf{y}_{1:t-1}$ is available at the transmitter. A channel coding scheme consists of a sequence of encoders with feedback given

by the functions $e_{n,t} : \{0,1\}^n \times \{0,1\}^{t-1} \to \{0,1\}$ which maps the n source bits given the past observation $\mathbf{y}_{1:t-1}$ to the channel input x_t as follows

$$x_t = e_{n,t}(\mathbf{b}_{1:n}, \mathbf{y}_{1:t-1}). \tag{3.2}$$

After observing τ (possibly random) number of channel outputs $\mathbf{y}_{1:\tau}$, the receiver guesses the n source bits as

$$\hat{\mathbf{b}}_{1:n} = d_{n,\tau}(\mathbf{y}_{1:\tau}) \tag{3.3}$$

where $d_{n,\tau}$ is the decoding function. After τ channel uses, the probability of error of the coding scheme is defined as

$$p_e(\tau) := \mathbb{P}(d_{n,\tau}(\mathbf{y}_{1:\tau}) \neq \mathbf{b}_{1:n}). \tag{3.4}$$

A variable length channel coding scheme $\gamma_{n,\epsilon}$ that transmits n bits consists of a sequence of encoding functions and a decoding functions $(e_{n,t}, d_{n,t})$ for $t \leq \tau_{n,\epsilon}$ where $\tau_{n,\epsilon}$ is a stopping rule such that $P_e(\tau_{n,\epsilon}) \leq \epsilon$ for a given target error probability $\epsilon \in (0,1)$. A rate R is said to be achievable by a variable length channel coding scheme γ if for all $\epsilon \in (0,1)$ there exists a sequence of schemes $\gamma_{n,\epsilon}$ for $n \geq 1$ such that

$$\lim_{n\to\infty} \frac{n}{\mathbb{E}[\tau_{n,\epsilon}]} \geq R. \tag{3.5}$$

Furthermore, we say that this scheme achieves rate–reliability pair (R, E) if there exists a sequence of schemes $\gamma_{n,\epsilon}$ for $n \geq 1$ such that

$$\lim_{n\to\infty} \frac{n}{\mathbb{E}[\tau_{n,\epsilon}]} \geq R, \quad \text{and} \quad \lim_{n\to\infty} \frac{\log(1/\epsilon)}{\mathbb{E}[\tau_{n,\epsilon}]} \geq E. \tag{3.6}$$

Fact 3.1. *No coding scheme can achieve diminishing error probability at rates higher than $C(p)$.*

Furthermore, no coding scheme can achieve positive rate–reliability pair (R, E) *unless*

$$E \leq C_1(p)\left(1 - \frac{R}{C(p)}\right),\ R \in (0, C(p)). \tag{3.7}$$

Fact 3.2 ([13])**.** *The expected stopping time of a variable length coding scheme* $\gamma_{n,\epsilon}$ *which transmits an* n *bit message such that* $P_e \leq \epsilon$ *for some positive* $\epsilon > 0$*, satisfies the following*

$$\mathbb{E}[\tau_{n,\epsilon}] \leq \left(\frac{n}{R^{\gamma_{n,\epsilon}}} + \frac{\log \frac{1}{\epsilon}}{E^{\gamma_{n,\epsilon}}}\right)(1 + o(1)) \tag{3.8}$$

for some positive values $E^{\gamma_{n,\epsilon}}$ *and* $R^{\gamma_{n,\epsilon}}$*. Then, the scheme* $\gamma_{n,\epsilon}$ *can achieve any rate* $R \in [0, R^{\gamma_{n,\epsilon}}]$ *with error exponent* E*, if it satisfies the following*

$$E \leq E^{\gamma_{n,\epsilon}}\left(1 - \frac{R}{R^{\gamma_{n,\epsilon}}}\right). \tag{3.9}$$

3.2.1 Bit-wise Coding

In this section, we provide a general class of encoding scheme with a specific structure. This family of encoding schemes relies on three sets of variables which indicate the state of the decoder. At time t and after receiving $\mathbf{y}_{1:t}$, let l_t be the number of bits decoded by the decoder at time t and $\hat{b}_{1:l_t}(t)$ be the decoder's estimate of these bits; let $\mathcal{I}_t \subseteq \{1, 2, ..., l_t\}$ be the index of the bits that decoder would like to receive confirmation on; finally, let $m_{t+1} \in \{\text{nt}, \text{cm}\}$ be the agreed-upon state between encoder and decoder regarding the nature of the transmitted bit after their shared observation $\mathbf{y}_{1:t}$. In particular, $m_{t+1} = \text{nt}$ indicates the next transmission to be a new bit b_{l_t+1} while $m_{t+1} = \text{cm}$ represents a confirmation on $\mathbf{b}_{\mathcal{I}_t} = \hat{\mathbf{b}}_{\mathcal{I}_t}$. Now given these four agreed-upon variables (as a function of $\mathbf{y}_{1:t}$ which is shared by both encoder and decoder), the

encoding scheme can be written as

$$x_{t+1} = \begin{cases} b_{l_t+1} & \text{, if } m_{t+1} = \text{nt}, \\ \mathbb{1}(\mathbf{b}_{\mathcal{I}_t} = \hat{\mathbf{b}}_{\mathcal{I}_t}(t)) & \text{, if } m_{t+1} = \text{cm}. \end{cases} \tag{3.10}$$

3.2.2 Prior work

In this subsection, we detail, to the best of our knowledge, the only known bit-wise schemes and show that they can be viewed as a special case in our family of encoding schemes.

Repetition coding: When $\mathcal{I}_t = \{l_t\}$ for all t and while using an ACK/NACK feedback, the bit-wise encoder given by (3.10) reduces to a simple repetition code where the number of outputs l_t and the next state m_{t+1} are determined as

$$(l_t, m_{t+1}) = \begin{cases} (l_{t-1} + 1, \text{nt}) & \text{if ACK of } b_{l_{t-1}}, \\ (l_{t-1}, \text{cm}) & \text{if NACK of } b_{l_{t-1}}, \end{cases} \tag{3.11}$$

where ACK of $b_{l_{t-1}}$ implies that the decoder can decode the bit $b_{l_{t-1}}$ with sufficient confidence (for instance when the probability of error in decoding the bit $b_{l_{t-1}}$ is at most ϵ for some $\epsilon \in (0, 1)$) and NACK of $b_{l_{t-1}}$ implies that decoder needs more information to decode the bit. While such a repetition code with feedback achieves capacity over BEC, this choice of $\mathcal{I}_t = \{l_t\}$ operates at zero rate over BSC with any crossover probability $p \in (0, \frac{1}{2})$.

Simsek bit-wise coding: Other than the simple repetition codes, to the best of our knowledge, [15] by Simsek et al. is the only other prior work that is of the bit-wise coding structure. The authors in [15] used their coding scheme to keep the estimation error bounded in a dynamical system with noisy observations (BSC). Their coding scheme chooses the confirmation

index set $\mathcal{I}_t = \{1, 2, ..., l_t\}$ such that

$$x_{t+1} = \begin{cases} b_{l_t+1} & , \text{if } m_{t+1} = \text{nt}, \\ \mathbb{1}(\mathbf{b}_{1:l_t} = \hat{\mathbf{b}}_{1:l_t}(t)) & , \text{if } m_{t+1} = \text{cm}, \end{cases} \tag{3.12}$$

where the decoder output $\hat{\mathbf{b}}_{1:l_t}(t)$ remains the same during confirmation and is updated for every new transmission, i.e.

$$\hat{b}_{l_t}(t) = \begin{cases} \hat{b}_{l_t}(t-1) & , \text{if } m_t = \text{cm} \\ y_t & , \text{if } m_t = \text{nt} \end{cases}. \tag{3.13}$$

The evolution to the next state m_{t+1} and the bit index l_t is determined by previous state m_t and the observation y_t. At time t after a new transmission (i.e., $m_t = \text{nt}$) of the $(l_{t-1}+1)^{th}$ bit, the decoder updates $(l_{t-1}+1)^{th}$ bit with y_t as given by (3.13). The coding scheme then switches to confirmation state (i.e., $m_{t+1} = \text{cm}$) confirming on all the bits of decoder's output $(1 : l_t)$. If at time t after a confirmation (i.e., $m_t = \text{nt}$) of the l_{t-1} bits, if $y_t = 0$ then the encoder/decoder discard one bit ($l_t = l_{t-1} - 1$) and confirm on $(1 : l_{t-1} - 1)$ bits. However, if $y_t = 1$ the coding scheme switches to new transmission as long as $l_{t-1} < n$. More precisely, the number of output bits l_t and the next state m_{t+1} evolve as

$$(l_t, m_{t+1}) = \begin{cases} (l_{t-1}+1, \text{cm}) & , m_t = \text{nt} \\ (l_{t-1}-1, \text{cm}) & , m_t = \text{cm}, y_t = 0, l_{t-1} > 1 \\ (l_{t-1}, \text{cm}) & , m_t = \text{cm}, y_t = 0, l_{t-1} = 1 \\ (l_{t-1}, \text{nt}) & , m_t = \text{cm}, y_t = 1, l_{t-1} < n \\ (l_{t-1}, \text{cm}) & , m_t = \text{cm}, y_t = 1, l_{t-1} = n \end{cases} \tag{3.14}$$

for $t \geq 1$ with initial state $(l_0, m_1) = (0, \text{nt})$.

This bit-wise transmission-confirmation scheme from [15] is shown to be able to stabilize

the estimation error with channel BSC for cross over probabilities in a small set given by $p < 0.05$. However, the analysis of achievable rates for this scheme for a communication problem with a variable length decoding time remains.

3.3 Main Results

3.3.1 Bit-wise Posterior Matching

In this section, we propose a special case of the family of encoding schemes represented by (3.10). We call the proposed scheme bit-wise Posterior Matching, denoted by bitPM, where here the state m_{t+1}, the number of the bits l_t output by the decoder, decoder's estimate $\hat{\mathbf{b}}_{1:l_t}(t)$, and the confirmation set $\mathcal{I}_t$, are chosen as a deterministic function of the posterior:

$$\pi_{\mathbf{b}'}(t) := \mathbb{P}(\mathbf{b} = \mathbf{b}' \mid \mathbf{y}_{1:t}). \tag{3.15}$$

In particular, let us consider the l_{th} bit sequential MAP decoder and the l bit resolution posterior

$$\hat{b}_l(t) = \max_{b=0,1} \pi^{\{1:l\}}_{(\hat{b}_{1:l-1}(t)\ b)}(t),\ l = 1, 2, ..., n, \tag{3.16}$$

$$\pi^l_{\mathbf{b}'}(t) := \mathbb{P}(\mathbf{b}_{1:l} = \mathbf{b}' \mid \mathbf{y}_{1:t}). \tag{3.17}$$

Now let us compute the posterior-matched resolution l^* as

$$l^*_t := \arg\min_l \left| \pi^*_{\hat{b}_{1:l}}(t) - \frac{1}{2} \right|. \tag{3.18}$$

We are now ready to provide the update rule for m_t, l_t, and $\mathcal{I}_t$:

$$(l_{t+1}, m_{t+1}) = \begin{cases} (l_t + 1, \text{nt}), & l_t^* > l_t \\ (l_t, \text{cm}), & l_t^* \leq l_t \text{ or } l_t = n \end{cases} \tag{3.19}$$

and $\mathcal{I}_t = \{1, 2, ..., l_t^*\}$. In other words, the decoder will use the posterior to find the optimal confirmation $1 : l_t^*$ (closet to Bern($\frac{1}{2}$). And if those $1 : l_t^*$ bits has all been transmitted before ($l_t^* \leq l_t$), the decoder asks the encoder to do confirmation on those $1 : l_t$ bits. Otherwise ($l_t^* > l_t$), the decoder asks the encoder to do a new transmission of the next bit b_{l_t+1}.

Lastly, the posterior of the bits is updated sequentially in time via Bayes' rule: for any $\mathbf{b}'_{1:n} \in \{0, 1\}^n$,

$$\pi_{\mathbf{b}'_{1:n}}(t) = \frac{\pi_{\mathbf{b}'_{1:n}}(t-1) p\big(y_t \mid x_t = \mathbb{1}(\mathbf{b}'_{1:l_t} = \hat{\mathbf{b}}_{1:l_t}(t))\big)}{\sum\limits_{\mathbf{b}'_{1:n}} \pi_{\mathbf{b}'_{1:n}}(t-1) p\big(y_t \mid x_t = \mathbb{1}(\mathbf{b}'_{1:l_t} = \hat{\mathbf{b}}_{1:l_t}(t))\big)}, \tag{3.20}$$

and the stopping time of the scheme is given by

$$\tau_{n,\epsilon} = \min\big\{t : \pi_{\hat{\mathbf{b}}(t)}(t) \geq 1 - \epsilon\big\}. \tag{3.21}$$

3.3.2 Rate-Reliability of Bit-wise Posterior Matching

Now we state our main result showing that bitPM achieves strictly positive rates for all BSCs and the best possible reliability with variable length decoding time.

Theorem 3.1. *Operating the bit-wise feedback coding scheme bitPM over BSC(p), the expected variable length decoding time $\tau_{n,\epsilon}$ of successfully decoding n bits reliability with probability $1 - \epsilon$, is upper bounded by*

$$\mathbb{E}[\tau_{n,\epsilon}] \leq \frac{n}{R_0(p)} + \frac{\log(\frac{1}{\epsilon})}{C_1(p)} + o(n \log(\frac{1}{\epsilon})), \tag{3.22}$$

where $C_1(p) := D(\textit{Bern}(p)\|\textit{Bern}(1-p))$ *and* $R_0(p) := I(\textit{Bern}(\frac{1}{3}), Y)$.

Proof. This theorem is a special case of Theorem 2.2 in Chapter 2 with query-independent Bernoulli noise. To avoid re-writing the proof with a minor change of notation, we omit the proof. We refer the reader to [16] for the proof under the notation of bit-transmission problem. □

Remark 3.1. *Note that* $R_0(p) > 0$ *for all* $p < 0.5$. *By Theorem 3.1, bitPM achieves at least rate* $R_0(p) = I(\textit{Bern}(\frac{1}{3}), Y)$ *which is strictly positive, and in fact, close to the channel capacity of* $BSC(p)$ *because of the concavity of the mutual information with respect to the input distribution. Numerical values of* $R_0(p)$ *and* $C(p)$ *are also compared across different value of* p *in the simulation session.*

Remark 3.2. *Intuitively, we achieve the rate* $R_0(p) = I(\textit{Bern}(\frac{1}{3}), Y)$ *since that the bitPM coding schemes gives the channel input* $x_t \sim \textit{Bern}(q_t)$ *where* $\frac{1}{3} \leq q_t \leq \frac{2}{3}$. *To see this, by the selection rule* (3.19)*, we have* $x_t \sim \textit{Bern}(\frac{1}{2})$ *if it's a new transmission. If it is a confirmation, the selection of* l_t^* (3.18) *and the sequential MAP estimate* (3.16) *ensure* $\frac{1}{3} \leq q_t \leq \frac{2}{3}$

Remark 3.3. *For brevity, we choose to present this chapter with* BSC. *The scheme can be applied on any binary input channel. Furthermore, our analysis remains valid for any binary input bounded symmetric output channels, e.g., binary input truncated Gaussian channels.*

3.4 Numerical Examples

In this section, we give numerical results for the proposed scheme bitPM as well as the bit-wise coding scheme in [15], which is labeled SJV'14 in the legend of Figure 3.1. To apply the scheme in [15] to a variable length coding problem, we added into SJV'14 the same stopping rule

$$\tau_{n,\epsilon} = \min\left\{t : \pi_{\hat{\mathbf{b}}(t)}(t) \geq 1-\epsilon\right\}. \tag{3.23}$$

We have also shown our analytic lower bound of the achievable rates of bitPM, $R_0(p)$, the analytic lower bound on anytime rate (always a lower bound for achievable rate) of [15], $R_S(p)$, along with the channel capacity of BSC(p) for comparison.

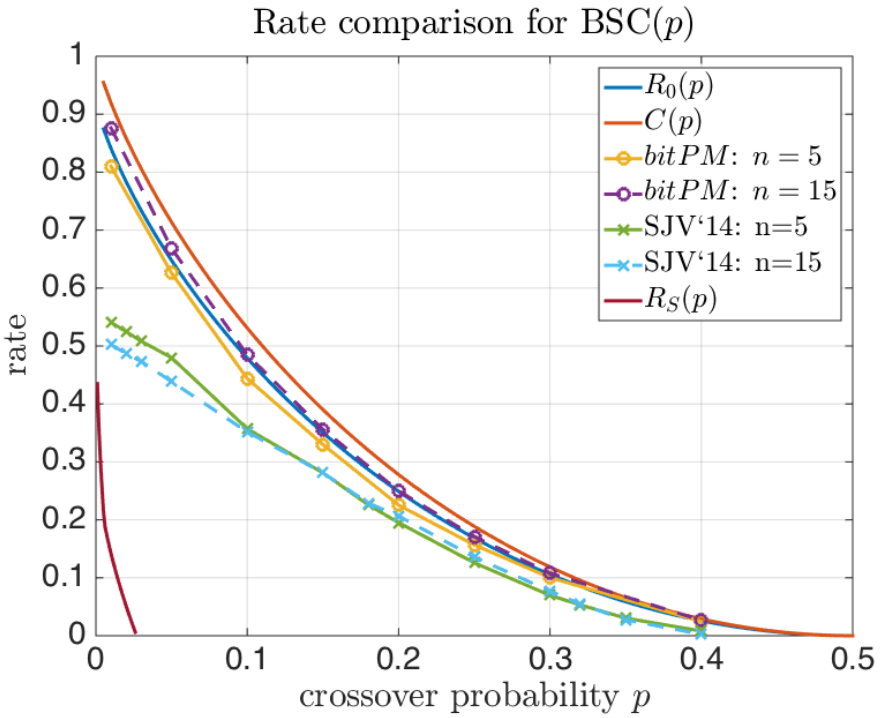

Figure 3.1: Rate comparison with target reliability $\epsilon = 10^{-2}$ over BSC(p)

As we can see in Fig. 3.1, numerically the proposed scheme bitPM has a higher rate than SJV'14 for all value of $p \in (0.0.5)$. On the other hand, the analytically achievable rate $R_0(p)$ of bitPM provided in our analysis is shown to be close to the channel capacity $C(p)$. Moreover, we also observe that numerically bitPM operates on a rate almost equal to the channel capacity when p is small.

3.5 Conclusions and Future Work

In this chapter, we provided a bit-wise sequential feedback code with a nested structure and obtained a strictly positive lower bound for its achievable rate over any BSC with arbitrary

cross-over probability p. The rate-reliability analysis of the proposed scheme is given using the Extrinsic Jensen Shannon divergence. We note that while for the simplicity of the exposition, we have focused our analysis on BSC, the result is shown to be generalizable to a large class of memoryless binary input symmetric output channels.

Furthermore, via numerical simulations, we have illustrated the performance of our proposed bit-wise sequential feedback code against the capacity of the channel. More specifically, we have shown that the achievable rate is near its optimal value even when the number of bits to be transmitted over the channel is small (known benefit of feedback). This observation motivates ongoing research on characterizing the non-asymptotic [17] analysis of our bit-wise sequential feedback codes.

Chapter 3, in full, is a reprint of the material as it appears in the paper: Sung-En Chiu, Anusha Lalitha and Tara Javidi, "Bit-wise Sequential Coding with Feedback." 2018 IEEE International Symposium on Information Theory (ISIT). IEEE, 2018. The dissertation author was the primary investigator and author of this paper.

Chapter 4

Active Learning and CSI acquisition for mmWave Initial Alignment

In this chapter, we demonstrate another application of $hiePM$ in Millimeter-wave (mmWave) communication. In particular, we apply $hiePM$ to the initial beam alignment problem. Numerical simulation shows that $hiePM$ is the state-of-art among other beam alignment algorithms.

4.1 Introduction

Millimeter wave (mmWave) communication with massive antenna arrays is a promising technique that increases the data rate significantly, thanks to the large available bandwidth in mmWave frequency bands. While an inherent challenge for mmWave communication is exceptionally high pathloss [18]- [19], resulting in low SNR and high link outage, the small wavelength can be exploited to deploy an array with a large number of antennas in a relatively small area. It has been shown [20] that massive MIMO mmWave systems can be deployed to form highly directional beams to mitigate the pathloss and the associated low SNR and high link

outage. However, it is essential to note that the realization of highly directional beams requires a precise and reliable estimate of channel state information (CSI) during the initial access phase. This chapter considers the problem of actively learning an optimum beamforming vector from a fundamental limit point of view.

With the scale of millimeter wavelength and the half wavelength spacing, a large number of antennas can be packed into a modest-sized device. For large antenna arrays, however, equipping each antenna with an RF chain is too hardware costly. This limitation prevents per antenna digital processing. A hardware friendly proposal for practically implementing large array systems in mmWave bands deploys a single RF chain where CSI acquisition reduces to finding the optimal analog beamforming along the dominant direction of the signals between the base station (BS) and the user that is trying to establish the communication link. In this chapter we consider this practical scenario of mmWave communication with massive MIMO technology and the practically designed low complexity hierarchical beamforming codebook of [21] to propose an efficient and adaptive beamforming algorithm that quickly identifies the optimal beamforming direction under a single dominant path channel model. Furthermore, we obtain bounds on the performance of this algorithm to asymptotically match the information theoretic limits on the speed and reliability of active learning and CSI acquisition with the given hardware constraints.

The exhaustive linear search, which utilizes beams that scan over all possible directions to pick the best one, and has been proposed in IEEE 802.15 and 5G standards, requires a relatively long initial access time that linearly grows with the angle resolution (highest resolution being the number of the antenna elements).

On the theoretical front, in contrast, prior work which is based on simple measurement models noted that the problem of CSI acquisition in mmWave is closely related to that of noisy search, which itself has been shown to be closely related to the problem of channel coding over a binary input channel with ([11,22,23]) and without ([24]) feedback. Under various noise models, it is shown that the number of measurements can be kept to grow only logarithmically with the

angular resolution and target error probability [11] and [23]. While these early studies did not take the practical beam patterns into account, this logarithmic scaling was later also confirmed and reported in more practical systems with realistic and empirically precise beam patterns ([21] and [25]) with the caveat of a sufficiently large SNR model. In particular, [21] carefully developed a hierarchical beamforming codebook which in the noiseless setting allows for an (adaptive) binary search over the angular space; increasing transmission power and time is then used to combat the measurement noise. The authors in [25] showed that a non-adaptive strategy can also achieve similar performance gains. More specifically, the authors of [25] proposed random hash functions to generate a random beamforming codebook whose acquisition time, they showed, grows only logarithmically with target resolution/error probability.

However, to guarantee coverage in low (< 5 dB) raw SNR regimes (cell-edge users), these techniques provide a marginal advantage over the exhaustive linear search as noted in [22]. We note that this logarithmic scaling (of search time with angular resolution) could also be obtained when viewing the problem as that of sparse estimation with compressive measurements (see [26] and references therein). As shown in [26], however, such an approach also requires large (> 5 dB) raw SNR to achieve reasonable accuracy for channel estimation.

We note that prior works that operate in higher raw SNR make them unsuitable for cell-edge users in mmWave communication. This limitation has significant practical system design implications. The current 5G mmWave communication in 3GPP standard [27] supports mainly non-standalone mmWave in which the initial access phase is covered by legacy sub-6G , which provides higher SNR. This constraint highlights the need for a strategy that can adaptively improve the measurement quality and is suitable for a low SNR regime.

4.1.1 Our work and contributions

In this chapter, we consider the problem of CSI acquisition during the initial access phase for designing the analog beamforming in an environment with a single-path channel. We

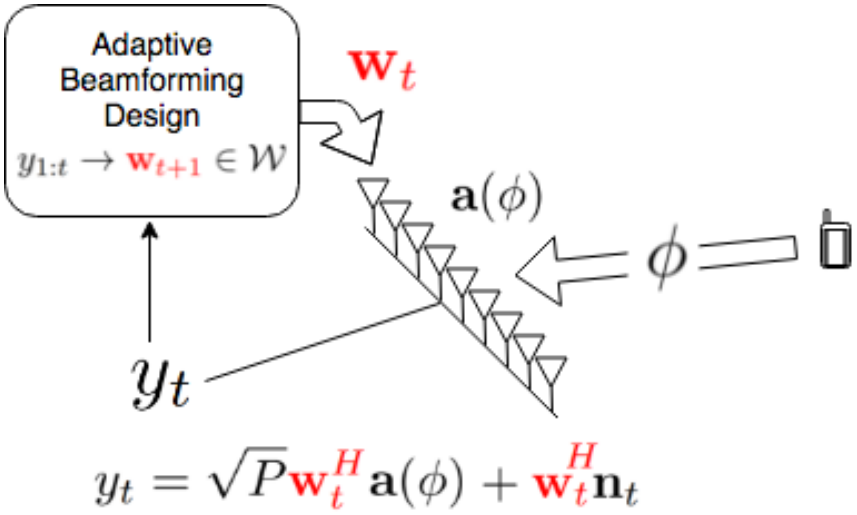

Figure 4.1: The active learning process of the AoA ϕ
The active learning process of the AoA ϕ is to design the beams $\mathbf{w}_t \in \mathcal{W}^S$ adaptively for the sequential collection of the observations y_t, from which at the ending of the collection is to be used for the estimation of the AoA ϕ.

formulate the CSI acquisition as active learning of the angle-of-arrival (AoA) at the base station (BS) side where the user's beamforming vector is assumed to be fixed as illustrated in Fig 4.1. We consider two measures of performance for the proposed search scheme: the (expected) resolved beam width (AoA resolution) and the (expected) error probability. Based on the nature of the initial access protocol, we consider two types of stopping criteria: fixed-length stopping, where a fixed amount of search time is allocated for the initial access phase, and variable-length stopping where the search is conducted over a random stopping time. The contributions of the chapter include:

- We formulate the initial beam alignment for massive MIMO as active learning of the AoA through multiple sequential and adaptive search beams. Our approach draws heavily from our prior work on algorithms for noisy search [14], active learning [28], and channel coding with feedback [23].

- We propose a new adaptive beamforming strategy utilizing the hierarchical beamforming codebook of [21]. The proposed adaptive strategy, hierarchical Posterior Matching

($hiePM$), accounts for the measurement noise and selects the beamforming vectors from the hierarchical beamforming codebook based on the posterior of the AoA. The design and analysis of $hiePM$ extend our prior work of sorted posterior matching [14] and [23] for noisy search in that it restricts the search and the measurements to the practical and hierarchical beamforming patterns of [21].

- We analyze the proposed $hiePM$ strategy and give an upper bound on the expected acquisition time of a variable-length $hiePM$ search strategy required to reach a fixed (predetermined) target resolution and error probability in the AoA estimate. Even when the measurements are hard detected (1-bit quantized measurements) the achievable AoA acquisition rate and the error exponent of $hiePM$ are shown (Corollary 4.2) to be significantly better than those for the search methods of [21] and the random hashing of [25] in all raw SNR regimes.

- We show, via extensive simulations that $hiePM$ is suitable for both fixed-length and variable-length initial beam alignment and significantly outperforms the state-of-art search strategies of [21] and [25]. The numerical simulation shows that $hiePM$ is capable of reaching a proper resolution and error probability even in a low (< 5dB) SNR regime with reasonable search time overhead, demonstrating the possibility of stand-alone mmWave communication for the first time

4.2 System Model

We consider a sectorized cellular communication system operating in EHF (30-300 GHz) bands, where a sector is formed by the BS serving users in a range of angles $[\theta_{\min}, \theta_{\max}]$ as depicted in Fig. 4.2. We focus on the model with one sector and a single user, where the interference from other sectors is assumed to be negligible. This assumption is justified due to high pathloss in the

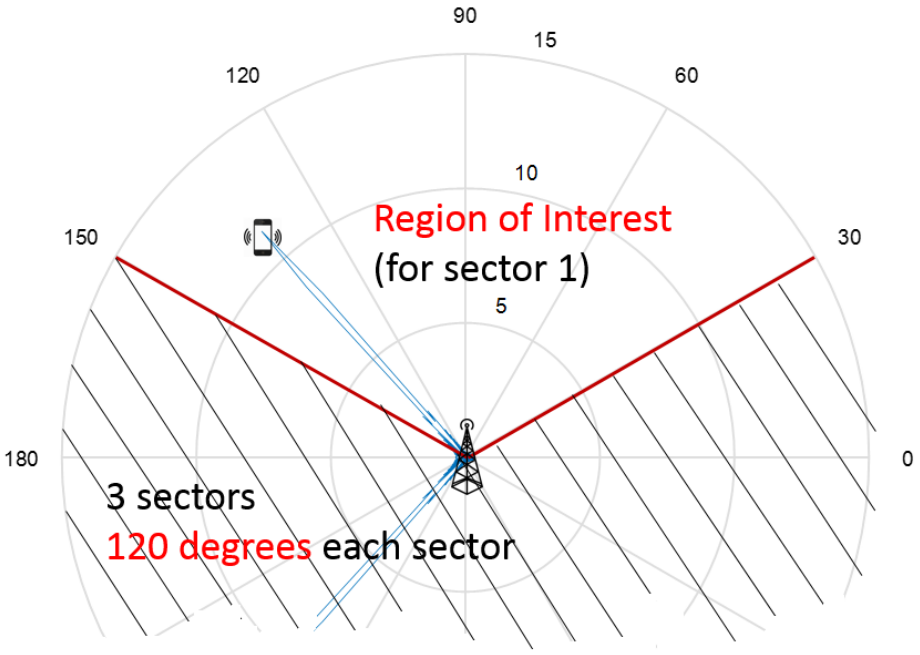

Figure 4.2: Base Station Serving sector $[30^o, 150^o]$

EHF bands [18], and the orthogonality (in time or code) of the transmissions from other users within the sector.

We consider a hardware architecture consisting of multiple antenna elements with a single RF chain [29] on both the BS and the user sides. The BS applies beamforming on the antenna elements such that the power gain due to beamforming may compensate the high pathloss in the mmWave communication system. We use a pilot-based procedure where the users send out pilots to the BS while the BS combines the signal from the antenna elements to the RF chain by the beamforming vector $\mathbf{w}_t \in \mathbb{C}^N$. We focus on the procedure of obtaining a suitable beamforming vector at the BS, while we assume a fixed beamforming vector at the user which allows us to model the user's antennas as a single virtual antenna.

Let N be the number of antennas at the BS, $\sqrt{P}$ be the combined effect of the transmit power and the large-scale fading (pathloss and shadowing), and $\mathbf{h} \in \mathbb{C}^N$ be the small-scale frequency flat fading vector, i.e., h_i is the small-scale fading between the single virtual antenna of the user and the ith antenna element at the BS. For small-scale channel modeling, we use

the stochastic multi-path modeling (see Ch.7 in [30]) assumption with a single dominant path. Furthermore, we assume that the user's mobility is negligible, i.e., the channel vector $\mathbf{h}$ is time invariant. In summary, we have the following assumption:

Assumption 4.1. *The small-scale channel can be described as:*

$$\mathbf{h} = \alpha \mathbf{a}(\phi), \tag{4.1}$$

where $\alpha \in \mathbb{C}$ is the fading coefficient and

$$\mathbf{a}(\phi) := [1, e^{j\frac{2\pi d}{\lambda}\sin\phi}, ..., e^{j(N-1)\frac{2\pi d}{\lambda}\sin\phi}] \tag{4.2}$$

is the array manifold created by the Angle-of-Arrival (AoA) $\phi \in [\theta_{min}, \theta_{max}]$ with antenna spacing d. Furthermore, we assume that the fading coefficient, α, and the AoA, ϕ, are static in time.

Let time index $t = 1, 2, ...$ be the time frame in which the BS can adapt the beamforming vector $\mathbf{w}_t$. Each beamforming slot consists of I samples of finer granularity either of time (e.g. CDMA) or of frequencies (e.g. OFDM subcarriers). Orthogonal spreading sequences $\mathbf{s}_k$ of length I are sent by each of the K users. In other words, we assume:

Assumption 4.2.

$$\mathbf{s}_k^H \mathbf{s}_{k'} = \begin{cases} 0 \, for \, k = k' \\ 1 \, for \, k \neq k' \end{cases} \tag{4.3}$$

With the assumption of orthogonality among users, correlating the pilot codes we can write the code-matched signal from a particular user as

$$\begin{aligned} y_t &= \sqrt{P}\mathbf{w}_t^H (\sum_{k'=1}^{K} \mathbf{h}_{k'} \mathbf{s}_{k'}^T)\mathbf{s}_k^* + \mathbf{w}_t^H \mathbf{N}_t \mathbf{s}_k^* \\ &\overset{(a)}{=} \alpha\sqrt{P}\mathbf{w}_t^H \mathbf{a}(\phi) + \mathbf{w}_t^H \mathbf{n}_t, \end{aligned} \tag{4.4}$$

where $\mathbf{N}_t$ is the $N \times I$ spatially uncorrelated AWGN noise matrix across the antenna elements (rows) and samples (columns). Note that in (a) we used single-path channel model (Assumption 4.1) and orthogonality of codes (Assumption 4.2) from different users as well as the static nature of the channel, $\mathbf{h}$, over the code resource I. Finally, $\mathbf{n}_t := \mathbf{N}_t \mathbf{s}_k^* \sim \mathcal{CN}(\mathbf{0}_{N\times 1}, \sigma^2 \mathbf{I})$ is the equivalent noise vector at the antenna array at the output of the code-matched filter, i.e. such that y_t has a raw SNR equal to P/σ^2 when no beamforming is applied.

In many practical scenarios, only partial information about y_t is available to the BS. As a result, we consider the available signal to BS, z_t, be of the form

$$z_t = q(y_t), \tag{4.5}$$

where $q(\cdot)$ represents a practically motivated partial information processing such quantization function. With the received signal model in (4.4) and (4.5), we are now ready to describe the sequential beam search problem which adaptively designs the beamforming vectors $\mathbf{w}_t$.

4.3 Active Learning and Hierarchical Posterior Matching

In this section, we present our main result. In subsection 4.3.1, we lay out the framework of active learning for sequential beam alignment. In subsection 4.3.2, we describe the hierarchical beamforming codebook. In subsection 4.3.3, we describe our proposed algorithm: Hierarchical Posterior Matching for sequentially selecting the beamforming vector from the codebook. Lastly, in subsection 4.3.4, we describe the posterior update for several measurement models.

4.3.1 Sequential Beam Alignment via Active Learning

A sequential beam alignment problem in the initial access phase consists of a beamforming design strategy (possibly adaptive), a stopping time τ, and a final beamforming vector

design. Specifically, we consider a stationary beamforming strategy as a causal (possibly random) mapping function from past observations to the beamforming vector: $\mathbf{w}_{t+1} = \gamma(z_{1:t}, \mathbf{w}_{1:t})$. Subsequently, the final beamforming vector selection $b(\cdot)$ is a (possibly random) mapping determining the final beamforming vector to be exploited for communication, $\hat{\mathbf{w}} = b(z_{1:\tau}, \mathbf{w}_{1:\tau})$, as a function of the sequence of the observations gathered during the initial access phase $[1 : \tau]$. To reduce the reconfiguration time of the beamforming vector from $\mathbf{w}_t$ to $\mathbf{w}_{t+1}$, we use a pre-designed beamforming codebook:

Assumption 4.3. *The beamforming vector is chosen from a pre-designed beamforming codebook $\mathcal{W}^S$ with finite cardinality.*

Based on the nature of the protocol, we consider two criteria for selection of the length of the initial access phase:

Fixed-length stopping time: the user transmits a pre-determined number of frames during which the base station uses the beamforming vectors $\mathbf{w}_1, \mathbf{w}_2, ..., \mathbf{w}_T$. After the total pre-determined number of frame, T, the BS makes a prompt decision on the final beamforming vector $\hat{\mathbf{w}}$

Variable-length stopping time: the user sends out the initial access signal continually until a specific target link quality can be achieved by the final beamforming vector $\hat{\mathbf{w}}$ with high probability. Under a variable-length setup, the BS sends an ACK to the user and ends the initial access phase.

In Sec. 4.4, we propose an adaptive beam alignment algorithm with both types of stopping rules, while our analysis in subsection 4.4 focuses on the variable-length stopping time τ. Our numerical studies consider the performance under both stopping rules.

The best beamforming vector, $\hat{\mathbf{w}} = \mathbf{a}(\phi)$, can boost the SNR by a factor of N, and the fading coefficient α can also be estimated and equalized if the SNR at the RF chain (after antenna combining) is high enough. Therefore, under Assumption 4.1, one of the primary goals of the initial access phase is to learn the AoA ϕ so that BS can form a proper beam toward that

direction. Therefore, we can treat the sequential beam alignment problem by the methods of active learning [28, 31], as shown in Fig. 4.1, where the beamforming vector $\mathbf{w}_t$ is equivalent to the query point and y_t the response in the learning problem. The adaptivity of $\mathbf{w}_t$ reflects that the learner chooses the query points actively as considered in the active learning tasks.

The quality of the established link, under a single-path channel model $\mathbf{h} = \alpha\mathbf{a}(\phi)$, is determined by the accuracy of the final point estimate $\hat{\phi}(y_{1:\tau}, \mathbf{w}_{1:\tau})$ of ϕ. In particular, a point estimate $\hat{\phi}$ together with a confidence interval δ provides robust beamforming with certain outage probability. Hence we measure the performance by the resolution and reliability of the final estimate $\hat{\mathbf{w}}$:

Definition 4.1. *Under Assumption 4.1, a sequential beam search strategy with an adaptive beamforming design γ, stopping time τ, and final AoA estimation $\hat{\phi}$ is said to have resolution $\frac{1}{\delta}$ with error probability ϵ if*

$$\mathbb{P}(\mid \hat{\phi} - \phi \mid > \delta) \leq \epsilon. \tag{4.6}$$

We note that, given a sufficiently large number of antennas, one can increase the resolution $1/\delta$ and decrease the error probability ϵ by increasing the time of sample collection τ or equivalently by prolonging the initial access phase. In other words, the expected number of samples $\tau_{\epsilon,\delta}$ necessary to ensure a resolution $1/\delta$ and error probability ϵ measures the effectiveness of an initial access algorithm. From an information theoretic viewpoint, one can think of a family of sequential adaptive initial access schemes that achieves acquisition rate R and reliability E:

Definition 4.2. *Under Assumption 4.1, a family of sequential adaptive initial access schemes achieves acquisition rate-reliability (R,E) if and only if*

$$R := \lim_{\delta \to 0} \frac{\log(\frac{1}{\delta})}{\mathbb{E}[\tau_{\epsilon,\delta}]}, \quad E := \lim_{\epsilon \to 0} \frac{\log(\frac{1}{\epsilon})}{\mathbb{E}[\tau_{\epsilon,\delta}]}. \tag{4.7}$$

Remark 4.1. *The final beamforming vector (hence the quality of the established link) is determined by both the target resolution and the error (δ, ϵ), written as $\hat{\mathbf{w}}(z_{1:\tau}, \mathbf{w}_{1:\tau}, \epsilon, \delta)$. Given a*

total communication time frame T, the expected spectral efficiency, under the final beamforming vector $\hat{\mathbf{w}}$, is given as

$$\mathbb{E}\left[\frac{T-\tau}{T}\log\left(1+\frac{P\mid \alpha\hat{\mathbf{w}}(z_{1:\tau},\mathbf{w}_{1:\tau},\epsilon,\delta)^H\mathbf{a}(\phi)\mid^2}{\sigma^2}\right)\right], \tag{4.8}$$

and is an important performance metric from a system point of view. This performance metric, however, requires a further system optimization over the length of the initial access phase, τ, and the length of the communication phase, T, which is outside the scope of this dissertation. Therefore, in our analysis, we focus on the parameters ϵ and δ. For a practically relevant comparison of different initial beam search algorithms, the system performance of (4.8) is also evaluated in the numerical simulations for some nominal choice of τ and T.

4.3.2 Hierarchical Beamforming Codebook

We adopt the hierarchical beamforming codebook $\mathcal{W}^S$ proposed in [21] with S levels of beam patterns such that the corresponding beams divide the space dyadically in a hierarchical manner such that the disjoint union of the beams in each level is the whole region of interest . The codebook consists of S different levels, i.e. $\mathcal{W}^S = \cup_{l=1}^{S}\mathcal{W}_l$ where $\mathcal{W}_l$ is all the beam patterns whose main beam has a width $\frac{|\theta_{\max}-\theta_{\min}|}{2^l}$. More specifically, for each level l, $\mathcal{W}_l$, contains 2^l beamforming vectors which divide the sector $[\theta_{\max},\theta_{\min}]$ into 2^l directions, i.e.,

$$[\theta_{\max},\theta_{\min}] = \bigcup_{m=0}^{2^l-1} H_l^m, \tag{4.9}$$

each associated with a certain range of AoA H_l^m. The beamforming vector $\mathbf{w}(H_l^m)$ is designed such that the beamforming gain $|\mathbf{w}(H_l^m)^H\mathbf{a}(\phi)|$ is almost constant for AoA $\phi \in H_l^m$ and almost zero for $\phi \notin H_l^m$.

Note that $\mathcal{W}^S$ can be represented as a binary hierarchical tree, where each level-l beam has

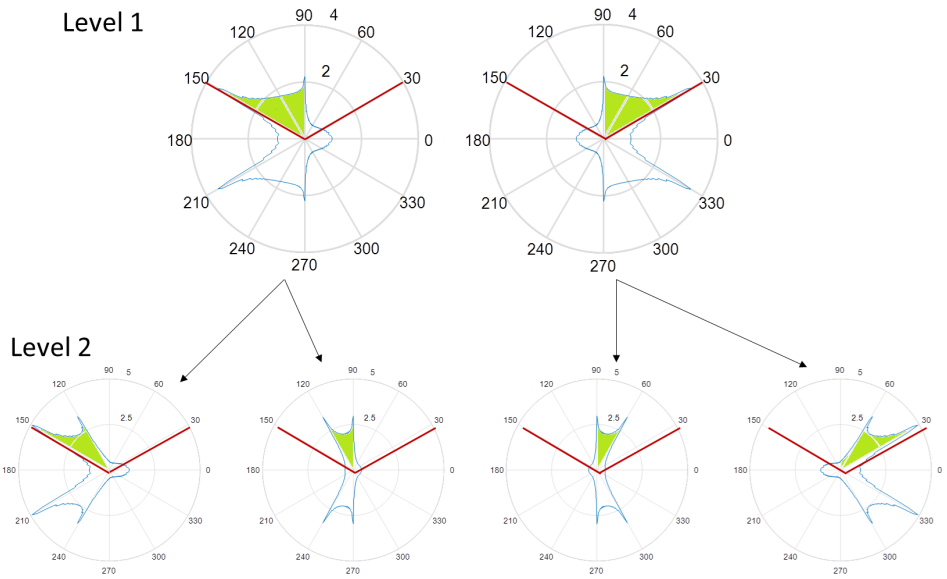

Figure 4.3: The first 2 levels of hierarchical beamforming codebook
The codebook is constructed by practical beam patterns formed by uniform linear array with 64 antenna

two descendants in level $l+1$ such that each level-l beam is the union of two disjoint beams, i.e., $H_l^m = H_{l+1}^{2m} \cup H_{l+1}^{2m+1}$. This binary tree hierarchy is illustrated in Fig. 4.3 with the beam patterns of the first two levels of the codebook. Note that, without loss of generality, the beamforming vectors in the codebook are assumed to have unit norm $\|\mathbf{w}\|^2 = 1$.

4.3.3 Hierarchical Posterior Matching

In this section, we propose a search mechanism based on the connection between initial access beamforming, noisy search [14], active learning [28], and channel coding with feedback [23], with the caveat that the beamforming vector is constrained to the practically feasible beamforming codebook of [21] as in set $\mathcal{W}^S$. Instead of using all past observations $\mathbf{w}_{t+1} = \gamma(z_{1:t}, \mathbf{w}_{1:t})$, $hiePM$ selects $\mathbf{w}_{t+1}$ based on the posterior of the AoA ϕ at time t, which is a sufficient statistic. We discretize the problem by assuming that the resolution $\frac{1}{\delta}$ is an integer and

that the AoA ϕ is from

$$\phi \in \{\theta_1, ..., \theta_{1/\delta}\},\ \theta_i = \theta_{\text{min}} + (i-1) \times \delta \times (\theta_{\text{max}} - \theta_{\text{min}}). \tag{4.10}$$

Such discretization approaches the initial beam alignment problem as $\delta \to 0$. To support resolution $1/\delta$, the corresponding size of the hierarchical beamforming codebook

$$S = \log_2(1/\delta) \tag{4.11}$$

is used. With this discretization, the posterior distribution can be written as a $\frac{1}{\delta}$-dimensional vector $\boldsymbol{\pi}(t)$, where the i^{th} component is of the form

$$\pi_i(t) := \mathbb{P}(\phi = \theta_i \mid z_{1:t}, \mathbf{w}_{1:t}),\ i = 1, 2, ..., \frac{1}{\delta}. \tag{4.12}$$

The posterior probability of the AoA ϕ being in a certain range, say, H_l^m, can be computed as

$$\pi_{H_l^m}(t) := \sum_{\theta_i \in H_l^m} \pi_i(t). \tag{4.13}$$

Now we are ready to present the proposed $hiePM$ algorithm. The proposed adaptive beamforming strategy, hierarchical Posterior Matching, $hiePM$, chooses a beamforming vector at each time t from the hierarchical beamforming codebook $\mathcal{W}^S$. The main idea of $hiePM$ is to select $\mathbf{w}_{t+1} \in \mathcal{W}^S$ by examining the posterior probability $\pi_{H_l^m}(t)$ for all $l = 1, 2, ..., S$ and $m = 0, 1, 2, ..., 2^l - 1$. Specifically, let

$$l_t^* = \arg\max_l \left\{ \max_m \pi_{H_l^m} \geq \frac{1}{2} \right\}, \tag{4.14}$$

the proposed $hiePM$ algorithm selects a codeword at either level l_t^* or $l_t^* + 1$ according to Alg. 1 below. Given a snapshot of posterior at time t, the selection rule is illustrated in Fig. 4.4. The

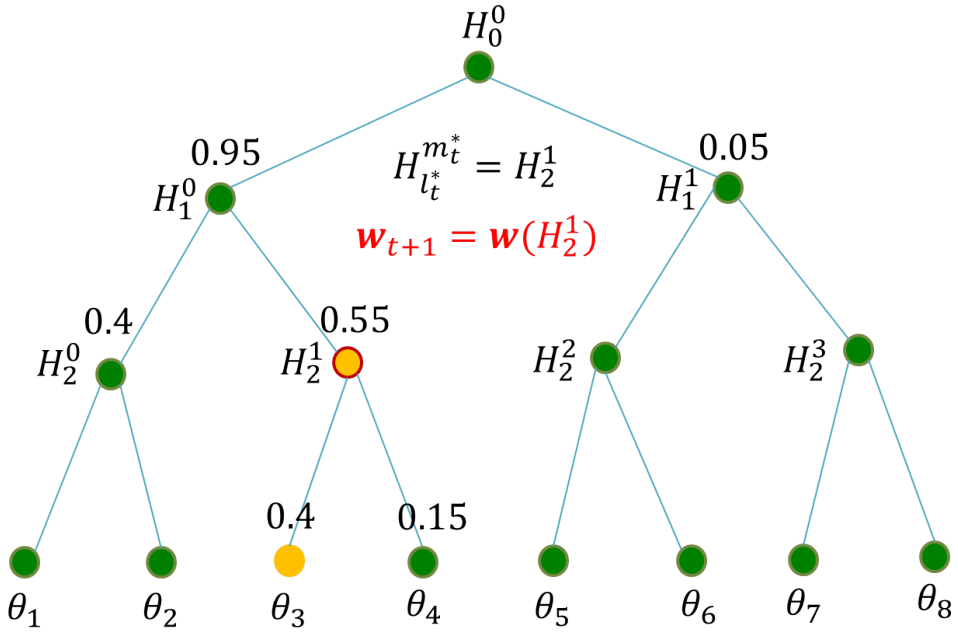

Figure 4.4: Illustration of the hierarchical posterior matching algorithm. In this example, we search down the tree hierarchy to levels 2 and 3, where level 3 has the first codeword that contains posterior lesser than half. Between level 2 and level 3, the codeword in level 2 of posterior 0.55 is selected since it's closer to half (0.55 v.s. 0.4).

algorithm runs for a fixed length of time (fixed-length stopping) or until a certain error probability ϵ for resolution $1/\delta$ is achieved (variable-length stopping). The final choice of beamforming vector is determined by the ϵ and δ. The details of $hiePM$ are summarized in Algorithm 1 below.

Remark 4.2. *The $hiePM$ algorithm can be thought of as a noisy generalization of a bisection search where the posterior is used to create almost equally-probable search subsets subject to the codebook $\mathcal{W}^S$. Compared with the vanilla bisection method proposed in [21], $hiePM$ allows for significantly lower SNR search outcomes whose reliability is dealt with over time, which can also be viewed as water-filling in the angular domain.*

Remark 4.3. *See [23, 24] for a detailed description of the connection between our beam search problem and a channel coding problem in data transmission. In this light, the vanilla noise-compensated bisection method of [21] can be viewed as a repetition coding strategy which is known to have zero rate, while $hiePM$ can be viewed as a constrained (subject to hierarchical*

Algorithm 4.1: Hierarchical Posterior Matching for Beamforming

Input: target resolution $\frac{1}{\delta}$, target error probability ϵ, codebook $\mathcal{W}^S$ $(S = \log_2(1/\delta))$, fixed stopping time n, *stopping-criterion*, *algorithm-type*

Initialization: $\pi_i(0) = \delta$ for all $i = 1, 2, ..., 1/\delta$,

for $t = 1, 2, ...$ **do**

  # Codeword selection from $\mathcal{W}^S$:

  $k = 0$;

  for $l = 1, 2, ..., S$ **do**

    if $\pi_{H_l^m}(t) > 1/2$ **then**

      $l_t^* = l$; $m \leftarrow \arg\max_{m' \in \{2m, 2m+1\}} \boldsymbol{\pi}_{H_{l+1}^{m'}}(t)$;

    else

      $(l_{t+1}, m_{t+1}) = \arg\min_{(l', m') \in \{(l_t^*, \lfloor \frac{m}{2} \rfloor), (l_t^*+1, m)\}} |\pi_{H_{l'}^{m'}}(t) - \frac{1}{2}|$; break;

  # Codeword selection result

  $\mathbf{w}_{t+1} = \mathbf{w}(H_{l_{t+1}}^{m_{t+1}})$

  # Take next measurement

  $y_{t+1} = \alpha\sqrt{P}\mathbf{w}_{t+1}^H \mathbf{a}(\phi) + \mathbf{w}_{t+1}^H \mathbf{n}_{t+1}$; $z_{t+1} = q(y_{t+1})$

  # Posterior update by Bayes' Rule (Sec. 4.3.4)

  $\boldsymbol{\pi}(t+1) \leftarrow z_{t+1}, \boldsymbol{\pi}(t)$

  case: stopping-criterion = fixed length (FL)

  if $t + 1 = n$ **then**

    break (to final beamforming);

  case: stopping-criterion = variable length (VL)

  if $\max_i \pi_i(t+1) > 1 - \epsilon$ **then**

    break (to final beamforming);

$\tau = t + 1$ (length of the initial access phase)

Final beamforming vector design

case: algorithm-type = fixed resolution (FR)

$(\hat{l}, \hat{m}) = (S, \arg\max_m \pi_{H_S^m}(\tau))$

case: algorithm-type = variable resolution (VR)

$$\hat{l} = \begin{cases} 1, \ \max_m \pi_{H_1^{\hat{m}}}(\tau) < 1 - \epsilon \\ \max\{l : \max_m \pi_{H_l^{\hat{m}}}(\tau) \geq 1 - \epsilon\}, \ o.w. \end{cases} \tag{4.15}$$

$$\hat{m} = \arg\max_m \ \pi_{H_{\hat{l}}^m}(\tau)$$

$\hat{\mathbf{w}} = \mathbf{w}(H_{\hat{l}}^{\hat{m}})$

codebook $\mathcal{W}^S$) approximation to the capacity achieving posterior matching feedback coding scheme of [8].

4.3.4 Posterior Update

Let $\gamma_h : \boldsymbol{\pi}(t) \to \mathcal{W}^S$ be the $hiePM$ sequential beamforming design given in Algorithm 1, i.e. let $\mathbf{w}_{t+1} = \gamma_h(\boldsymbol{\pi}(t))$. By the measurement model, the posterior update in Algorithm 1 in general can be written as

$$\pi_i(t+1) = \frac{\pi_i(t) f(z_{t+1}|\phi = \theta_i, \mathbf{w}_{t+1} = \gamma_h(\boldsymbol{\pi}(t)))}{\sum_{j \neq i} \pi_j(t) f(z_{t+1}|\phi = \theta_j, \mathbf{w}_{t+1} = \gamma_h(\boldsymbol{\pi}(t)))}, \tag{4.16}$$

where $f(z_{t+1}|\phi = \theta_i, \mathbf{w}_{t+1} = \gamma_h(\boldsymbol{\pi}(t)))$ is the conditional distribution of z_{t+1} and depends on the function $q(\cdot)$ as well as the channel state information (e.g. the fading coefficient α) known to the BS. Here we give a few examples:

1. *Full measurement $z_t = y_t$*:

   In the case of static channel (zero mobility), we may assume that the fading coefficient α is known to the BS. With full measurement $z_t = y_t$, the conditional distribution of z_t is a complex Gaussian, written as

$$\begin{aligned} &f(z_{t+1}|\phi = \theta_i, \mathbf{w}_{t+1} = \gamma_h(\boldsymbol{\pi}(t))) \\ &\quad = \mathcal{CN}(z_{t+1}; \alpha\sqrt{P}\mathbf{w}_{t+1}^H \mathbf{a}(\theta_i), \sigma^2) \end{aligned} \tag{4.17}$$

   In the case where α is not known, the algorithm is assumed to use an estimate $\hat{\alpha}$:

$$\begin{aligned} &f(z_{t+1}|\phi = \theta_i, \mathbf{w}_{t+1} = \gamma_h(\boldsymbol{\pi}(t))) \\ &\quad \approx \mathcal{CN}(z_{t+1}; \hat{\alpha}\sqrt{P}\mathbf{w}_{t+1}^H \mathbf{a}(\theta_i), \sigma^2) \end{aligned} \tag{4.18}$$

   for the posterior update.

2. *1-bit measurement* $z_t = \mathbb{1}\left(|y_t| > v_t\right)$:

   For practical high speed ADC implementation, we consider an extreme quantization function of a 1-bit [26, 32] measurement model $z_t = \mathbb{1}\left(|y_t| > v_t\right)$, where at each time instance t the BS only has 1-bit of information about whether or not the received power passes the threshold v_t. Equivalently, we can write the measurement model as

$$z_t = \mathbb{1}(\phi \in H_{l_t}^{m_t}) \oplus u_t(\phi), \;\; u_t(\phi) \sim \text{Bern}(p_t(\phi)) \tag{4.19}$$

   where $u_t(\phi)$ is the equivalent Bernoulli noise with flipping probability $p_t(\phi)$, and $\oplus$ denotes the exclusive OR operator. The setting of the threshold v_t and the corresponding flipping probability $p_t(\phi)$ is given in Lemma 4.1. In this case, the conditional distribution of z_t can therefore be written as

$$\begin{aligned} &f(z_{t+1}|\phi = \theta_i, \mathbf{w}_{t+1} = \gamma_h(\boldsymbol{\pi}(t))) \\ &\qquad = \text{Bern}(z_{t+1} \oplus \mathbb{1}(\theta_i \in H_{l_t}^{m_t}); p_{t+1}(\theta_i)). \end{aligned} \tag{4.20}$$

4.4 Analysis

Our analysis for $hiePM$ focuses on the variable-length stopping criteria with a fixed resolution and a fixed target error probability ϵ, where by Algorithm 1 the variable-length stopping time $\tau_{\epsilon,\delta}$ can be written as

$$\tau_{\epsilon,\delta} = \min\{t : 1 - \max_i \pi_i(t) \leq \epsilon\}. \tag{4.21}$$

We will also focus on the 1-bit measurement model described in Sec. 4.3.4. Furthermore, we make the assumption of an ideal hierarchical beamforming codebook for the analysis:

Assumption 4.4. *The beam formed by the beamforming vector* $\mathbf{w}(H_l^m) \in \mathcal{W}^S$ *has constant beamforming power gain for any signal of AoA* $\phi \in H_l^m$ *and rejects any signal outside of* H_l^m*,* $i.e.$

$$|\mathbf{w}(H_l^m)^H \mathbf{a}(\phi)| = \begin{cases} G_l, & \text{if } \phi \in H_l^m \\ 0, & \text{if } \phi \notin H_l^m \end{cases}. \tag{4.22}$$

Remark 4.4. *Assumption 4.4 is mainly for better presentation. This assumption is approximately true when we have a massive number of antennas* $N \gg \frac{1}{\delta}$*. The deterioration of performance due to the imperfect beamforming, such as that resulting from sidelobe leakage, is not the focus of our analysis. In our numerical simulations, however, we remove this assumption by investigating the performance of the algorithms under the actual beamforming pattern with a finite number of antennas.*

Under the 1-bit measurement $z_t = \mathbb{1}(|y_t| > v_t)$ with Assumption 4.4 and the optimal choice of the threshold v_t in Lemma 4.1, the flipping probability $p_t(\phi)$ of the Bernoulli noise in (4.19) is independent of the AoA ϕ and only depends on the beamforming codeword level l_t selected at time t. In particular, we have

$$p_t(\phi) = p[l_t] := \int_0^{v_t} \text{Rice}(x; PG_l^2, \sigma^2)\, dx, \tag{4.23}$$

where $p[l] > p[l+1]$ and $p[l] \to 0$ since $G_l < G_{l+1}$ and $G_l \to \infty$ as $l \to \infty$ (assuming unlimited number of antenna) by the design of the codebook. Furthermore, we assume that $\log_2(1/\delta)$ is an integer. Now we are ready to give an upper bound of the expected stopping time $\tau_{\epsilon,\delta}$ with resolution $\frac{1}{\delta}$ and outage probability ϵ of the proposed $hiePM$ sequential beam search algorithm:

Theorem 4.1. *By using codebook* $\mathcal{W}^S$ *with* $S = \log_2(1/\delta)$ *levels and assuming the perfect beamforming assumption (Assumption 4.4) and the 1-bit measurement model* $z_t = \mathbb{1}(|y_t| > v_t)$ *with the optimal choice of* v_t *in Lemma 4.1, the expected stopping time of* $hiePM$*, of resolution*

$\frac{1}{\delta}$ *and error probability* ϵ*, can be upper bounded by*

$$\mathbb{E}[\tau_{\epsilon,\delta}] \leq \frac{\log(1/\delta)}{R_h} + \frac{\log(1/\epsilon)}{E_h} + o(\log(\frac{1}{\delta\epsilon})), \tag{4.24}$$

where $E_h = C_1(p[\log_2(1/\delta)])$*,* $R_h = I(1/3, p[l'])$ *with* $l' = \left\lfloor \frac{K_0 \lceil \log\log \frac{1}{\delta} \rceil}{\log 2} - 1 \right\rfloor$ *and* K_0 *is a constant defined in Lemma A.3.*

Proof. The 1-bit quantization in section 4.7, the problem is equivalent to Theorem 2.2 in Chapter 2. □

Corollary 4.1. *Let,* $\mathbb{E}[\tau_{\epsilon,\delta}] = n$*. For all values of* δ *such that* $\delta \leq 2^{-nR_h}$*, the error probability of* $hiePM$ *can be approximately upper bounded by*

$$\mathbb{P}(\mid \hat{\phi} - \phi \mid > \delta) \lessapprox \exp\left(-nE_h\left(1 - \frac{\log(1/\delta)}{nR_h}\right)\right) \tag{4.25}$$

when δ *is small enough.*

Corollary 4.2. *Under the same conditions and by Theorem 4.1,* $hiePM$ *achieves acquisition rate*

$$\begin{aligned} \lim_{\delta\to 0} \frac{\log(1/\delta)}{\mathbb{E}[\tau_{\epsilon,\delta}]} &\geq \lim_{\delta\to 0} R_h \\ &= \lim_{\delta\to 0} I(1/3, p^*(\delta,\epsilon)) = 1 \end{aligned} \tag{4.26}$$

for arbitrarily small error $\epsilon > 0$*, and error exponent*

$$\lim_{\epsilon\to 0} \frac{\log(1/\epsilon)}{\mathbb{E}[\tau_{\epsilon,\delta}]} \geq \lim_{\epsilon\to 0} E_h = C_1(p[\log_2(1/\delta)]) \tag{4.27}$$

for any $\delta > 0$*.*

Remark 4.5. *The integer assumption of* $\log_2(1/\delta)$ *is for notational simplicity. If the desired resolution* $1/\delta$ *is not of power of 2, one can simply take a higher resolution* $1/\delta' = 2^{\lceil \log_2(1/\delta) \rceil}$*.*

The corresponding upper bound in Theorem 4.1 can be written accordingly and the conclusion in Corollary 4.2 remains true.

Remark 4.6. *The rate one in equation (4.26) implies that $hiePM$ performs asymptotically ($\delta \to 0$) in the same manner as a noiseless bisection search which is the optimal usage of the hierarchical beamforming codebook $\mathcal{W}^S$. The asymptotically noiseless behavior is due to the fact that $hiePM$ shrinks the AoA D_l^m quickly, together with Assumption 4.4 that an unlimited number of antennas allow the beamforming gain $|\mathbf{w}(H_l^m)^H \mathbf{a}(\phi)|^2 = \frac{\pi}{|D_l^m|} \to \infty$ as $l \to \infty$. Compared with other beam alignment algorithms, non-adaptive random coding based strategies [25] are not able to shrink the AoA region of the search beam. Therefore, the corresponding acquisition rate of [25] rate is strictly lesser than 1. On the other hand, the adaptive noisy vanilla bisection algorithm in [21] has rate zero, albeit the AoA region of the search beam shrinks over time. This phenomenon is because the noisy bisection of [21] in effect employs the repetition coding, which has rate zero even with feedback (adaptivity).*

Remark 4.7. *To further compare our theoretical result of $hiePM$ with prior works, we plot Corollary 4.2 together with error probability upper bounds of [21] and [25] in Fig. 4.5 with $\mathbb{E}[\tau] = 28$, $1/\delta = 128$ and $|\theta_{max} - \theta_{min}| = 120^o$ and the ideal beamforming assumption (Assumption 4.4). For the bisection algorithm of [21], we take the upper bound from the author's analysis for equal power allocation with fixed fading coefficient $\alpha = 1$. While for the random hashing of [25], we take an optimization of the number of directions over Gallager's random coding bound of BSC as*

$$P_e \leq \min_q \exp\left(-28 \times E_{RC}(q)\right), \tag{4.28}$$

where $E_{RC}(q) = \max_{0\leq\rho\leq 1}\left(E_0(\rho, q) - \rho \times \frac{\log_2(128)}{28}\right)$ and

$$\begin{aligned} E_0(\rho, q) = -\log\Bigg(&\left(q(p_q)^{\frac{1}{1+\rho}} + (1-q)(1-p_q)^{\frac{1}{1+\rho}}\right)^{1+\rho} \\ &+ \left(q(1-p_q)^{\frac{1}{1+\rho}} + (1-q)(p_q)^{\frac{1}{1+\rho}})\right)^{1+\rho}\Bigg) \end{aligned} \tag{4.29}$$

with

$$p(q) := \int_0^{v_t} \textit{Rice}(x; P\frac{3}{2q}, \sigma^2)\, dx, \tag{4.30}$$

where again v_t is optimally chosen according to Lemma 4.1. The illustration of Corollary 4.2 in Fig. 4.5 predicts the superior performance of $hiePM$ over the prior works [21] and [25]. We note that for these upper bounds, $hiePM$ and random hashing of [25] assumes a 1-bit quantizer, whereas the bisection method of [21] is favorably given the unquantized amplitude information. We further show in numerical simulation (Fig. 4.7) that with practical beam patterns and unquantized measurements, the actual performance of $hiePM$ not only is indeed better than the prior works but achieves a significantly smaller error probability than our theoretical upper bound. Furthermore, we will see that the non-adaptive random hashing based method in [25], in fact, outperforms the adaptive bisection in [21] due to the lack of a good coding of [21].

4.5 Numerical Results

In this section, we compare the performance of our proposed *hiePM* algorithms against the bisection algorithm of [21], and an optimized random-code-based strategy, which is taken as an upper bound on the performance of the random hash-based solution of [25]. Before we proceed with this performance analysis, however, we first provide a summary of the simulation setup and parameters.

4.5.1 Simulation Setup and Parameters

We use the hybrid analog/digital system architecture described in 4.2, where the BS has $N = 64$ antenna elements of uniform linear array with antenna spacing $\frac{\lambda}{2}$, and the user has a single (virtual) antenna. Furthermore, due to the use of orthogonal spreading sequences, we focus on the single user case $K = 1$. The channel consists of a single path with the fast fading

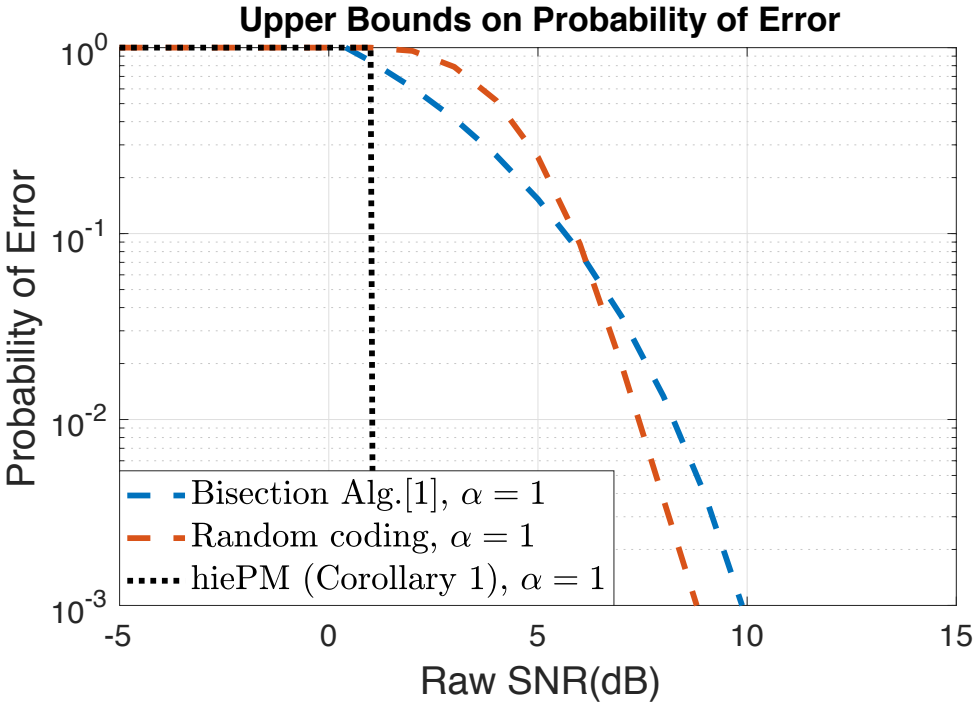

Figure 4.5: Comparison of the theoretical upper bounds on error probability
We compare between $hiePM$, random coding, and the bisection algorithm of [21] as a function of raw SNR. The upper bound on $hiePM$ is given by Corollary 4.1. While the upper bound on random coding is given by Gallager's bound as in (4.28), and the upper bound on the bisection algorithm is provided by [21].

coefficient α. The rule-of-thumb [33] estimate of channel coherence time given by

$$T_c \approx \frac{0.432}{f_m} = \frac{0.432c}{f_c v}, \tag{4.31}$$

where c is the speed light, f_c is the carrier frequency, and v is the user speed. So even for mmWave communication with 73GHz, at walking speed (< 3 km/hour) the coherence time is

$$T_c = \frac{0.432 \times 3 \times 10^9 \text{ (m/s)}}{73 \times 10^9 \text{ (Hz)} \times 3 \text{ (km/hour)}} \approx 8.127 \text{ millisecond}. \tag{4.32}$$

Note that, additionally, narrow beamforming and the existence of a dominated sub-path (e.g., Line-Of-Sight) can both increase the coherence time significantly [34]. Therefore, in subsection 4.5.3, we assume that the fading coefficient α is static during the entire initial access duration of 2 milliseconds. We consider both the case when the fading coefficient α is known exactly $\hat{\alpha} = \alpha$, and the case when it is estimated with the estimation inaccuracy modelled as $\hat{\alpha} \sim \mathcal{CN}(\alpha, \sigma_\alpha^2)$. In subsection 4.5.4, we further study the robustness of $hiePM$ with a static estimate of the time-varying fading coefficient α_t of a Rician AR-1 model with a coherence time corresponding to higher user mobility. Finally, we consider learning the AoA with an angular resolution of $1/\delta = 128$, and an (expected) stopping time of $E[\tau] = 28$, i.e., with $E[\tau]$ selections of beamforming vectors, hence, samples.

To provide a sense for the normalized parameters, let us consider some candidate PHY layer solutions. In particular, when using the 5G new radio Physical Random Access Channel (PRACH) format B4 [35], the $E[\tau] = 28$ samples translate to less than 2 ms acquisition time for sub-1-degree angular resolution within a $[0, 120]$ sector. We present our results as a function of raw SNR $\frac{P}{\sigma^2}$ to get a sense for reasonable values of SNR. In Fig. 4.6 we compute and illustrate the expected distance at which a raw target SNR is obtained. Under 3GPP TR 38.901 UMi LOS pathloss channel model (summarized in [36]), with 23 dBm maximum user power, -174 dBm/Hz thermal noise density, 5 dB receiver noise figure at BS, with a bandwidth of 100 MHz. As seen in

Fig. 4.6, one can argue that given our selection of this PHY layer and parameters, the practical raw SNR regime of interest is within -15 dB to 10 dB.

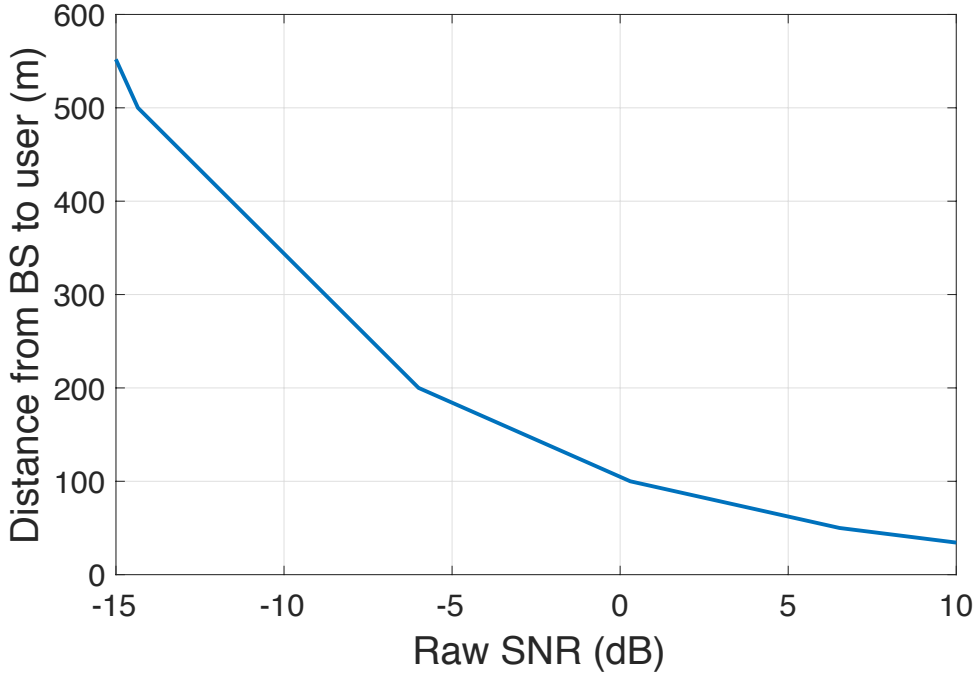

Figure 4.6: Relationship between raw SNR P/σ^2 and distance from BS to user
This relationship is generated by the 3GPP TR 38.901 UMi LOS pathloss channel model (summarized in [36]), with 73GHz carrier frequency, 23 dBm maximum user power, -174 dBm/Hz thermal noise density, 5 dB receiver noise figure at BS, and a bandwidth of 100 MHz.

4.5.2 Algorithm Details and Parameters

The proposed algorithm *hiePM* is based on sequential beam refinement but implements additional coding techniques; thus we focus our comparison to that of the bisection refinement of [21] to highlight that the use of this coding strategy differentiates *hiePM* from existing beam refinement strategies. For the bisection algorithm of [21], the number of beamforming vectors in each level is 2, and the power is allocated according to the equal power distribution strategy.

For both $hiePM$ and the bisection algorithm of [21], the finite set of beamforming vectors $\mathcal{W}^S$ are designed with a hierarchical structure where individual beamforming vectors

$\mathbf{w}(\mathcal{D}_l^m) \in \mathcal{W}_l$ are designed with the objective of near-constant gain for directions $\phi \in \mathcal{D}_l^m$ and zero otherwise (Assumption 4). In other words, each beamforming vector solves

$$\mathbf{A}_{BS}^H \mathbf{w}(\mathcal{D}_l^m) = C_s \mathbf{G}_{\mathcal{D}_l^m}, \tag{4.33}$$

where $\mathbf{A}_{BS}$ is the $N \times (1/\delta)$ matrix of array manifolds

$$\mathbf{A}_{BS} = [\mathbf{a}(\phi_1), \mathbf{a}(\phi_2), \dots \mathbf{a}(\phi_{1/\delta})] \tag{4.34}$$

C_s is a normalization constant, and $\mathbf{G}_{\mathcal{D}_l^m}$ is an $1/\delta \times 1$ vector indicating probed directions

$$\mathbf{G}_{\mathcal{D}_l^m} = \begin{cases} 1, & \text{if } \phi \in H_l^m \\ 0, & \text{if } \phi \notin H_l^m \end{cases}. \tag{4.35}$$

An approximate solution to (4.33), obtained using the pseudo inverse is

$$\mathbf{w}(\mathcal{D}_l^m) = C_s (\mathbf{A}_{BS} \mathbf{A}_{BS}^H)^{-1} \mathbf{A}_{BS} \mathbf{G}_{\mathcal{D}_l^m}. \tag{4.36}$$

The resulting beamforming weight vectors, applied with phase and gain control at each element, produce beam patterns with improved sidelobe suppression and near-constant gain in the intended search directions. We can use these vectors in our simulations to ensure that our analytic Assumption 4.4 is a matter of analytic simplicity but is not consequential in a realistic setting.

To represent non-adaptive algorithms that are a variation of random coding, such as the random hashing algorithm of [25], we compare to the random search algorithm that randomly scans the region of interest. The random search algorithm uses a codebook $\mathcal{W}^{\frac{q}{n}}$ of size $|\mathcal{W}^{\frac{q}{n}}| = \binom{n}{q}$ which consists of all possible beam patterns with total width $\frac{q}{n}|\theta_{\max} - \theta_{\min}|$, where the region of interest $|\theta_{\max} - \theta_{\min}|$ has been divided into n non-overlapping directions, and q directions

are probed in each beam pattern. At any time instant t, the random search algorithm randomly selects a beamforming vector $\mathbf{w}_{t+1}$ from the pre-designed codebook $\mathcal{W}_n^q$. A fixed number of measurements τ are taken. The discretization parameter is set to $n = 1/\delta = 128$, we set $\tau = 28$, and we plot various values of q. The performance of $hiePM$ over the optimized choice of q is important as it provides a first order insight into "adaptivity gain."

4.5.3 Simulation Results

In this section, we provide a comparative analysis of our proposed *hiePM* algorithm against prior work [21] and [25]. In particular, Fig. 4.7 plots the error probability as a function of raw SNR. In summary, Fig. 4.7 shows that both fixed-length and variable-length stopping variations of *hiePM* outperform the bisection algorithm of [21] as well as random coding, or random-hash based solutions of [25]. We also note that random beamforming codebooks outperform the bisection algorithm of [21] as expected by our analysis in Remark 4.6. By optimizing the coding rate q, and comparing against *hiePM* one can also fully characterize the adaptivity gain. Finally, we note that our analytic upper bound (in Fig. 4.5) is rather loose and $hiePM$ performs significantly better than our analysis predicted.

Probability of Error versus Raw SNR

For the system and channel described above, we conduct the simulation scenario where the average error probability as a function of raw SNR is analyzed. We take the error probability of the AoA estimation to be the probability of selecting an erroneous final beamforming vector $\text{Prob}\{\hat{\mathbf{w}}(z_{1:\tau}, \mathbf{w}_{1:\tau}, \epsilon, \delta) \neq \mathbf{w}(\{\phi\})\}$.

For clarity, from now on we use the naming convention *hiePM(stopping-criterion, resolution-criterion)* to specify the case selections of stopping criteria and resolution-criteria in the proposed *hiePM* algorithm (detailed in algorithm 1). To ensure a reasonable comparison, we first discuss *hiePM*(FL, FR) which is most comparable to the bisection algorithm of [21] and the

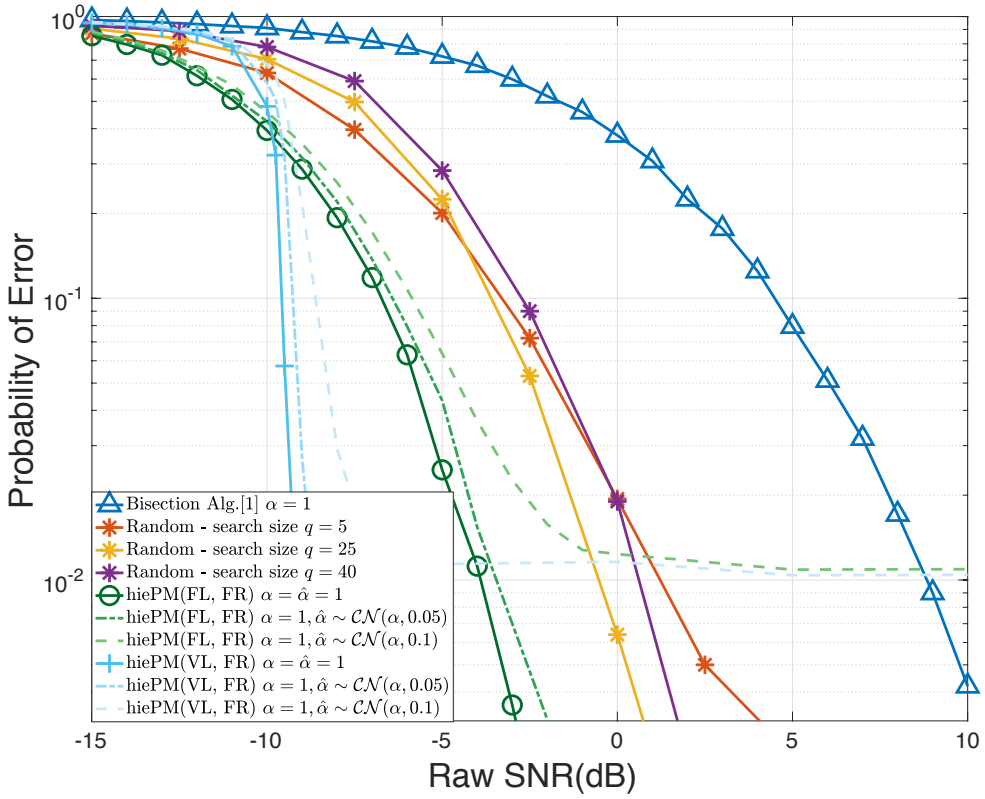

Figure 4.7: Comparison of the error probability (static fading).
We compared *hiePM*, the random search algorithm, and the vanilla bisection algorithm of [21] as a function of raw SNR. Initial access length $\tau = 28$, achieved under 2 ms using the 5G NR PRACH format B4 [35] ($E[\tau] = 28$ for variable-length stopping type), is used for acquiring the AoA with resolution $1/\delta = 128$.

random search algorithm described above. Fig. 4.7 shows the superior performance of *hiePM*(FL, FR) with fixed and known fading coefficient $\alpha = 1$ over both the bisection algorithm of [21] and the random search algorithm. We also notice that under reasonable tuning of parameter q, even the non-adaptive random search algorithm achieves better performance than the adaptive bisection algorithm of [21]. As we expected from Remark 4.6, the best performance is achieved by *hiePM* due to its sequential coding strategy, while the performance of the bisection algorithm of [21] suffers as it resembles a repetition code.

Improvements in the probability of error are further demonstrated by *hiePM*(VL, FR) with targeted error probability ϵ selected such that $\mathbb{E}[\tau] = 28$. The benefit of allowing a variable stopping time is evident in that it causes a sharp drop in the error probability at approximately -10 dB raw SNR. The error probability upper bound (Corollary 4.1) on *hiePM*(VL, FR) is also plotted. We see in Fig. 4.7 that this upper bound predicts the sharp slope of *hiePM*(VL, FR), theoretically guaranteeing a significant performance improvement in error probability for *hiePM*(VL, FR) over the bisection algorithm of [21] and the random search algorithm for large SNR. Further exploration of this sharp transition in the low (< 0 dB) raw SNR regime is beyond the scope of this dissertation.

Investigating effects of imperfect channel knowledge

The bisection algorithm of [21] learns the AoA without any knowledge of the channel. It combines the procedures of AoA estimation and channel estimation. On the other hand, our proposed algorithm, *hiePM*, requires the knowledge of the fading coefficient α in the posterior update. While a channel estimation procedure can be used to learn α preceding *hiePM*, perhaps in a short preliminary phase, we explore the performance achieved using an estimate for the fading coefficient $\hat{\alpha}$ instead. We find that the improved performance by *hiePM* over the bisection algorithm of [21] and the random search algorithm holds even without full knowledge of the fading coefficient α. To see this, we consider the case of a mismatched update rule with an estimate for

the fading coefficient $\hat{\alpha} = \mathcal{CN}(\alpha, \sigma_\alpha^2)$. We see that even under a reasonably mismatched estimate of the fading coefficient ($\sigma_\alpha^2 = 0.05$), all *hiePM* based algorithms still achieve a lower probability of error than the bisection algorithm of [21]. In other words, the degradation due to estimation error is far less significant, saturating in error probability only at high SNR (> 5 dB). As we can see in Fig. 4.7 using a mismatched estimate of the fading coefficient α causes the performance of probability of error to saturate at large SNR (> 0 dB). This phenomenon reflects the events when the estimate of the fading coefficient α is very inaccurate, which occurs with a constant probability regardless of the SNR value, due to our modeling of $\hat{\alpha}$. In practice, the accuracy of the estimate $\hat{\alpha}$ improves as SNR increases. However, this is beyond the scope of this dissertation, and we refrain from investigating such effects.

Spectral efficiency versus Raw SNR

Practically speaking, a more efficient AoA learning algorithm is advantageous in that it both reduces communication overhead and increases the accuracy of the final beamforming vector. Next, we empirically analyze the overall performance of a communication link established by the proposed algorithm *hiePM* in terms of the data spectral efficiency. The spectral efficiency is evaluated according to equation (4.8), using the final beamforming vector $\hat{\mathbf{w}}(z_{1:\tau}, \mathbf{w}_{1:\tau}, \epsilon, \delta)$ resulting from each algorithm. Due to its dependence on the final beamforming vector, $\hat{\mathbf{w}}$, the spectral efficiency encompasses both the design parameters ϵ and δ, and also the total communication time. We set the total communication time frame to $T = 100 \times \mathbb{E}[\tau]$ (further optimization of this parameter beyond the scope of this dissertation).

Fig. 4.8 shows the gain in spectral efficiency obtained by various implementations of the proposed algorithm *hiePM* over both the bisection algorithm of [21] and the random search algorithm for the system and channel described above as a function of raw SNR. We also provide spectral efficiency without beamforming for reference. Fig. 4.8 shows that all variants of *hiePM* outperform the bisection algorithm of [21] significantly in the SNR regime of (-5dB to 5dB). On

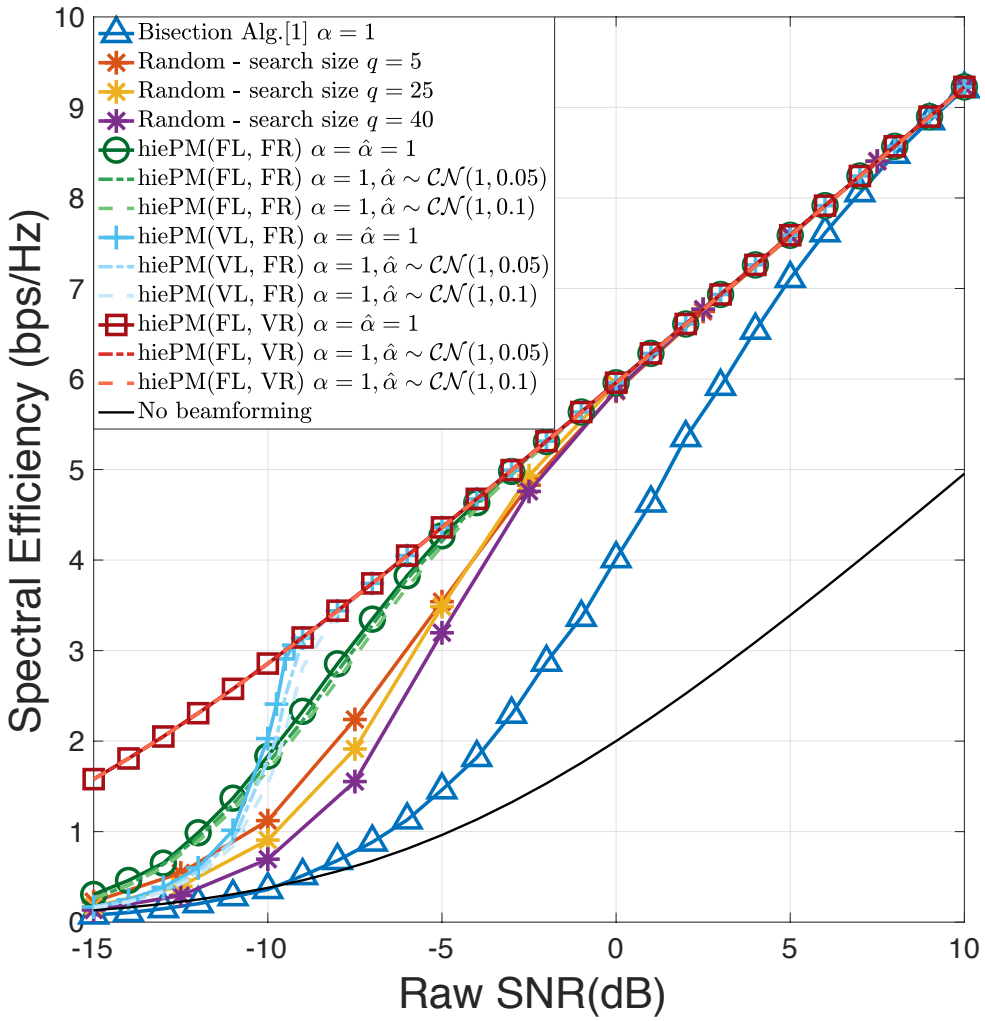

Figure 4.8: Comparison of the spectral efficiency (static fading)
We compare the spectral efficiency obtained by *hiePM*, the random search algorithm, and the vanilla bisection algorithm of [21] as a function of raw SNR P/σ^2. Initial access time $\tau = 28$, achieved under 2 ms using the 5G NR PRACH format B4 [35] ($E[\tau] = 28$ for variable-length stopping). The spectral efficiency is given by (4.8) with the final beamforming vector $\hat{\mathbf{w}}$ designed by the respective algorithm.

the other hand, the performance of the bisection algorithm of [21] approaches the performance of *hiePM* as SNR grows beyond 7dB or so. Fig. 4.8 also shows the benefits of opportunistically selecting the resolution of the final beam as is done under *hiePM*(FL, VR) according to (4.15). This advantage is particularly important in a low SNR regime (-15dB to -7dB) where *hiePM*(FL, VR) adapts the final beamforming vector to the final posterior distribution at time τ, hence setting the angular resolution of the communication beam opportunistically. Moreover, this significant performance improvement is robust to channel estimation error and a mismatched estimate of the fading coefficient $\hat{\alpha}$. To understand this phenomenon, we refer to Fig. 4.7, where the error probability of finding the correct beam with resolution $1/\delta$, when SNR is less than -5dB, is non-negligible under *hiePM*(FL, FR), and *hiePM*(VL, FR).

4.5.4 Time varying channel

In this subsection, we discuss the channel coherence time and how our initial beam alignment algorithm works in a time-varying channel scenario. We verify our framework by extending our algorithms to be adapted to a simple Rician AR-1 model. Let us consider a Rician AR-1 fading channel of factor K_r with perfect knowledge of the operating SNR (large-scale fading) as well as perfect frequency/phase synchronization, i.e., the fading coefficient is given as

$$\alpha_t = \sqrt{\frac{K_r}{1+K_r}}\mu + \sqrt{\frac{1}{1+K_r}}\beta_t,\ t = 0, 1, 2, ..., \tau. \tag{4.37}$$

where $\mu = 1$ and $\beta_t \sim CN(0, 1)$ is the complex Gaussian diffusion AR process given as

$$\beta_{t+1} = \beta_t\sqrt{1-g} + e_t\sqrt{g},\ \ t = 0, 1, 2, ..., \tau, \tag{4.38}$$

where $e_t \sim \mathcal{CN}(0, 1)$ is the independent noise term. The correlation parameter g is set such that

$$1 - (1-g)^{14T_c} = 0.5, \tag{4.39}$$

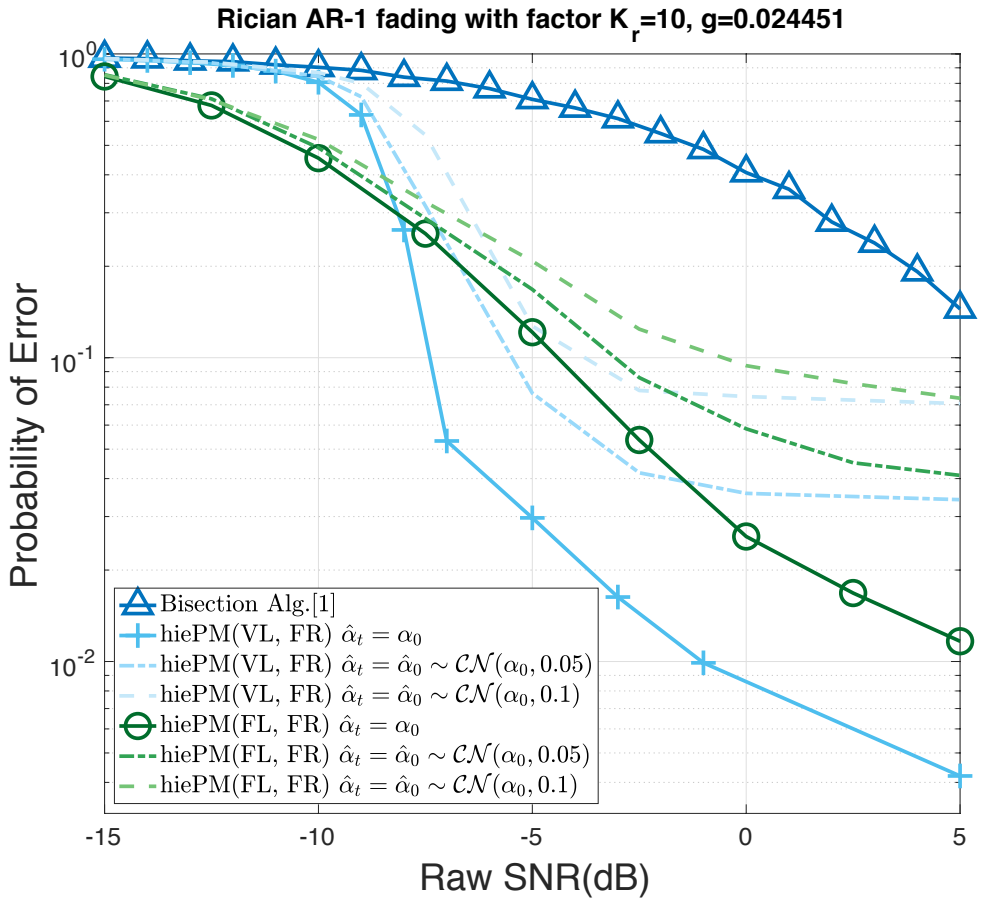

Figure 4.9: Comparison of the error probability (time-varying fading)
We compared *hiePM*, the random search algorithm, and the vanilla bisection algorithm of [21] as a function of raw SNR P/σ^2 under Rician AR-1 fading with factor $K_r = 10$, and $g = 0.024451$ (i.e. $T_c = 2$). Initial access length $\tau = 28$, achieved under 2 ms using the 5G NR PRACH format B4 [35] ($E[\tau] = 28$ for variable-length stopping type), is used for acquiring the AoA with resolution $1/\delta = 128$.

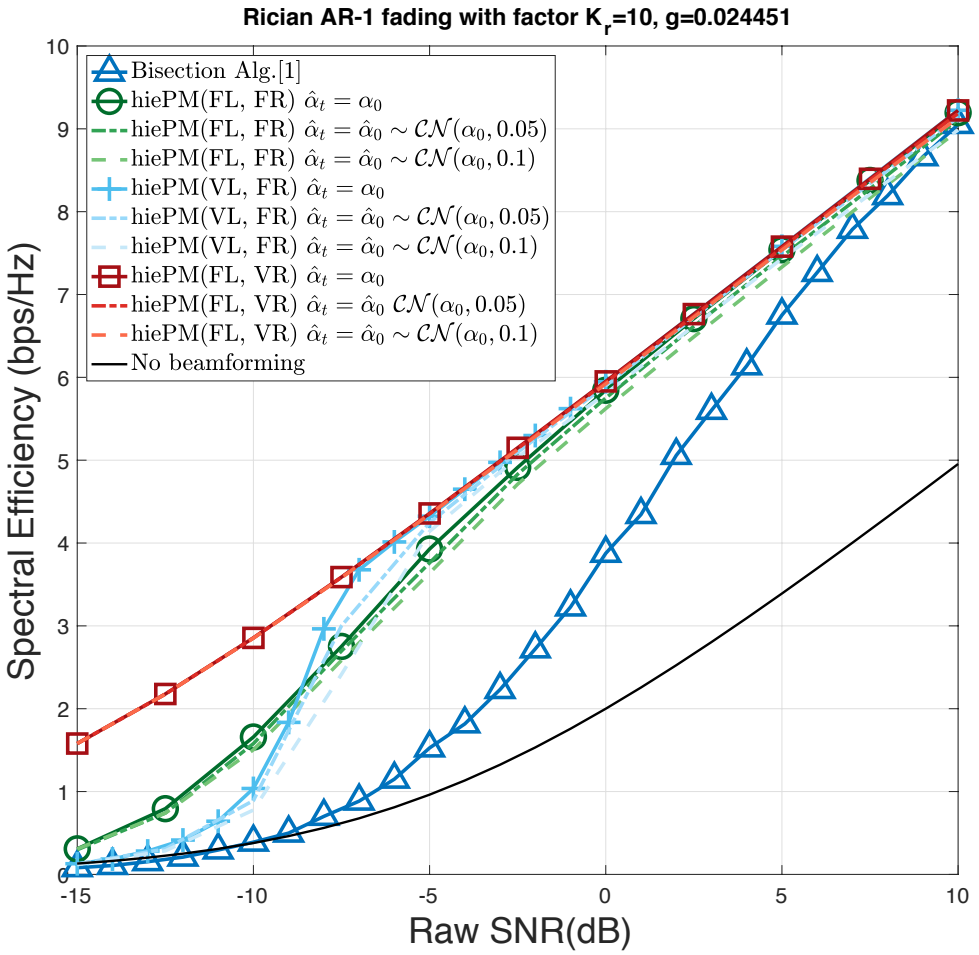

Figure 4.10: Comparison of the spectral efficiency (time-varying channel)
We compared the spectral efficiency obtained by *hiePM* and the vanilla bisection algorithm of [21] as a function of raw SNR P/σ^2 under Rician AR-1 fading with factor $K_r = 10$, and $g = 0.024451$, (i.e. $T_c = 2$). Initial access time $\tau = 28$, achieved under 2 ms using the 5G NR PRACH format B4 [35] ($E[\tau] = 28$ for variable-length stopping). The spectrum efficiency is given by (8) - in original manuscript with the final beamforming vector $\hat{\mathbf{w}}$ designed by the respective algorithm.

where T_c is the 50% time of the diffusion β_t in ms (recall that we assume a system with 14 beam slots in $1ms$). Combining (4.37) and (4.38), the Rician AR-1 model can be written as

$$\begin{aligned}\alpha_{t+1} =& \sqrt{\frac{K_r}{1+K_r}}\mu + \left(\alpha_t - \sqrt{\frac{K_r}{1+K_r}}\mu\right)\sqrt{1-g} \\ &+ e_t\sqrt{\frac{g}{1+K_r}}, \;\; t = 0, 1, 2, ..., \tau.\end{aligned} \tag{4.40}$$

Fig. 4.9 demonstrates the robustness of $hiePM$ to the Rician AR-1 fading channel model described above with coherence time $T_c = 2$ ms of the AR process β_t, and a Rician factor $K_r = 10$ (this is a reasonable value for, e.g. indoor mmWave channel models [37]). We again use an erroneous/mismatched and fixed estimate of the fading coefficient $\hat{\alpha}_t = \hat{\alpha}_0 \sim \mathcal{CN}(\alpha_0, \sigma_\alpha^2)$ for $t = 1, 2, \ldots, \tau$. In particular, we compare the performance achieved by our $hiePM$ algorithms with different degrees of knowledge of the fading estimate (i.e., $\sigma_\alpha^2 = 0, 0.05, 0.1$) against the performance obtained by the bisection algorithm of [21]. As expected, the performance of the probability of error worsens for both algorithms in a time-varying fading, as compared to the static model $\alpha = 1$ in Fig. 4.7. However, even under a mismatched and fixed estimate of the fading coefficient $\hat{\alpha}_t$, our main conclusions still hold. In particular, the performance degradation in spectral efficiency due to time-varying channel is almost negligible, as we show in Fig. 4.10 (note that this is the effect of time-varying channel during initial access, where for communication phase the spectral efficiency is calculated by (4.8) as our focus is the impact of a time-varying channel on the initial beam alignment). Our variable resolution algorithm $hiePM$(FL,VR) (with opportunistic choice of final beamwidth) is unaffected in terms of spectral efficiency, while the $hiePM$(FL,FR) and $hiePM$(VL,FR) cases incur a small loss of spectral efficiency due to the degree of the mismatched estimate (i.e., correlated to the severity of σ_α^2).

4.6 Conclusion and Future Work

In this chapter, we addressed the initial access problem for mmWave communication with beamforming techniques. With a single-path channel model, the proposed sequential beam search algorithm $hiePM$ demonstrates a systematic way of actively learning an optimal beamforming vector among the hierarchical beamforming codebook of [21].

Using a single-path channel model, we characterize the performance of the proposed learning algorithm $hiePM$ by the resolution and the error probability of learning the AoA, which are closely related to the link quality established by the final beamforming vector. We analyze $hiePM$ by giving an upper bound of the expected search time $\tau_{\epsilon,\delta}$ required to achieve a resolution $\frac{1}{\delta}$ and error probability ϵ in Theorem 4.1. As a corollary, we provide an upper bound on the error probability achieved with a search time $\mathbb{E}[\tau_{\epsilon,\delta}]$, and resolution $\frac{1}{\delta}$ for $hiePM$ in Corollary 4.1. We also specialize our analysis and compare the error exponent obtained by $hiePM$ and the bisection method in [21]. A higher error exponent is shown across a wide range of SNR even when only 1-bit of information about the measurement is available to $hiePM$. The numerical simulations show a significant improvement on the communication rate over the previous vanilla bisection algorithm of [21] and the random search algorithm from [25], demonstrating the first work of possibilities of standalone mmWave communication.

The future direction of this work includes generalizing the channel model and considering multiple paths, as well as learning the fading coefficient together with the direction during the beam search. On the theoretical end, closing the gap between the upper bound of error probability and its actual performance (demonstrated in Fig. 4.7) is worth pursuing of theoretical interest. On the practical side, reducing the computation complexity of posterior and the need of the statistics is helpful for implementation purpose.

4.7 Optimal Threshold for 1-bit measurement model

The complete 1-bit measurement model in Sec. 4.3.4 is written as

$$\begin{aligned} y_{t+1} &= \alpha\sqrt{P}\mathbf{w}_{t+1}^H\mathbf{a}(\phi) + \mathbf{w}_{t+1}^H\mathbf{n}_{t+1} \\ z_{t+1} &= \mathbb{1}(|y_{t+1}|^2 > v_t) \\ &= \mathbb{1}(\phi \in H_{l_t}^{m_t}) \oplus u_t(\phi), \;\; u_t(\phi) \sim \text{Bern}(p_t(\phi)) \end{aligned} \tag{4.41}$$

Lemma 4.1. *The threshold v_t that minimizes the maximum flipping probability $p_t(\phi)$ for all ϕ is given by the solution of the following equation*

$$\int_0^{v_t} \textit{Rice}(x; PG, \sigma^2)\, dx = \int_{v_t}^{\infty} \textit{Rice}(x; Pg, \sigma^2)\, dx, \tag{4.42}$$

where

$$\begin{aligned} G &:= \min_{\phi \in H_{l_t}^{m_t}} |\mathbf{w}^H(H_{l_t}^{m_t})\mathbf{a}(\phi)|^2 \\ g &:= \max_{\phi \in [\theta_{min}, \theta_{max}] \setminus H_{l_t}^{m_t}} |\mathbf{w}^H(H_{l_t}^{m_t})\mathbf{a}(\phi)|^2. \end{aligned} \tag{4.43}$$

Proof. Since $|y_t| \sim \text{Rice}(P|\mathbf{w}_t^H\mathbf{a}(\phi)|, \sigma^2)$, we can write the flipping probability $p_t(\phi)$ as:

if $\phi \in H_{l_t}^{m_t}$,

$$\begin{aligned} p_t(\phi) &= \int_0^{v_t} \text{Rice}(x; P|\mathbf{w}^H(H_{l_t}^{m_t})\mathbf{a}(\phi)|^2, \sigma^2)\, dx \\ &\leq \int_0^{v_t} \text{Rice}(x; PG, \sigma^2)\, dx, \end{aligned} \tag{4.44}$$

and if $\phi \notin H_{l_t}^{m_t}$,

$$\begin{aligned} p_t(\phi) &= \int_{v_t}^{\infty} \text{Rice}(x; P|\mathbf{w}^H(H_{l_t}^{m_t})\mathbf{a}(\phi)|^2, \sigma^2)\, dx \\ &\leq \int_{v_t}^{\infty} \text{Rice}(x; Pg, \sigma^2)\, dx, \end{aligned} \tag{4.45}$$

where the upper bound in (4.44) and (4.45) is reached by the minimizer and maximizer in 4.43, respectively. Since (4.44) is increasing in v_t and (4.45) is decreasing in v_t, setting them equal

gives the minimax optimizer. □

Chapter 4, in full, has been submitted for publication as Sung-En Chiu, Nancy Ronquillo and Tara Javidi, Active Learning and CSI Acquisition for mmWaveInitial Alignment, available on arXiv:1812.07722. The dissertation author was the primary investigator and author of this paper

Chapter 5

Conclusions and Future Works

In this dissertation, we formulated the query-dependent noisy search problem with practical metrics motivated by many applications in networking [10], robotics [13] and wireless communication [38]. We proposed three novel search strategies $sortPM$, $dyaPM$ and $hiePM$. The expected *query time complexity* is analyzed under a unified framework of the EJS divergence. We show that $sortPM$, $dyaPM$ both achieve asymptotic optimality in expected search time, whereas $hiePM$ achieves a sub-optimal time complexity. Low *computational and Memory complexity* implementation of $dyaPM$ and $hiePM$ is given in details in Algorithm 2.3 and 2.2, showing a logarithmic reduction over prior works [6, 39]. Furthermore, not only the low complexity of the proposed strategies but also *query geometry* of the strategies is shown to be suitable for practical applications. The connected *query geometry* of $dyaPM$ is suitable for applications in visual search [6]. The hierarchical *query geometry* of $hiePM$ ($\mathcal{H}$) is suitable for applications such as heavy hitter detection [10], hierarchical beamforming [38] and bit-wise feedback coding [16]. Numerically, we show that all the proposed search strategies have superior non-asymptotic performance.

We addressed the application of the proposed algorithm $hiePM$ on the data transmission problem with noiseless feedback in Chapter 3, which demonstrated a simple adaptive encoding

scheme and allowed a bit-wise encoding. We also considered the application of $hiePM$ in the initial beam alignment problem in 5G mmWave communication using beamforming in Chapter 4. With a single-path channel model, the problem is reduced to actively searching the Angle-of-Arrival (AoA) of the signal sent from the user to the Base Station (BS). $hiePM$ is applied to adaptively and sequentially choose the beamforming from the hierarchical beamforming codebook. The proposed algorithm is compared to prior works of initial beam alignment that employs linear beam search, repeat binary search, or random beam search, respectively, and gives the state-of-art performance in terms of both AoA estimation error at the end of the initial alignment, and the spectral efficiency during the communication phase.

5.1 Multi-Dimension Extension

By the hierarchical query geometry, $hiePM$ offers a natural generalization to a higher dimension or any structure that can be bisected. Fig. 5.1 illustrates an example of two-dimensional search. $hiePM$ is therefore readily applicable to the visual search problem with the abstract formulation in [6]. Applying $hiePM$ to more practical settings such as a target localization using drone [40] is one of interesting extension of this dissertation. On the other hand, by Theorem 2.2, we know that the (expected) number of queries grows only linearly in the number of dimensions. This benefit also renders $hiePM$ suitable for active learning problem where a learner tries to learn a classifier in multi-dimension by actively querying examples for labels.

5.2 Multiple Targets

Generalizing the work in this dissertation to deal with the case of multiple targets is also an important research direction. Search problem that involves multiple targets are in the scope of *Group Testing* [41] and/or *Compressive Sensing*.

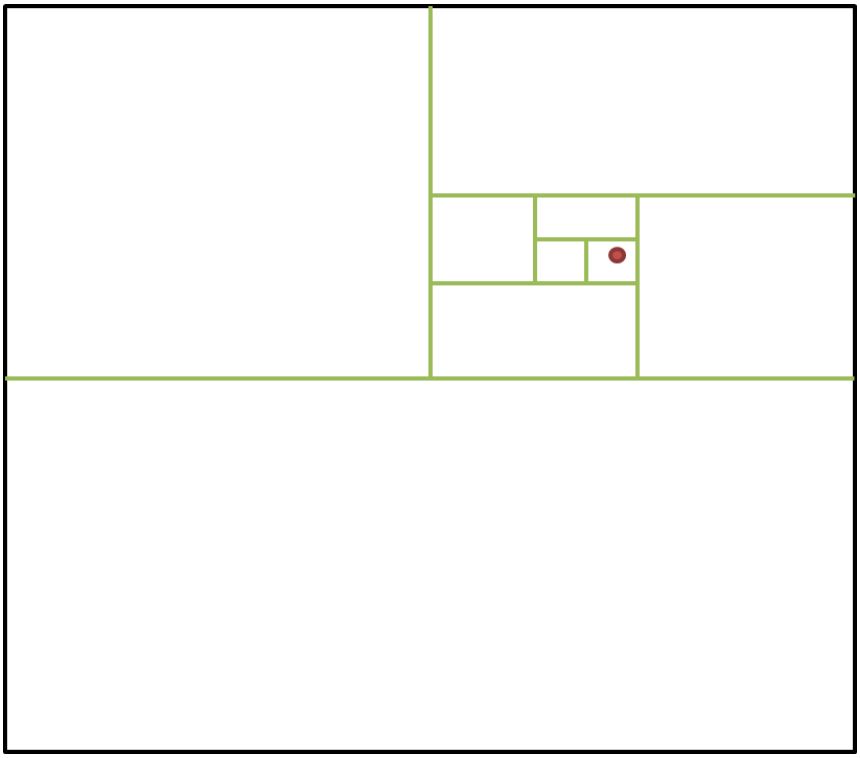

Figure 5.1: Hierarchical Query Set in 2D

As opposed to non-adaptive noisy group testing, no known algorithm can achieve the converse bound in the number of tests (queries) of adaptive noisy group testing. One of the difficulties is that it unclear incorporate the observations into the design of the test. A simple extension of the proposed algorithms in this dissertation to noisy adaptive group testing is to track the posterior of the locations of the multiple targets and then apply the Posterior Matching. However, tracking such a high dimensional posterior can be problematic. Simplifying tracking of the posterior by the hierarchical structure of $hiePM$ provides a possible approach of solving the open problem in noisy adaptive group testing, as well as providing practical algorithms for noisy group testing.

On the other hand, in some applications such as the initial beam alignment in Chapter 4, the measurements from multiple users or multiple sub-paths may create destructive adding. Randomness in phase or amplitude may offer an advantage over constant amplitude within the

query area. A combination of the query size reduction by $hiePM$ and the amplitude/phase randomness from Compressive Sensing may be a proper solution for such an issue.

Bibliography

[1] A. Rényi, "On a problem in information theory," *Magyar Tudományos Akadémia Matematikai Kutató Intézetének Közleményei (in Hungarian)*, no. 6, pp. 505–516, 1961.

[2] M. Horstein, "Sequential transmission using noiseless feedback," *Information Theory, IEEE Transactions on*, vol. 9, no. 3, pp. 136–143, Jul 1963.

[3] M. V. Burnashev and K. Zigangirov, "An interval estimation problem for controlled observations," *Problemy Peredachi Informatsii*, vol. 10, no. 3, pp. 51–61, 1974.

[4] S. M. Ulam, *Adventures of a mathematician.[Book (life of SM Ulam)].* Univ of California Press, 1976.

[5] M. B. Or and A. Hassidim, "The Bayesian learner is optimal for noisy binary search (and pretty good for quantum as well)," *Proceedings - Annual IEEE Symposium on Foundations of Computer Science, FOCS*, pp. 221–230, 2008.

[6] M. Naghshvar and T. Javidi, "Two-Dimensional Visual Search," *IEEE International Symposium on Information Theory*, pp. 1262–1266, 2013.

[7] ——, "Active sequential hypothesis testing," *Annals of Statistics*, vol. 41, no. 6, pp. 2703–2738, 2013.

[8] O. Shayevitz and M. Feder, "Optimal feedback communication via posterior matching," *Information Theory, IEEE Transactions on*, vol. 57, no. 3, pp. 1186–1222, March 2011.

[9] N. Ronquillo and T. Javidi, "Multiband noisy spectrum sensing with codebooks," in *Asilomar Conference on Signals, Systems and Computers*, no. 978. IEEE, 2017, pp. 1687–1691.

[10] C. Wang, K. Cohen, and Q. Zhao, "Information-Directed Random Walk for Rare Event Detection in Hierarchical Processes." *arXiv Information Theory (cs.IT)*, pp. 1–30, 2018. [Online]. Available: http://arxiv.org/abs/1612.09067

[11] Y. Kaspi, O. Shayevitz, and T. Javidi, "Searching with Measurement Dependent Noise," *IEEE Transactions on Information Theory*, vol. 64, no. 4, pp. 2690–2705, 2018.

[12] C. E. Shannon, "The zero-error capacity of a noisy channel," *IRE. Trans. Info. Theory*, vol. IT-2, pp. 8–19, Sept 1956.

[13] M. Naghshvar, T. Javidi, and M. Wigger, "Extrinsic Jensen-Shannon divergence: Applications to variable-length coding," *IEEE Transactions on Information Theory*, vol. 61, no. 4, pp. 2148–2164, 2015.

[14] S. E. Chiu and T. Javidi, "Sequential measurement-dependent noisy search," in *2016 IEEE Information Theory Workshop, ITW 2016*, 2016.

[15] T. Simsek, R. Jain, and P. Varaiya, "Scalar Estimation and Control With Noisy Binary Observations," *IEEE Transactions on Automatic Control*, vol. 49, no. 9, pp. 1598–1603, 2004.

[16] S.-E. Chiu, A. Lalitha, and T. Javidi, "Bit-wise Sequential Coding with Feedback," in *IEEE International Symposium on Information Theory*, 2018.

[17] Y. Polyanskiy, H. V. Poor, and S. Verd, "Variable-length coding with feedback in the non-asymptotic regime," in *2010 IEEE International Symposium on Information Theory*, June 2010, pp. 231–235.

[18] G. R. Maccartney, J. Zhang, S. Nie, and T. S. Rappaport, "Path loss models for 5G millimeter wave propagation channels in urban microcells," *GLOBECOM - IEEE Global Telecommunications Conference*, pp. 3948–3953, 2013.

[19] T. S. Rappaport, Y. Xing, G. R. MacCartney, A. F. Molisch, E. Mellios, and J. Zhang, "Overview of Millimeter Wave Communications for Fifth-Generation (5G) Wireless Networks-With a Focus on Propagation Models," *IEEE Transactions on Antennas and Propagation*, vol. 65, no. 12, pp. 6213–6230, 2017.

[20] A. F. Molisch, V. V. Ratnam, S. Han, Z. Li, S. L. H. Nguyen, L. Li, and K. Haneda, "Hybrid Beamforming for Massive MIMO: A Survey," *IEEE Communications Magazine*, vol. 55, no. 9, pp. 134–141, 2017.

[21] A. Alkhateeb, O. E. Ayach, G. Leus, and R. W. Heath, "Channel Estimation and Hybrid Precoding for Millimeter Wave Cellular Systems," *IEEE Journal of Selected Topics in Signal Processing*, vol. 8, no. 5, pp. 831–846, 2014.

[22] M. Giordani, M. Mezzavilla, C. N. Barati, S. Rangan, and M. Zorzi, "Comparative analysis of initial access techniques in 5g mmwave cellular networks," in *Proceedings of the 2016 Annual Conference on Information Science and Systems (CISS)*, March 2016, pp. 268–273. [Online]. Available: http://dx.doi.org/10.1109/CISS.2016.7460513

[23] A. Lalitha, N. Ronquillo, T. Javidi, and S. Member, "Improved Target Acquisition RatesWith Feedback Codes," *IEEE Journal of Selected Topics in Signal Processing*, vol. 12, no. 5, pp. 871–885, 2018.

[24] Y. Shabara, C. E. Koksal, and E. Ekici, "Linear Block Coding for Efficient Beam Discovery in Millimeter Wave Communication Networks," *arXiv preprint arXiv:1712.07161*, 2017. [Online]. Available: http://arxiv.org/abs/1712.07161

[25] O. Abari, H. Hassanieh, M. Rodriguez, and D. Katabi, "Millimeter Wave Communications: From Point-to-Point Links to Agile Network Connections," in *Proceedings of the 15th ACM Workshop on Hot Topics in Networks - HotNets '16*, 2016, pp. 169–175. [Online]. Available: http://dl.acm.org/citation.cfm?doid=3005745.3005766

[26] Y. Ding, S. E. Chiu, and B. D. Rao, "Bayesian Channel Estimation Algorithms for Massive MIMO Systems with Hybrid Analog-Digital Processing and Low Resolution ADCs," *IEEE Journal on Selected Topics in Signal Processing*, vol. 12, no. 3, pp. 499–513, 2018.

[27] 3GPP, "NR - Multi-connectivity - Overall description (Stage 2)," *3GPP TS 37.340*, 2018.

[28] M. Naghshvar, T. Javidi, and K. Chaudhuri, "Bayesian Active Learning With Non-Persistent Noise," *IEEE Transactions on Information Theory*, vol. 61, no. 7, pp. 4080–4098, 2015. [Online]. Available: http://ieeexplore.ieee.org/lpdocs/epic03/wrapper.htm?arnumber=7105932

[29] W. Roh, J. Y. Seol, J. H. Park, B. Lee, J. Lee, Y. Kim, J. Cho, K. Cheun, and F. Aryanfar, "Millimeter-wave beamforming as an enabling technology for 5G cellular communications: Theoretical feasibility and prototype results," *IEEE Communications Magazine*, vol. 52, no. 2, pp. 106–113, 2014.

[30] D. Tse and P. Viswanath, *Fundamentals of Wireless Communication, Chapter 07: MIMO I : spatial multiplexing and channel modeling*. Cambridge University Press, 2005.

[31] S. Dasgupta, D. Hsu, and C. Monteleoni, "A general agnostic active learning algorithm," *Nips*, vol. 20, no. 2, pp. 353–360, 2007. [Online]. Available: http://dblp.uni-trier.de/db/conf/nips/nips2007.html#DasguptaHM07

[32] J. Choi, J. Mo, S. Member, and R. W. H. Jr, "Near Maximum-Likelihood Detector and Channel Estimator for Uplink Multiuser Massive MIMO Systems With One-Bit ADCs," *IEEE Transactions on Communications*, vol. 64, no. 5, pp. 2005–2018, 2016.

[33] T. S. Rappaport, *Wireless Communications: Principles and Practice*. NJ: Prentice-Hall, 2002.

[34] V. Va, J. Choi, and R. W. Heath, "The Impact of Beamwidth on Temporal Channel Variation in Vehicular Channels and Its Implications," *IEEE Transactions on Vehicular Technology*, vol. 66, no. 6, pp. 5014–5029, 2017.

[35] X. Lin, J. Li, R. Baldemair, T. Cheng, S. Parkvall, D. Larsson, H. Koorapaty, M. Frenne, S. Falahati, A. Grövlen, and K. Werner, "5g new radio: Unveiling the essentials of the next generation wireless access technology," *CoRR*, vol. abs/1806.06898, 2018.

[36] T. S. Rappaport, Y. Xing, G. R. MacCartney, A. F. Molisch, E. Mellios, and J. Zhang, "Overview of millimeter wave communications for fifth-generation (5g) wireless network-swith a focus on propagation models," *IEEE Transactions on Antennas and Propagation*, vol. 65, no. 12, pp. 6213–6230, Dec 2017.

[37] S. Mukherjee, S. S. Das, A. Chatterjee, and S. Chatterjee, "Analytical calculation of rician k-factor for indoor wireless channel models," *IEEE Access*, vol. 5, pp. 19 194–19 212, 2017.

[38] S.-E. Chiu, N. Ronquillo, and T. Javidi, "Active Learning and CSI acquisition for mmWave Initial Alignment," pp. 1–14, 2018. [Online]. Available: http://arxiv.org/abs/1812.07722

[39] Y. Kaspi, O. Shayevitz, and T. Javidi, "Searching with measurement dependent noise," *2014 IEEE Information Theory Workshop, ITW 2014*, pp. 267–271, 2014.

[40] Y. Lu, Z. Wang, Z. Tang, and T. Javidi, "Target Localization with Drones using Mobile CNNs," in *International Conference on Intelligent Robots and Systems (IROS)*, 2018, pp. 2566–2573.

[41] M. Aldridge, O. Johnson, and J. Scarlett, "Group testing: an information theory perspective," vol. 19, 2019. [Online]. Available: http://arxiv.org/abs/1902.06002

[42] F. Chung and L. Lu, "Concentration Inequalities and Martingale Inequalities: A Survey," *Internet Mathematics*, vol. 3, no. 1, pp. 79–127, 2006.

Appendix A

Asymptotic Analysis for Expected Query Time Complexity

A.1 Preliminaries: Average Log-Likelihood and the Extrinsic Jensen-Shannon Divergence

In this subsection, we review some useful concepts in [13]. The average log-likelihood of the posterior is defined as

$$U(t) \equiv U(\boldsymbol{\pi}(t)) := \sum_{i=1}^{1/\delta} \pi_i(t) \log \frac{\pi_i(t)}{1-\pi_i(t)}, \tag{A.1}$$

with the following property:

1. $U(t)$ is a submartingale with drift EJS.

$$\mathbb{E}[U(t+1) \mid \boldsymbol{\pi}(t)] = U(t) + EJS(\boldsymbol{\pi}(t), \gamma), \tag{A.2}$$

where EJS is the Extrinsic Jensen-Shannon divergence, defined as

$$EJS(\boldsymbol{\pi}(t), \gamma) = \sum_{i=1}^{1/\delta} \pi_i(t) D\left(P_{y_t|i,S_{t+1}} \middle\| P_{y_{t+1}|\neq i,S_{t+1}}\right) \tag{A.3}$$

with

$$\begin{aligned} P_{y_{t+1}|i,S_{t+1}} &:= \mathbb{P}(Y_{t+1} = y_{t+1} \mid \theta = i; S_{t+1} = \gamma(\boldsymbol{\pi}(t))) \\ &= \mathbb{P}(Y_{t+1} = y_{t+1} \mid X_{t+1} = \mathbb{1}(i \in S_{t+1})) \end{aligned} \tag{A.4}$$

and

$$\begin{aligned} P_{y_{t+1}|\neq i,S_{t+1}} &:= \mathbb{P}(Y_{t+1} = y_{t+1} \mid \theta \neq i; S_{t+1}) \\ &= \sum_{j \neq i} \frac{\pi_j(t)}{1 - \pi_i(t)} P_{y_{t+1}|j,S_{t+1}}. \end{aligned} \tag{A.5}$$

2. Initial value $U(0) = -\log(\frac{1}{\delta} - 1)$ is directly related to the logarithm of resolution and hence the targeting rate

3. Level crossing of U is directly related to the error probability, since $\pi_i(t) < 1 - \epsilon \; \forall i \; \Rightarrow U(t) < \log \frac{1-\epsilon}{\epsilon}$.

Analyzing the random drift from time 0 with the initial value $U(0)$ up to the first crossing time $\nu := \min\{t : U(t) \geq \log \frac{1}{\epsilon}\}$ is closely related to the expected drift given by EJS. In particular, we can then establish an upper bound for the expected targeting time $\mathbb{E}[\tau_{\epsilon,\delta}]$ in terms of the predefined error probability ϵ and the resolution δ. Specifically we have the following theorem:

Fact A.1 (Theorem 1 in [13])**.** *Define*

$$\tilde{\pi} := 1 - \frac{1}{1 + \max\{\log(1/\delta), \log(1/\epsilon)\}}. \tag{A.6}$$

For adaptive search strategy with search region S_t, if

$$EJS(\boldsymbol{\pi}(t), \gamma) \geq R \quad \forall t \geq 0 \tag{A.7}$$

and

$$EJS(\boldsymbol{\pi}(t),\gamma) \geq \tilde{\pi}E \quad \forall t \geq 0 \textit{ s.t. } \max_i \pi_i(t) \geq \tilde{\pi}, \tag{A.8}$$

we have the expected targeting time associated with error probability ϵ and resolution δ bounded by

$$E[\tau_{\epsilon,\delta}] \leq \frac{\log(1/\delta)}{R} + \frac{\log(1/\epsilon)}{E} + f_{R,E}(\epsilon,\delta) \tag{A.9}$$

where $f_{R,E}(\epsilon,\delta) = \frac{\log\log\frac{1}{\delta\epsilon}}{R} + \frac{1}{E} + \frac{96}{RE}(\frac{1-p[\delta]}{p[\delta]})^2$.

Proof. The proof of Fact A.1 follows similarly the proof of [Theorem 1, [13]]. □

Fact A.2. *For both search strategies $sortPM$ and $dyaPM$ with resolution $1/\delta$ and reliability ϵ, we have*

$$EJS(\boldsymbol{\pi}(t),\gamma) \geq I(1/2, p[\delta|S_{t+1}|]),\ \forall\, t \tag{A.10}$$

$$EJS(\boldsymbol{\pi}(t),\gamma) \geq \tilde{\boldsymbol{\pi}} C_1(p[\delta]),\ \forall \max_i \boldsymbol{\pi}_i \geq \tilde{\pi}, \tag{A.11}$$

where $\tilde{\pi} := 1 - \frac{1}{1+\max\{\log(1/\delta),\log(1/\epsilon)\}}$.

Proof. The proof of Fact A.2 follows along the proof of [Proposition 3, [13]]. □

Fact A.3. *The absolute difference between $U(\boldsymbol{\pi}(t+1))$ and $U(\boldsymbol{\pi}(t))$ is bounded by the entropy of $\boldsymbol{\pi}(t)$, written as*

$$|U(\boldsymbol{\pi}(t+1)) - U(\boldsymbol{\pi}(t))| \leq \log\frac{1-p_{min}}{p_{min}} + H(\boldsymbol{\pi}(t)) + e, \tag{A.12}$$

Proof.

$$
\begin{aligned}
&|U(\boldsymbol{\pi}(t+1)) - U(\boldsymbol{\pi}(t))| \\
&= \sum_{i=1}^{1/\delta} \pi_i(t+1) \log \frac{\pi_i(t+1)}{1-\pi_i(t+1)} - \sum_{i=1}^{1/\delta} \pi_i(t) \log \frac{\pi_i(t)}{1-\pi_i(t)} \\
&\leq \sum_{i=1}^{1/\delta} \pi_i(t+1) \left| \log \frac{\pi_i(t+1)}{1-\pi_i(t+1)} - \log \frac{\pi_i(t)}{1-\pi_i(t)} \right| + \sum_{i=1}^{1/\delta} |\pi_i(t+1) - \pi_i(t)| \left| \log \frac{\pi_i(t)}{1-\pi_i(t)} \right| \\
&\overset{(a)}{\leq} \log \frac{1-p_{\min}}{p_{\min}} + \sum_{\pi_i(i)<\frac{1}{2}} \pi_i(t)(1-\pi_i(t)) \log \frac{1-\pi_i(t)}{\pi_i(t)} + \sum_{\pi_i(i)\geq\frac{1}{2}} \pi_i(t)(1-\pi_i(t)) \log \frac{\pi_i(t)}{1-\pi_i(t)} \\
&\leq \log \frac{1-p_{\min}}{p_{\min}} + H(\boldsymbol{\pi}(t)) + \max_x x \log \frac{1}{x},
\end{aligned}
\tag{A.13}
$$

where (a) is by lemma 6 in [13] and that $p[\cdot] \geq p_{\min}$. □

Fact A.4 (Lemma 2 in [13])**.** *The EJS divergence is lower bounded by the Jensen Shanon (JS) divergence :*

$$EJS(\boldsymbol{\pi}(t), \gamma) \geq JS(\boldsymbol{\pi}(t), \gamma), \tag{A.14}$$

where

$$JS(\boldsymbol{\pi}(t), \gamma) = \sum_{i=1}^{1/\delta} \pi_i(t) D\left(P_{y_t|i,S_{t+1}} \middle\| P_{y_{t+1}|S_{t+1}}\right) \tag{A.15}$$

with $P_{y_{t+1}|S_{t+1}} := \sum_i \pi_(t) P_{y_{t+1}|i,S_{t+1}}$.

Fact A.5. *Using the search strategy* $hiePM$ *with resolution* $1/\delta$ *and reliability* ϵ *on codebook* $\mathcal{W}^L$ *with* $L = \log_2(1/\delta)$*, we have*

$$EJS(\boldsymbol{\pi}(t), \gamma_h) \geq I(1/3, p[\delta|D_{l_{t+1}}|]),\ \forall\, t \tag{A.16}$$

$$EJS(\boldsymbol{\pi}(t), \gamma_h) \geq \tilde{\boldsymbol{\pi}} C_1(p_{min}),\ \forall \max_i \boldsymbol{\pi}_i \geq \tilde{\pi}, \tag{A.17}$$

where $\tilde{\pi} := 1 - \frac{1}{1+\max\{\log(1/\delta), \log(1/\epsilon)\}}$.

Proof. The proof of Fact A.5 is a modification from proof of [Proposition 3, [13]] by using Fact

A.4. We first prove equation (A.17). By the selection rule of $hiePM$, the last level codebook $S_{t+1} = D^{(l_{t+1}=\log_2(\frac{1}{\delta}))}$ is used whenever $\max_i \pi_i(t) \geq \tilde{\pi} > 1/2$. Therefore,

$$\begin{aligned} EJS(\boldsymbol{\pi}(t), \gamma_h) &= \sum_{i=1}^{1/\delta} \pi_i(t) D\left(P_{\hat{y}_{t+1}|i,\gamma_h} \middle\| P_{\hat{y}_{t+1}|\neq i,\gamma_h}\right) \\ &\geq \tilde{\pi} D\left(P_{\hat{y}_{t+1}|i,\gamma_h} \middle\| P_{\hat{y}_{t+1}|\neq i,\gamma_h}\right) \\ &= \tilde{\pi} D(\text{Bern}(1-p[S]) \| \text{Bern}(p[S])) \\ &= \tilde{\pi} C_1(p[\log_2(1/\delta)]). \end{aligned} \tag{A.18}$$

It remains to show equation (A.16). For notational simplicity, let

$$\rho \equiv \pi_{D^{l_{t+1}}}(t) := \sum_{i \in D^{l_{t+1}}} \pi_i(t) \tag{A.19}$$

and $B^0 \equiv \text{Bern}(p[l_{t+1}])$, $B^1 \equiv \text{Bern}(1-p[l_{t+1}])$. We separate the proof into two cases:

If $\rho > 2/3$, we know that $l_{t+1} = \log_2(\frac{1}{\delta})$ by the selection rule of $hiePM$. Therefore, the set $D^{l_{t+1}}$ is of the smallest size 1. Let $D^{l_{t+1}} = \{\, i_{t+1}\}$, we have

$$\begin{aligned} &EJS(\boldsymbol{\pi}(t), \gamma_h) = \sum_{i=1}^{1/\delta} \pi_i(t) D\left(P_{\hat{y}_{t+1}|i,\gamma_h} \middle\| P_{\hat{y}_{t+1}|\neq i,\gamma_h}\right) \\ &= \rho D\big(B^1 \big\| B^0\big) \\ &+ \sum_{i \neq i_{t+1}} \pi_i(t) D\left(B^0 \middle\| \frac{\rho}{1-\pi_i(t)} B^1 + \frac{1-\rho-\pi_i(t)}{1-\pi_i(t)} B^0\right) \\ &\overset{(a)}{\geq} D\left(B^0 \middle\| \frac{1}{2} B^1 + \frac{1}{2} B^0\right) \\ &= I(1/2, p[l_{t+1}]) \geq I(1/3, p[l_{t+1}]), \end{aligned} \tag{A.20}$$

where (a) is by the fact that $D(B^1\|B^0) = D(B^0\|B^1)$ and that $D(B^0\|\alpha B^1 + (1-\alpha)B^0)$ is increasing in α for $0 \leq \alpha \leq 1$, together with $\frac{\rho}{1-\pi_i(t)} > 2/3 > 1/2$.

For the other case where $\rho \leq 2/3$, again by the selection rule of $hiePM$, we have $1/3 \leq \rho \leq 2/3$. Now we can lower bound the EJS as

$$\begin{aligned} EJS(\boldsymbol{\pi}(t), \gamma_h) &\overset{(a)}{\geq} JS(\boldsymbol{\pi}(t), \gamma_h) \\ &= \rho D\left(B^1 \middle\| \rho B^0 + (1-\rho)B^1\right) \\ &\quad + (1-\rho) D\left(B^0 \middle\| \rho B^0 + (1-\rho)B^1\right) \\ &= I(\rho, p[l_{t+1}]) \overset{(b)}{\geq} I(1/3, p[l_{t+1}]) \end{aligned} \tag{A.21}$$

where (a) is by Fact A.4 and (b) is by the concavity of the mutual information with respect to the input distribution, the symmetric of $I(\rho, p[l_{t+1}])$ around $\rho = 1/2$ for symmetric channels, and together with $1/3 \leq \rho \leq 2/3$. This concludes the assertion.

□

A.1.1 Upper-bounding the Expected Search Time with Query-Dependent Noise

From the expected search time upper bound via the use of EJS (Fact A.1) and the search size $\delta|S_{t+1}|$ dependent lower bound of EJS given in Fact A.2 and Fact A.5, we see that intuitively we need $I(1/2, p[\delta|S_{t+1}|])$ or $I(1/3, p[\delta|S_{t+1}|])$ to be large, or equivalently the size of the search region $|S_{t+1}|$ to be small, in a certain sense. In particular, we can handle the search size shrinkage in a probabilistic manner by providing an exponentially decay tail. Indeed, we have the following proposition:

Proposition A.1. *Given any search strategy γ with $\delta|S_{t+1}| \leq 1/2$ and*

$$EJS(\boldsymbol{\pi}(t), \gamma) \geq R(\delta|S_{t+1}|), \ \forall\, t \tag{A.22}$$

$$EJS(\boldsymbol{\pi}(t), \gamma) \geq \tilde{\boldsymbol{\pi}} E, \ \forall \max_i \boldsymbol{\pi}_i \geq \tilde{\pi}, \tag{A.23}$$

for some $R(\delta|S_{t+1}|) > 0$ *increasing in* $\delta|S_{t+1}|$ *and* $E > 0$. *If further*

$$\mathbb{P}(\delta \mid S_{t+1} \mid \ > \alpha) \leq k_0 e^{-tE_0}, \ \forall\, t > T_0 \tag{A.24}$$

for some $1/2 > \alpha > \delta$, $k_0 > 0$, $E_0 > 0$, *and* $T_0 > \lceil \log\log(\frac{1}{\delta\epsilon}) \rceil$, *the expected time of the strategy* γ *achieving resolution* $1/\delta$ *and reliability* ϵ *can be upper bounded by*

$$E[\tau_{\epsilon,\delta}] \leq \frac{\log(1/\delta)}{R(\alpha)} + \frac{\log(1/\epsilon)}{E} + g_{R,E}(\epsilon,\delta), \tag{A.25}$$

where

$$\begin{aligned} g_{R,E}(\epsilon,\delta) :=& \frac{k_0 e^{-E_0}}{(1-e^{-e_0})(\log\frac{1}{\delta\epsilon})^{E_0}} \left(\lceil \log\log\frac{1}{\delta\epsilon} \rceil + \frac{\log\frac{1}{\delta}}{R(1/2)} + \frac{\log\frac{1}{\epsilon}}{E} + f_{R(1/2),E}(\epsilon,\delta) \right) \\ &+ \frac{k_0 e^{-2E_0}}{(1-e^{-e_0})^2(\log\frac{1}{\delta\epsilon})^{2E_0}} + \lceil \log\log\frac{1}{\delta\epsilon} \rceil + f_{R(\alpha),E}(\epsilon,\delta) \end{aligned} \tag{A.26}$$

is of $o(\frac{1}{\delta\epsilon})$ *as* $\delta \to 0$ *or* $\epsilon \to 0$.

Proof. We prove this proposition via the total probability theorem and the re-start of the time homogeneous Markov chain $\boldsymbol{\pi}(t)$. Specifically, let us define the "bad" event $E_t = \{\delta|S_{t+1}| > \alpha\}$ and the "good" event $F_n = \bigcup_{t=n}^{\infty} E_t$. For every n, by total probability theorem and the union

bound, we have

$$\begin{aligned}
\mathbb{E}[\tau_{\epsilon,\delta}] &= \int_{\Omega} \tau_{\epsilon,\delta}\, d\mathbb{P} \leq \sum_{t=n}^{\infty} \int_{E_t} \tau_{\epsilon,\delta}\, d\mathbb{P} + \int_{F_n^C} \tau_{\epsilon,\delta}\, d\mathbb{P} \\
&= \sum_{t=n}^{\infty} \int_{E_t} \mathbb{E}[\tau_{\epsilon,\delta} \mid \boldsymbol{\pi}(t)]\, d\mathbb{P} + \int_{F_n^C} \tau_{\epsilon,\delta}\, d\mathbb{P} \\
&\overset{(a)}{\leq} \sum_{t=n}^{\infty} \mathbb{P}(E_t) \left(t + \frac{\log \frac{1}{\delta}}{R(1/2)} + \frac{\log \frac{1}{\epsilon}}{E} + f_{R(1/2),E}(\epsilon,\delta) \right) \\
&\qquad + \int_{F_n^C} \tau_{\epsilon,\delta}\, d\mathbb{P} \\
&\overset{(b)}{\leq} \sum_{t=n}^{\infty} \mathbb{P}(E_t) \left(t + \frac{\log \frac{1}{\delta}}{R(1/2)} + \frac{\log \frac{1}{\epsilon}}{E} + f_{R(1/2),E}(\epsilon,\delta) \right) \\
&\qquad + n + \frac{\log \frac{1}{\delta}}{R(\alpha)} + \frac{\log \frac{1}{\epsilon}}{E} + f_{R(\alpha),E}(\epsilon,\delta),
\end{aligned} \tag{A.27}$$

where $f_{R,E}(\epsilon,\delta)$ is as defined in Fact A.1. Here (a) follows from the time homogeneity of the Markov Chain $\boldsymbol{\pi}(t)$ re-starting at time t, together with Fact A.1 and $\delta|S_{t+1}| \leq 1/2$, written as

$$\mathbb{E}[\tau_{\epsilon,\delta} \mid \boldsymbol{\pi}(t)] \leq t + \frac{\log \frac{1}{\delta}}{R(1/2)} + \frac{\log \frac{1}{\epsilon}}{E} + f_{R(1/2),E}(\epsilon,\delta). \tag{A.28}$$

Similar argument can be made for (b) with $\delta|S_{t+1}| \leq \alpha$ for $t \geq n$ under event F_n^C. Now, plugging the assumption $\mathbb{P}(E_t) = \mathbb{P}(\delta \mid S_{t+1} \mid > \alpha) \leq k_0 e^{-tE_0}$ into (A.27) with some algebra, we have

$$\begin{aligned}
E[\tau_{\epsilon,\delta}] \leq & \frac{k_0 e^{-nE_0}}{1-e^{-E_0}} \left(n + \frac{e^{-nE_0}}{1-e^{-E_0}} + \frac{\log \frac{1}{\delta}}{R(1/2)} + \frac{\log \frac{1}{\epsilon}}{E} + f_{R(1/2),E}(\epsilon,\delta) \right) \\
& + n + \frac{\log \frac{1}{\delta}}{R(\alpha)} + \frac{\log \frac{1}{\epsilon}}{E} + f_{R(\alpha),E}(\epsilon,\delta).
\end{aligned} \tag{A.29}$$

Letting $n = \lceil \log \log \frac{1}{\delta\epsilon} \rceil$, we have the assertion of the proposition. □

By proposition A.1, we can see that for proving Theorem 2.1,2.3,2.2, it is sufficient to provide exponential decay tail probability of a large search size $\mathbb{P}(\delta \mid S_{t+1} \mid > \alpha)$ for each of the proposed algorithm $S_{t+1} = \gamma(\boldsymbol{\pi}(t))$. The main idea of studying the event $\{\delta|S_{t+1}| > \alpha\}$ is to

group the region into coarse bins of size α according to each of the search algorithm. And by the nature of each algorithm the event $\{\delta|S_{t+1}| > \alpha\}$ is equivalent to the event that one coarse bin has posterior larger than half. By further considering a similar submartingale of an average log-likelihood as in (A.1) but over the coarse bin posterior, the problem is then transformed to be the tail probability of a level crossing of a strictly positively drifted submartingle, where we can bound it by the Azuma's Inequality (Lemma A.4). Now let us provide the details:

Proof of Theorem 2.1

Along with the operation of $sortPM$, we first sort the posterior, and then group into bins with size $\delta|\text{bin}(q)| = \alpha$, written as

$$\pi_q^\alpha(t) := \sum_{i \in \text{bin}(q)} \pi_i^\downarrow(t),\ q = 1, 2, ..., 1/\alpha, \tag{A.30}$$

where $\pi^\downarrow$ is the sorted posterior, $\text{bin}(q) := \{\frac{\alpha}{\delta}(q-1)+1, \frac{\alpha}{\delta}(q-1)+2, ..., \frac{\alpha}{\delta}q\}$. For notational simplicity, we deal with the case where $1/\alpha$ and α/δ are both integer (the proof follows similarly for non-integer case). Let us further define the average log-likelihood of the binned sorted posterior

$$\begin{aligned} U_\alpha(t) &:= U\left(\boldsymbol{\pi}^\alpha(t)\right) \\ &= \sum_{q=1}^{1/\alpha} \pi_q^\alpha(t) \log \frac{\pi_q^\alpha(t)}{1-\pi_q^\alpha(t)}. \end{aligned} \tag{A.31}$$

By the search set selection rule in Algorithm 2.1 together with the definition of $U_\alpha(t)$, under $sortPM$ strategy we have

$$\begin{aligned} \mathbb{P}(\delta \mid S_{t+1} \mid\ > \alpha) &\leq \mathbb{P}\left(\pi_1^\alpha(t) < \frac{1}{2}\right) \\ &\leq \mathbb{P}(U_\alpha(t) < 0). \end{aligned} \tag{A.32}$$

Now, by fact A.3 and lemma A.1, $U_\alpha(t)$ is a submartingale with bound difference

$$\begin{aligned} &|U_\alpha(t+1) - U_\alpha(t)| \\ &\leq B_\alpha := \log(1/\alpha) + \log \frac{1-p_{\min}}{p_{\min}} + e. \end{aligned} \tag{A.33}$$

Further note that $U_\alpha(0) = -\log(1/\alpha - 1) < -\log(1/\alpha)$ and together with lemma A.4, we have

$$\begin{aligned} \mathbb{P}(\delta \mid S_{t+1} \mid \ > \alpha) &\leq \mathbb{P}(U_\alpha(t) < 0) \\ &\leq k_s e^{-t\frac{K_s^2}{2(B_\alpha + K_s)^2}} \ \ \forall t > \frac{\log(\frac{1}{\alpha})}{K_s}, \end{aligned} \tag{A.34}$$

where $k_s = e^{\frac{K_s \log(1/\alpha)}{K_s + B_\alpha}}$. Since $\alpha > (e \log \frac{1}{\delta\epsilon})^{-K_s}$ and therefore $\frac{\log(1/\alpha)}{K_s} < \lceil \log\log \frac{1}{\delta\epsilon} \rceil$, by proposition A.1, we conclude the assertion.

Proof of Theorem 2.2 and 2.3

Without loss of generality, we may assume that the resolution δ is such that $L = \log_2(1/\delta)$ is an integer. If otherwise, we can choose a smaller δ' such that $\log_2(1/\delta')$ is an integer and the analysis will follow similarly without affecting the asymptotic conclusions. One of the key attribute of $dyaPM$ and $hiePM$ is the nested resolution due to the natural bisection. To analyze it, we introduce the posterior vector $\boldsymbol{\pi}^{\{l\}}(t)$ of a nested resolution level $l < L$ with length 2^l where its elements are defined as

$$\pi_q^{\{l\}}(t) := \sum_{i \in \text{bin}(q)} \pi_i(t), \quad q = 1, 2, ..., 2^l, \tag{A.35}$$

where bin$(q) := \{(q-1)2^{L-l}+1, (q-1)2^{L-l}+2, ..., q2^{L-l}\}$. Further, we can also define the average log-likelihood on $\boldsymbol{\pi}^{\{l\}}$ as

$$U^{\{l\}}(t) := \sum_{q=1}^{2^l} \pi_q^{\{l\}}(t) \log \frac{\pi_q^{\{l\}}(t)}{1-\pi_q^{\{l\}}(t)}. \tag{A.36}$$

We have

$$\begin{aligned} \mathbb{P}(\delta \mid S_{t+1} \mid \ > 2^{-l}) &\leq \mathbb{P}\bigg(\max_q \pi_q^{\{l\}}(t) < \frac{1}{2}\bigg) \\ &\leq \mathbb{P}\big(U^{\{l\}}(t) < 0\big). \end{aligned} \tag{A.37}$$

The proof then follows similarly as in the proof of Theorem 2.1: Applying proposition A.1 with $\alpha = 2^{-l}$, where the corresponding submartingale properties of $U^{\{l\}}(t)$ is by Lemma A.2 and Lemma A.3 for $dyaPM$ and $hiePM$, respectively, hence we omitted the rest.

A.1.2 Technical Lemmas

Lemma A.1. *Using $sortPM$ with resolution δ, the coarse binned sorted log-likelihood $U_\alpha(t)$ defined by (A.30) and (A.31) is a submartigale with respect to $\boldsymbol{\pi}(t)$. In particular, we have*

$$\begin{aligned} &\mathbb{E}[U_\alpha(t+1) \mid \boldsymbol{\pi}(t)] - U_\alpha(t) \\ &\geq K_s := \max\left\{\frac{1}{2}D\left(\frac{1}{4}B_1 + \frac{3}{4}B_0 \middle\| B_0\right), \frac{1}{8}D\left(B_1 \middle\| \frac{3}{4}B_1 + \frac{1}{4}B_0\right)\right\} \end{aligned} \tag{A.38}$$

for all $t > 0$ where $B_1 =$ Bern$(1-p[1/2])$ and $B_0 =$ Bern$(p[1/2])$.

Proof. Let σ_t be the permutation such that $\sigma_t(\boldsymbol{\pi}(t)) = \boldsymbol{\pi}^{\downarrow}(t)$. To emphasize the effect of the different permutations at different time t, for a given permutation σ we define $\boldsymbol{\pi}^{\sigma}(t) := \sigma(\boldsymbol{\pi}(t))$ and

$$\begin{aligned} U_\alpha^\sigma(t) &:= U(\boldsymbol{\pi}^{\alpha,\sigma}) \\ &= \sum_{q=1}^{1/\alpha} \pi_q^{\alpha,\sigma}(t) \log \frac{\pi_q^{\alpha,\sigma}(t)}{1-\pi_q^{\alpha,\sigma}(t)}, \end{aligned} \tag{A.39}$$

where

$$\pi_q^{\alpha,\sigma}(t) := \sum_{i \in \text{bin}(q)} \pi_i^{\sigma}(t),\ q = 1, 2, ..., 1/\alpha. \tag{A.40}$$

By definition, we have $U_\alpha(t) \equiv U_\alpha^{\sigma_t}(t)$. Now, we can lower bound the expected drift as

$$\begin{aligned}
&\mathbb{E}[U_\alpha(t+1) \mid \boldsymbol{\pi}(t)] - U_\alpha(t) = \mathbb{E}[U_\alpha^{\sigma_{t+1}}(t+1) \mid \boldsymbol{\pi}(t)] - U_\alpha^{\sigma_t}(t) \\
&\overset{(a)}{\geq} \mathbb{E}[U_\alpha^{\sigma_t}(t+1) \mid \boldsymbol{\pi}(t)] - U_\alpha^{\sigma_t}(t) \\
&\overset{(b)}{=} \sum_{q=1}^{1/\alpha} \pi_q^{\sigma_t,\alpha}(t) D\left(P^{\sigma_t}_{y_{t+1}|\text{bin}(q),S_{t+1}} \middle\| P^{\sigma_t}_{y_{t+1}|\notin\text{bin}(q),S_{t+1}}\right),
\end{aligned} \tag{A.41}$$

where

$$\begin{aligned}
P^{\sigma_t}_{y_{t+1}|\text{bin}(q),S_{t+1}} &:= \frac{1}{\pi_q^{\alpha,\sigma_t}(t)} \sum_{i \in \text{bin}(q)} \pi_i^{\sigma_t}(t) P_{y_{t+1}|\sigma_t(i),S_{t+1}} \\
P^{\sigma_t}_{y_{t+1}|\notin\text{bin}(q),S_{t+1}} &:= \sum_{q' \neq q} \frac{\pi_{q'}^{\sigma_t,\alpha}(t)}{1 - \pi_q^{\sigma_t,\alpha}(t)} P^{\sigma_t}_{y_{t+1}|\text{bin}(q),S_{t+1}}
\end{aligned} \tag{A.42}$$

and $P_{y_{t+1}|\cdot,S_{t+1}}$ is as defined in (A.4). Here the inequality (a) follows from $\boldsymbol{\pi}^{\sigma_t,\alpha}(t+1) \succeq \boldsymbol{\pi}^{\sigma_{t+1},\alpha}(t+1)$ and that $U(\boldsymbol{\pi})$ is Schur-convex with respect to $\boldsymbol{\pi}$. And (b) is a similar manipulation using Bayes's rule as was done in the proof of [Theorem 1 in [13]].

We now further lower bound (A.41) by positivity and convexity of the KL divergence. We seperate the discussion into two cases:

1. If $q^* = 1$:

   By the selection rule of k^* in $sortPM$, we have $\pi_1^\alpha(t) \geq 1/2$ and $\pi_{[1,k^*]}^{\sigma_t}(t) \geq 1/4$.

Therefore,

$$
\begin{aligned}
(A.41) &\geq \sum_{q=1}^{1/\alpha} \pi_q^{\sigma_t,\alpha}(t) D\left(P^{\sigma_t}_{y_{t+1}|\text{bin}(q),S_{t+1}} \middle\| P^{\sigma_t}_{y_{t+1}|\notin\text{bin}(q),S_{t+1}}\right) \\
&\overset{(c)}{\geq} \pi_1^{\sigma_t,\alpha}(t) D\left(\frac{\pi^{\sigma_t}_{[1,k^*]}(t)}{\pi_1^{\alpha}(t)} B_1 + \frac{\pi^{\sigma_t}_{[k^*+1,\frac{\alpha}{\delta}]}(t)}{\pi_1^{\alpha}(t)} B_0 \;\middle\|\; B_0\right) \\
&\overset{(d)}{\geq} \frac{1}{2} D\left(\frac{1}{4}B_1 + \frac{3}{4}B_0 \middle\| B_0\right),
\end{aligned}
\tag{A.43}
$$

where (c) is by positivity of KL divergence and (d) is by $\pi_1^{\alpha}(t) \geq 1/2$ and $\pi^{\sigma_t}_{[1,k^*]}(t) \geq 1/4$.

2. If $q^* > 1$:

   By the selection rule of k^* in $sortPM$, we have $\pi^{\sigma_t}_{[1,k^*]}(t) \leq 3/4$.

   WLOG, we assume that $k^* < \max \text{bin}(q^*)$ otherwise it reduces to the case of Fact A.2. Together with the selection rule of k^*, we have $\pi^{\sigma_t,\alpha}_{[1,q^*]}(t) \geq \frac{1}{2}$. By sorting we aslo have $\pi^{\sigma_t,\alpha}_{[1,q^*-1]}(t) \geq \pi^{\sigma_t,\alpha}_{q^*}(t)$. Therefore $\pi^{\sigma_t,\alpha}_{[1,q^*-1]}(t) \geq \frac{1}{4}$.

   Now can proceed the lower bound as

$$
\begin{aligned}
(A.41) &\geq \sum_{q=1}^{1/\alpha} \pi_q^{\sigma_t,\alpha}(t) D\left(P^{\sigma_t}_{y_{t+1}|\text{bin}(q),S_{t+1}} \middle\| P^{\sigma_t}_{y_{t+1}|\notin\text{bin}(q),S_{t+1}}\right) \\
&\overset{(e)}{\geq} \pi^{\sigma_t,\alpha}_{[1,q^*-1]}(t) D(B_1 \| \pi^{\sigma_t}_{[1,k^*]} B_1 + \pi^{\sigma_t}_{[k^*+1,\frac{1}{\delta}]} B_0) \\
&\overset{(f)}{\geq} \frac{1}{4} D\left(B_1 \middle\| \frac{3}{4}B_1 + \frac{1}{4}B_0\right),
\end{aligned}
\tag{A.44}
$$

where (e) is by Fact A.4 and positivity of the KL divergence, and (f) is from $\pi^{\sigma_t,\alpha}_{[1,q^*-1]}(t) \geq \frac{1}{4}$ and $\pi^{\sigma_t}_{[1,k^*]}(t) \leq 3/4$.

Let

$$
K_s := \max\left\{\frac{1}{2} D\left(\frac{1}{4}B_1 + \frac{3}{4}B_0 \middle\| B_0\right), \frac{1}{4} D\left(B_1 \middle\| \frac{3}{4}B_1 + \frac{1}{4}B_0\right)\right\},
\tag{A.45}
$$

and by (A.43) and (A.43), we conclude the assertion of this lemma.

□

Lemma A.2. *Using $dyaPM$ with resolution δ, the nested log-likelihood $U^{\{l\}}(t)$ of lower resolution level $l < \log_2(1/\delta))$ defined in (A.36) is a submartigale. In particular, we have*

$$\begin{aligned}&\mathbb{E}[U^{\{l\}}(t+1) \mid \boldsymbol{\pi}(t)] - U^{\{l\}}(t)\\ &\geq K_d := \min\Big\{ \min_{\rho\in(0,0.1]} \max\{f(\rho), g(\rho)\}, \frac{1}{4} D\left(\frac{1}{4}B_1 + \frac{3}{4}B_0 \Big\| B_0\right)\Big\} > 0,\end{aligned} \tag{A.46}$$

for all $t > 0$, for any $l < \log_2(1/\delta)$, where $B_1 = Bern(1 - p[1/2])$, $B_0 = Bern(p[1/2])$

$$\begin{aligned}f(\rho) &= \rho D\left(B_1 \Big\| (3/4)B_1 + (1/4)B_0\right)\\ g(\rho) &= \begin{cases}(1/2-\rho)D\left((1-4\rho)B_1 + 4\rho B_0 \Big\| (1/2+\rho)B_1 + (1/2-\rho)B_0\right), & \rho \in [0, 0.1)\\ 0, \quad o.w,\end{cases}\end{aligned} \quad \cdot \tag{A.47}$$

Proof. By similar algebraic effort as in [Theorem 1 in [13]], the expected drift can be written as

$$\begin{aligned}&\mathbb{E}[U^{\{l\}}(t+1) \mid \boldsymbol{\pi}(t)] - U^{\{l\}}(t)\\ &= \sum_{q=1}^{2^l} \pi_q^{\{l\}}(t) D\left(P_{y_{t+1}|\in \text{bin}(q),\gamma} \Big\| P_{y_{t+1}|\notin \text{bin}(q),\gamma}\right),\end{aligned} \tag{A.48}$$

where

$$\begin{aligned}P_{y_{t+1}|\in \text{bin}(q),\gamma} &:= \frac{1}{\pi_q^{\{l\}}(t)}\\ &\times \sum_{i\in \text{bin}(q)} \pi_i(t) p\big(y_{t+1} \big| \theta = i, S_{t+1} = \gamma(\boldsymbol{\pi}(t))\big)\end{aligned} \tag{A.49}$$

and

$$\begin{aligned}P_{y_{t+1}|\notin \text{bin}(q),\gamma} &:= \frac{1}{\sum_{i\notin \text{bin}(q)} \pi_i(t)}\\ &\times \sum_{i\notin \text{bin}(q)} \pi_i(t) p\big(y_{t+1} \big| \theta = i, S_{t+1} = \gamma(\boldsymbol{\pi}(t))\big).\end{aligned} \tag{A.50}$$

We drop (t) and write $\boldsymbol{\pi} \equiv \boldsymbol{\pi}(t)$ in the proof frequently for notational simplification. We

write the starting index of $H_{l_t^*}^{m_t^*}$ as $d \equiv m_t^* 2^{L-l_t^*}$. Furthermroe, let the bin of level l that contains k^* be q^*, *i.e.* $k^* \in \text{bin}(q^*)$ and $b_m = \min(\text{bin}(q^*))$ and $b_M = \max(\text{bin}(q^*))$.

The case of $l = \log_2(1/\delta)$ is done by Fact A.2. For any given $l < \log_2(1/\delta)$, we separate into two cases:

1. $S_{t+1} = \gamma_d(\boldsymbol{\pi}(t))$ contains at least one bin of level l, *i.e.* $\text{bin}(q) \subseteq S_{t+1}$ for some q:

$$\begin{aligned}
&\mathbb{E}[U^{\{l\}}(t+1) \mid \boldsymbol{\pi}(t)] - U^{\{l\}}(t) \\
&= \sum_{q=1}^{2^l} \pi_q^{\{l\}}(t) D\left(P_{y_{t+1}|\in\text{bin}(q),\gamma} \middle\| P_{y_{t+1}|\notin\text{bin}(q),\gamma}\right) \\
&\overset{(a)}{\geq} \max\Big\{ \pi_{[d,b_m-1]} D\left(B_1 \middle\| \pi_{[d,k^*]} B_1 + (1-\pi_{[d,k^*]}) B_0\right), \\
&\qquad \pi_{q^*}^{\{l\}} D\left(\frac{\pi_{[b_m,k^*]}}{\pi_{q^*}^{\{l\}}} B_1 + \frac{\pi_{[k^*+1,b_M]}}{\pi_{q^*}^{\{l\}}} B_0 \middle\| \pi_{[d,k^*]} B_1 + (1-\pi_{[d,k^*]}) B_0\right) \Big\},
\end{aligned} \tag{A.51}$$

where we used

$$\begin{aligned}
&D\left(P_{y_{t+1}|q,\gamma} \middle\| P_{y_{t+1}|\neq q,\gamma}\right) \geq D\left(P_{y_{t+1}|q,\gamma} \middle\| P_{y_{t+1}|\gamma}\right) \\
&D\left(P_{y_{t+1}|q,\gamma} \middle\| P_{y_{t+1}|\neq q,\gamma}\right) \geq 0
\end{aligned} \tag{A.52}$$

in (a). Note that by the binary tree construction of H_l^m, we have $[b_m, k^*] \subseteq \text{bin}(q^*) \subseteq H_{l_t^*+1}^{2m_t^*}$. Therefore,

$$\pi_{[b_m,k^*]} \leq \pi_{q^*}^{\{l\}} \leq \pi_{H_{l^*t+1}^{2m_t^*}} \leq \frac{1}{2}. \tag{A.53}$$

By the selection rule of k^* and that $\pi_k \leq 1/2$, we also know that $\pi_{[d,k^*]} \leq 3/4$. Together with (A.53) we can lower bound the first part in (A.51) as

$$\begin{aligned}
&\pi_{[d,b_m-1]} D\left(B_1 \middle\| \pi_{[d,k^*]} B_1 + (1-\pi_{[d,k^*]}) B_0\right) \\
&\geq \rho D\left(B_1 \middle\| (3/4) B_1 + (1/4) B_0\right) := f(\rho)
\end{aligned} \tag{A.54}$$

where we used $\rho \equiv \pi_{[d,b_m-1]}$ for further simplification of the notation.

On the other hand, without loss of generality we assume that $k^* < b_M$ (otherwise if

$k^* = b_M$, it reduces to the case of Fact A.2). By the selection rule of k^* and that $k^* < b_M$, we have

$$0 \leq \frac{1}{2} - \pi_{[d,k^*]} \leq \pi_{[d,b_M]} - \frac{1}{2} \tag{A.55}$$

which can be re-written as

$$0 \leq \frac{1}{2} - \rho - \pi_{[b_m,k^*]} \leq \rho + \pi_{q^*}^{\{l\}} - \frac{1}{2}. \tag{A.56}$$

Therefore,

$$\begin{aligned} \frac{\pi_{[b_m,k^*]}}{\pi_{q^*}^{\{l\}}} &\overset{(b)}{\geq} \frac{1 - \pi_{q^*}^{\{l\}} - 2\rho}{\pi_{q^*}^{\{l\}}} \\ &= \frac{1-2\rho}{\pi_{q^*}^{\{l\}}} - 1 \overset{(c)}{\geq} 1 - 4\rho, \end{aligned} \tag{A.57}$$

where (b) is by (A.56) and (c) by (A.53). And again by (A.53) we also have

$$\pi_{[d,k^*]} \leq \pi_{[d,b_M]} = \rho + \pi_{q^*}^{\{l\}} \leq \rho + \frac{1}{2}. \tag{A.58}$$

With (A.56), (A.57) and (A.58), the second part in equation (A.51) can then be lower bounded as

$$\begin{aligned} &\pi_{q^*}^{\{l\}} D\left(\frac{\pi_{[b_m,k^*]}}{\pi_{q^*}^{\{l\}}} B_1 + \frac{\pi_{[k^*+1,b_M]}}{\pi_{q^*}^{\{l\}}} B_0 \middle\| \pi_{[d,k^*]} B_1 + (1 - \pi_{[d,k^*]}) B_0\right) \\ &\geq \begin{cases} (1/2-\rho) D\left((1-4\rho)B_1 + 4\rho B_0 \middle\| (1/2+\rho)B_1 + (1/2-\rho)B_0\right), & \rho \in [0, 0.1) \\ 0, \quad o.w, \end{cases} \\ &:= g(\rho). \end{aligned} \tag{A.59}$$

Now, since $f(\rho) > 0$ for $\rho \in (0, 1]$ and $g(0) > 0$, we have

$$(A.51) \geq \min_{\rho \in (0, 0.1]} \max\{f(\rho), g(\rho)\} > 0. \tag{A.60}$$

2. $S_{t+1} = \gamma_d(\boldsymbol{\pi}(t))$ is within a bin of level l, *i.e.* $S_{t+1} \subseteq \text{bin}(q^*)$:

$$\begin{aligned}
&\mathbb{E}[U^{\{l\}}(t+1) \mid \boldsymbol{\pi}(t)] - U^{\{l\}}(t) \\
&\quad = \sum_{q=1}^{2^l} \pi_q^{\{l\}}(t) D\left(P_{y_{t+1}|q,\gamma} \middle\| P_{y_{t+1}|\neq q,\gamma}\right) \\
&\quad \geq \pi_{q^*}^{\{l\}} D\left(\frac{\pi_{[b_m,k^*]}}{\pi_{q^*}^{\{l\}}} B_1 + \frac{\pi_{[k^*+1,b_M]}}{\pi_{q^*}^{\{l\}}} B_0 \middle\| B_0\right)\Big\}.
\end{aligned} \tag{A.61}$$

By the selection rule of k^* and that $S_{t+1} \subseteq \text{bin}(q^*)$, we know that $\pi_{q^*}^{\{l\}} \geq \pi_{S_{t+1}} \geq 1/4$ and that $\frac{\pi_{[b_m,k^*]}}{\pi_{q^*}^{\{l\}}} \geq \pi_{[b_m,k^*]} = \pi_{S_{t+1}} \geq 1/4$. Therefore,

$$(A.61) \geq \frac{1}{4} D\left(\frac{1}{4} B_1 + \frac{3}{4} B_0 \middle\| B_0\right). \tag{A.62}$$

The result is concluded by combining the two cases from (A.60) and (A.62) □

Lemma A.3. *Using $hiePM$ with resolution $\frac{1}{\delta}$, the nested log-likelihood $U^{\{l\}}(t)$ of lower resolution level $l < \log_2(1/\delta))$ defined in (A.36) is a submartigale. In particular, we have*

$$\begin{aligned}
&\mathbb{E}[U^{\{l\}}(t+1) \mid \boldsymbol{\pi}(t)] - U^{\{l\}}(t) \\
&\geq K_h := \min\left\{ I\Big(\frac{1}{3}, p[\frac{1}{2}]\Big), \frac{2}{3} D\Big(\frac{1}{3}\textit{Bern}(1-p[\frac{1}{2}]) + \frac{2}{3}\textit{Bern}(p[\frac{1}{2}]) \Big\| \textit{Bern}(p[\frac{1}{2}])\Big)\right\}
\end{aligned} \tag{A.63}$$

for all $t > 0$, for any $l < S$.

Proof. Given any $l < S$, if the selected codeword $D^{(l_{t+1})}$ is such that $l_{t+1} \leq l$, by Fact A.5 we conclude the results. If otherwise $l_{t+1} > l$, then we have $D^{(l_{t+1})} \subseteq \text{bin}(q_t)$ for some q_t. For notational simplicity, let $\rho \equiv \pi_{D^{(l_{t+1})}}(t) := \sum_{i \in D^{(l_{t+1})}} \pi_i(t)$ and $B^0 \equiv \text{Bern}(p[2^{-l_{t+1}}])$,

$B^1 \equiv \text{Bern}(1 - p[2^{-l_{t+1}}])$. We have

$$\begin{aligned}
&\mathbb{E}[U^{\{l\}}(t+1) \mid \boldsymbol{\pi}(t)] - U^{\{l\}}(t) \\
&= \sum_{q=1}^{2^l} \pi_q^{\{l\}}(t) D\left(P_{y_{t+1}|q,\gamma} \middle\| P_{y_{t+1}|\neq q,\gamma}\right) \\
&\overset{(a)}{\geq} \frac{2}{3} D(\rho B^1 + (1-\rho)B^0 \| B^0) \overset{(b)}{\geq} \frac{2}{3} D(\frac{1}{3}B^1 + \frac{2}{3}B^0 \| B^0) \\
&\geq \frac{2}{3} D\Big(\frac{1}{3}\text{Bern}(1 - p[\frac{1}{2}]) + \frac{2}{3}\text{Bern}(p[\frac{1}{2}]) \Big\| \text{Bern}(p[\frac{1}{2}])\Big)\Big\}.
\end{aligned} \tag{A.64}$$

where (a) and (b) are by the selection rule of $hiePM$ that $\boldsymbol{\pi}_{q_t}^{\{l\}}(t) > 2/3$ whenever $l_t > l$ and that $1/3 \leq \rho \leq 2/3$. This concludes the assertion. □

Lemma A.4 (Azuma's Inequality)**.** *Given a submartingale $U(t)$ with $U(0) < 0$ with respect to another random process $\boldsymbol{\pi}(t)$. If $U(t)$ has bounded difference, $i.e.$ $|U(t+1) - U(t)| < B$ for some $B \in \mathbb{R}^+$, and that the expected difference is strictly positive, i.e.*

$$\mathbb{E}[U(t+1) - U(t) \mid \boldsymbol{\pi}(t)] \geq K > 0, \tag{A.65}$$

then we have

$$\mathbb{P}(U(t) < 0) < k e^{-t\frac{K^2}{2(B+K)^2}} \quad \forall t > \frac{-U(0)}{K} \tag{A.66}$$

where $k = e^{-\frac{KU(0)}{(B+K)^2}}$.

Proof. By the positive drift, $U(t) - tK$ is also a submartingale with bounded difference

$$|U(t+1) - (t+1)K - (U(t) - tK)| \leq B + K, \tag{A.67}$$

for all $t \geq 0$. Applying Azuma's inequality [42] on $U(t) - tK$, we have

$$\begin{aligned}
&\mathbb{P}(U(t) < 0) \\
&= \mathbb{P}\big(U(t) - tK - U(0) < -U(0) - tK\big) \\
&\leq \exp\left(-\frac{(U(0) + tK)^2}{2t(B+K)^2}\right) \\
&= \exp\left(-\frac{K^2 t}{2(B+K)^2}\right) \exp\left(-\frac{KU(0)}{(B+K)^2}\right) \exp\left(-\frac{(U(0))^2}{2t(B+K)^2}\right) \\
&\leq e^{-\frac{KU(0)}{(B+K)^2} - \frac{K^2}{2(B+K)^2}t}
\end{aligned} \tag{A.68}$$

for $t > \frac{-U(0)}{K}$, concluding the results. □